Spring 2021

Fabrication, characterization and environmental monitoring of polymer-based materials for biomedical and structural applications

Mousumi Bose

Department: Chemistry

FABRICATION, CHARACTERIZATION AND ENVIRONMENTAL MONITORING OF POLYMER-BASED MATERIALS FOR BIOMEDICAL AND STRUCTURAL APPLICATIONS

by

MOUSUMI BOSE

A DISSERTATION

Presented to the Graduate Faculty of the

MISSOURI UNIVERSITY OF SCIENCE AND TECHNOLOGY

In Partial Fulfillment of the Requirements for the Degree

DOCTOR OF PHILOSOPHY

in

CHEMISTRY

2021

Approved by:

Paul Nam, Advisor
Honglan Shi
Philip Whitefield
Risheng Wang
K. Chandrashekhara

PUBLICATION DISSERTATION OPTION

This dissertation consists of the following three articles, formatted in the style used by the Missouri University of Science and Technology:

Paper I, found on pages 22–47, has been submitted to *IEEE Sensors Journal*.

Paper II, found on pages 48–74, has been submitted to *Journal of Applied Polymer Science*.

Paper III, found on pages 75–98, has been submitted to *Chromatographia*.

ABSTRACT

Polymers are versatile materials utilized for variety of applications. In biomedical field, luminescence quenching based optical oxygen sensors encapsulated in polymeric substances are gaining attention for early detection of surface wounds associated with tissue oxygen. A simple and low-cost fabrication technique was developed to produce sensor arrays for continuous two-dimensional oxygen tension measurement. Sensor patch along with smart phone-based readout technique is being evaluated as a smart bandage.

The environmental concerns and limited petroleum supply demand for replacing petroleum-based polymers with renewable bio-based sources while maintaining comparable properties. A sustainable and green approach was adopted to synthesize soy polyol-derived rigid polyurethane foam for structural and thermal insulation applications. The focus was to investigate the effect of different additives on synthesis of these foams and their mechanical and thermal properties. Its potential for use in structural insulated panel for energy-efficient and modular building construction is being evaluated.

The emission of hazardous volatile organic compounds (VOCs) is of great concern when the recycled materials such as rubber and motor oil are used as processing aids with asphalt pavement materials for road construction. To monitor the potential environmental risks, a portable gas chromatography (GC) was employed in the development of a rapid and sensitive detection method for on-site monitoring of toxic VOCs, such as benzene, toluene, ethylbenzene, and xylenes (BTEX). The method was applied for on-line monitoring of BTEX gas emission during the hot-mix-asphalt processing with recycled materials.

ACKNOWLEDGMENTS

First and foremost, I express my heartfelt gratitude to my advisor, Dr. Paul Nam, for his invaluable guidance and support throughout my doctoral degree. Thanks to all his constructive suggestions and belief in me, which helped me to carry out my research in multiple areas.

I would like to thank Dr. Honglan Shi, Dr. K. Chandrashekhara, Dr. Chang-Soo Kim and Dr. William Stoecker for all their advice and numerous discussions. I also wish to thank Dr. Philip Whitefield and Dr. Risheng Wang for their time and valuable inputs.

I am thankful to my colleagues, especially Dr. Gurjot Dhaliwal, Xiaolong He, Jason Hagerty and Jason Boes, who worked with me extensively during my doctoral program. I am grateful to the professors, especially Dr. Wenyan Liu, and entire staff of the Department of Chemistry for helping me throughout my graduate study at Missouri S&T.

I would also like to thank the funding agencies National Institute of Health (NIH), Missouri Soybean Merchandising Council, US Department of Agriculture and Nanova Environmental, Inc. for their support during my doctoral program.

Finally, I am forever indebted to my husband, Dr. Soumava Chakraborty, for his unconditional support, understanding and belief in me. I would like to express my love to my little daughter, Samsthita, who joined us in the final year of my PhD, for giving me unlimited pleasure and happiness. I would also like to thank my parents for their encouragement, unconditional love, and support. I owe my thanks to Almighty for His graces and blessings on me, so that I have been finally able to accomplish my PhD.

TABLE OF CONTENTS

SECTION

LIST OF ILLUSTRATIONS

PAPER III

LIST OF TABLES

1. INTRODUCTION

1.1. BACKGROUND

Emerging polymers and its versatile applications are adopted in almost every area of modern living. It has incredibly diverse uses from high strength structural materials through sophisticated biomedical applications. With huge increase of polymer consumption, its environmental impact attracted researchers' attention towards its recyclability or replacement of the conventional petroleum-based polymers with renewable bio-based sources. This research explores different aspects of use of polymers.

1.2. OPTICAL OXYGEN SENSOR

Oxygen concentration is very important to measure for many different applications such as prevention of ulcers, wound healing, cell metabolism, packaged food conditions, and water quality monitoring, etc. [1]–[5]. Excess pressure over bony prominences leads to insufficient blood flow and subsequently causes pressure ulcer [6]. Healing process of any types of wounds, such as burn wound or any minor cut to major accident, involves four different steps and each step requires adequate oxygen supply. Oxygen plays major roles in production of cytokines and growth factors, cell recruitment and proliferation, protein synthesis, and extracellular matrix reorganization, etc. Since, oxygen cannot be stored in the cells, continuous supply of oxygen to the cells is necessary for wound healing. Therefore, obvious requirement is continuous monitoring of oxygen levels in those areas [7]–[9].

Sensing of oxygen using optical oxygen sensor has attracted huge attention. Over the last 20 years polymers are extensively utilized to develop variety of sensors, which largely used for various biomedical applications. Polymers are used for optical sensors due to their low cost, tailor-made structures, tunable properties, easy processing, etc. Flexibility to change the chemical and physical properties of polymers reversibly or irreversibly depending on interest, make them the materials of choice for fabrication of sensors [10], [11].

Optical sensors utilize optical transduction techniques and measure optical properties of the opto-active reagents on interaction with an analyte of interest, such as oxygen. Optical properties include fluorescence intensity and decay time, absorption, reflectance, refractive index, light scattering and polarization etc. Polymers used for optical sensors either can participate in sensing method or can immobilize the chemicals responsible for sensing the analyte [12].

1.2.1. Working Principle of Ratiometric Luminescent Optical Sensor. On stimulation with light wave fluorescent/ phosphorescent molecules are excited to higher energy state. When molecules return to ground energy state, they emit light with higher wavelength compared to their excited stimulation light, known as stokes shift. Fluorescence is emission from spin-paired singlet excited state, whereas phosphorescence occurs from triplet excited state due to change in electron spin. Since the probability of later transition is lower, phosphorescence is long lived (10^{-5} – 10 s) emission, whereas fluorescence is short lived (10^{-9} - 10^{-7} s) emission. Phosphorescence also occurs at higher wavelength than fluorescence. Perrin-Jablonski diagram in Figure 1.1 explains the process well. Photo-luminescent intensity and lifetime are utilized extensively to build

oxygen sensors, since presence of O_2 can alter the intensity and lifetime effectively. Polymers are used either to immobilize such opto-active chemicals or conjugated polymers are prepared with active photo-luminescent properties [13].

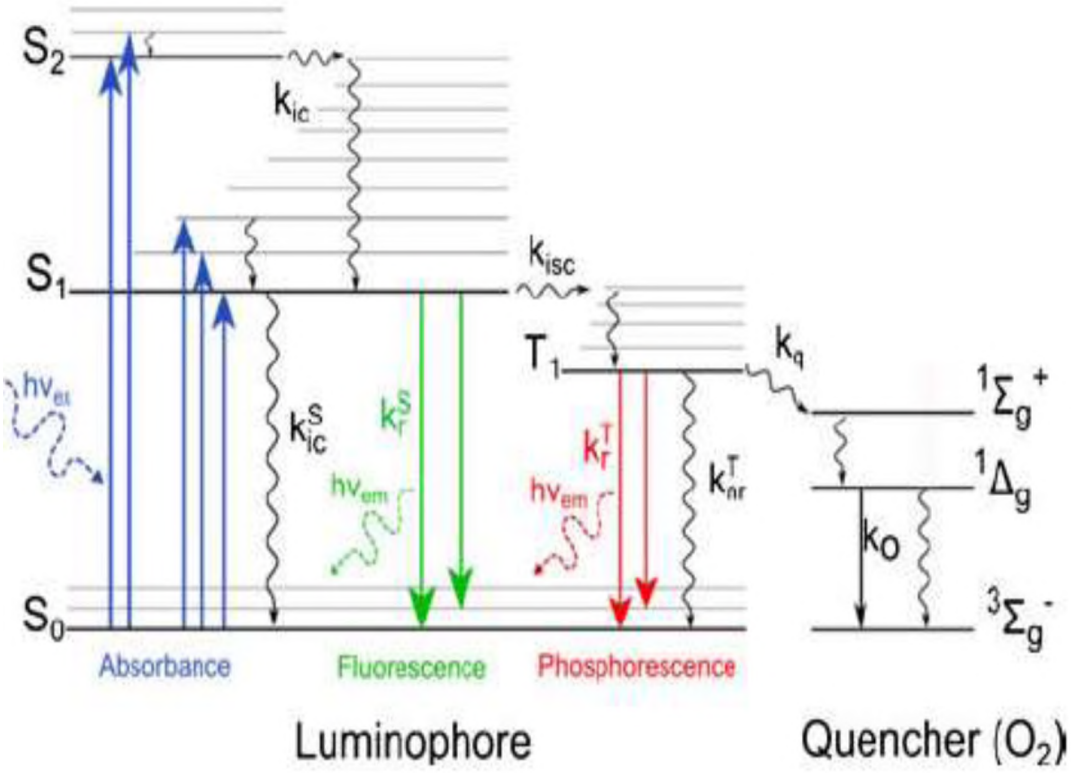

Figure 1.1. Perrin-Jablonski diagram [13].

Dynamic collision of oxygen molecules with excited luminescent molecules causes quenching (return from excited state to ground state) of the oxygen sensitive luminescent probes, thus decreases its intensity and lifetime effectively. During the collision triplet oxygen converted to singlet oxygen, which is not easy to detect reversibly. But the dynamic quenching of luminescent molecules is completely reversible and does not affect the absorption maxima. The relationship between luminescent

intensity and lifetime with partial pressure of oxygen is expressed by Stern-Volmer equation, Equation (1).

$$\frac{I_0}{I} = \frac{\tau_0}{\tau} = 1 + K_{SV} P_{O_2} \quad (1)$$

where I_0 and I are the intensity, τ_0 and τ are the lifetime of luminescent probe in absence and presence of O_2 respectively. K_{sv} is the Stern-Volmer constant and P_{O_2} is the partial pressure of oxygen. Figure 1.2 is the elastration of Stern-Volmer equation i.e. intensity quenching of photo-luminescent dye in presence of oxygen. The dynamic range of analytical measurement can be adjusted by proper choice of luminescent molecule, matrix materials and other additives required to fabricate the probe [13]–[15].

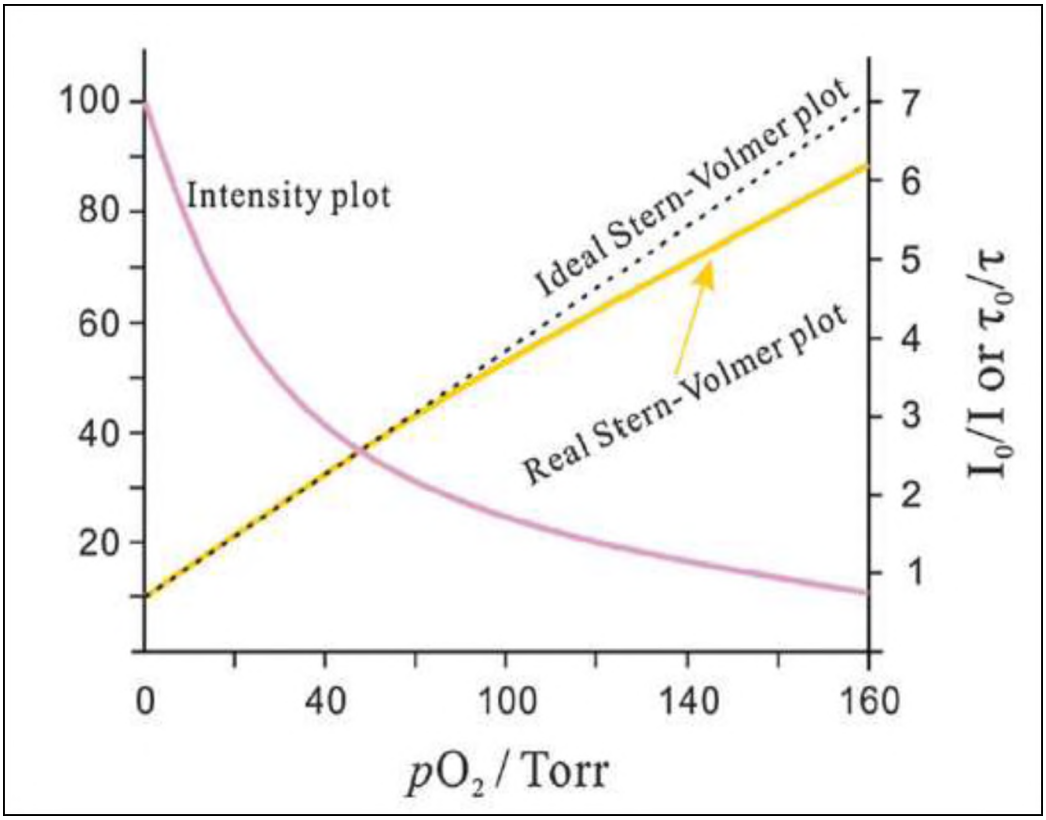

Figure 1.2. Stern-Volmer plot showing luminescent intensity quenching in presence of O_2 [15].

1.2.2. Fluorophore. Encapsulating fluorophore in a suitable polymer matrix is common practice to fabricate optical sensors. Metalloporphyrin-based luminophores are most popular due to their intense red phosphorescence with larger Stokes shift, longer lifetimes, etc. Halogen substitution further improves its chemical stability and photostability. Fluorine substituted Pt(II) porphyrin (PtTFPP), as shown in Figure 1.3, has become the most frequently used fluorophore for intensity-based sensing system [13], [18].

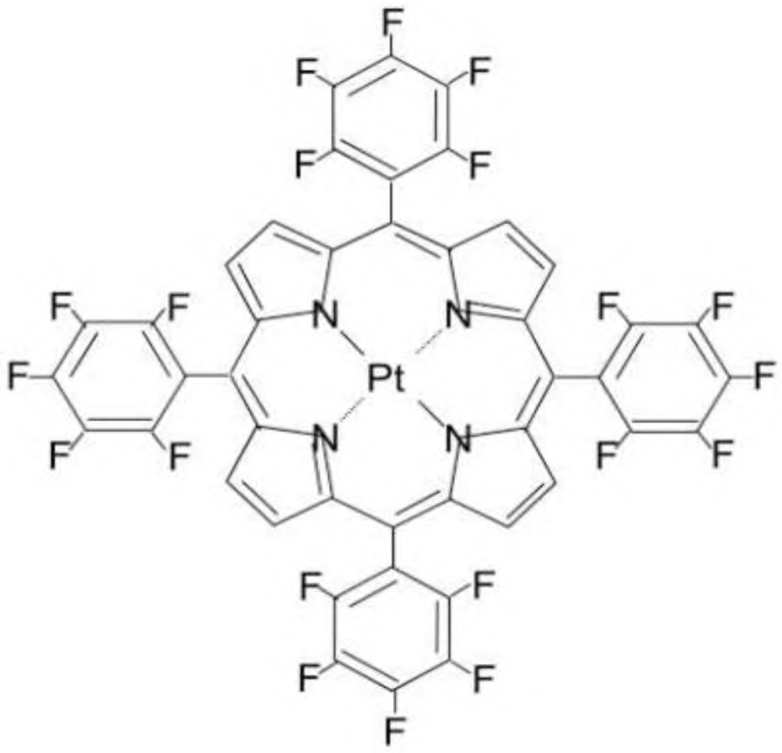

Figure 1.3. Chemical structure of platinum tetrakis(pentafluorophenyl)porphyrin (PtTFPP) [13].

1.2.3. Host Polymer. Host polymer should be compatible and inert to fluorophores, provide long-term stability and should have optimum O_2 permeability and

diffusion rate to achieve significant sensitivity. Silicone rubber is commonly used FDA approved polymer, but it has very high oxygen permeability. To obtain better sensitivity polystyrene (PS) is more suitable option due its lower oxygen diffusion. It can be used with fluorophore of higher quenching constant and provides wide dynamic range 0-21% of O_2 [16], [17].

Online monitoring of oxygen either in gas or dissolved in liquid requires luminescent material (oxygen sensitive probe or dye) should be firmly immobilized on a host material. There is a large number of optical oxygen sensors have been developed where polymers are used as a solid support material. Use of polymers as host material for biomedical applications, such as blood or skin oxygen monitoring, minimizes leaching of dye. In addition to that, use of polymer matrix provides microenvironment to reduce potential interferences with sample, selective permeation of oxygen while minimize permeation of other compounds like moisture, tune down oxygen permeability to obtain proper quenching constant (K_{sv}) [14].

There are three most common methods for immobilizing luminescent dye in a polymer host, shown in Figure 1.4. In Figure 1.4.(A) dye is homogeneously distributed in polymer matrix. It can be either dissolved or bonded covalently with polymer matrix. This is the easiest method, but leakage of dye depends on strength of interaction between the dye and host polymer. In Figure 1.4.(B) dye is adsorbed on particle (e.g. alumina, silica) surface followed by incorporation of such particles in polymer host materials, such as silicone rubber, polystyrene (PS), poly(methyl methacrylate) (PMMA) etc. This method minimizes aggregation of luminescent dye and hence self-quenching. It also reduces leakage of dye in contact with liquid sample. Finally, in Figure 1.4.(C)

luminescent dye is completely dissolved or absorbed (not surface adsorbed) in a polymeric particles, then the particles are incorporated in a different host polymer. This method helps in precise loading of dye, minimizes energy transfer between oxygen sensitive dye and reference dyes, reduces dye leakage, and gives flexibility in adopting more biocompatible host polymer [15].

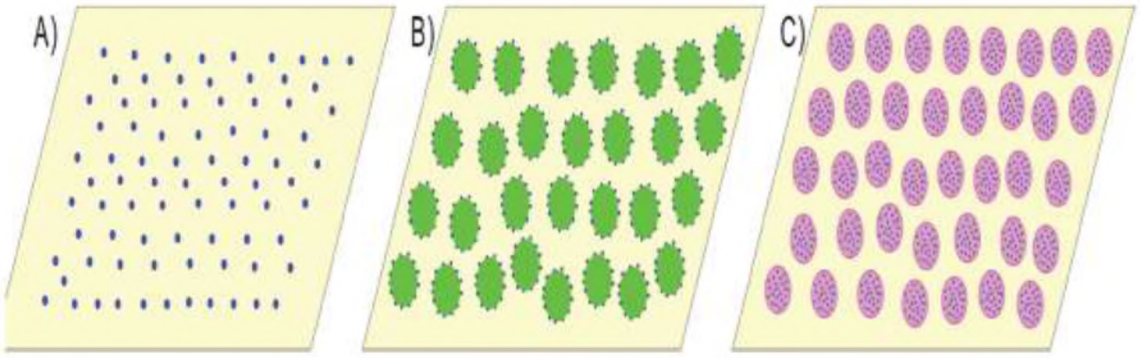

Figure 1.4. Most common methods for immobilizing oxygen sensitive probe in a polymer host [15].

Properties of these polymers required to match with an ideal host material: (1) host polymers and luminescent dyes are compatible to each other so that dyes remain inside the polymers without leaching or aggregation; (2) host polymers should be inert to dyes, so that intensity or lifetime of dyes does not altered by the host polymers; (3) polymers should be completely transparent, (4) oxygen permeability and diffusion rate should match with requirement for the sensors, (5) long-term stability, (6) biocompatibility for medical uses, etc. Permeability (P), solubility (S) and diffusion (D) of oxygen in a polymer matrix are related by the equation: P = S*D. Solubility of oxygen in polymer decreases with increase in temperature above glass transition temperature

(T_g). Diffusion rate increases with increase in temperature following Arrhenius law, but it is temperature independent for silicone polymer in the temperature range of 5 to 45 °C. Silicone rubber (poly(dimethyl siloxane) or PDMS) is the most extensively used FDA approved polymer for this purpose due to its very high oxygen permeability, excellent biocompatibility, high thermal and chemical stability, mechanical strength, optical transparency, low T_g (thus flexible at ambient temperature), etc. Diffusion coefficient of oxygen in PDMS is 0.115 cm^2 sec^{-1} and does not depend on the concentrations of oxygen and fluorophore in the ambient temperature and pressure range. Other polymers show much lower diffusion coefficient for oxygen in the range of 10^{-9} - 10^{-7} cm^2 sec^{-1}. For reduced oxygen permeability polystyrene (PS), poly(methyl methacrylate) (PMMA) are also used with high quenching coefficient probes for better sensitivity and high dynamic range. Poly(hydroxylethyl methacrylate), chitosan, polyurethane, poly(ethylene glycol) based hydrogels are also used to immobilize oxygen sensitive probes [14], [15].

1.3. SOY POLYOL-BASED RIGID POLYURETHANE FOAM

Polyurethane (PU) is a versatile material used in many different applications due to its wide range of stiffness, hardness, and densities. It was first discovered by Bayer and his coworkers in 1937, and then onwards it is widely used materials for a large variety of products [19]. PU foam is a commonly used material in construction, automobile and packaging industries due to its high strength to weight ratio and high thermal insulation properties. PU foam can be synthesized as both flexible and rigid foam depending on its density and cell size. Different types of PUs are result of different formulations and

fabrication methods. Rigid PU foam is about 23% of all types of PU production and is a versatile material with easily tunable properties [20], [21].

Recently environmental concerns triggered the challenge to replace petroleum-based products with renewable ones completely or at least partially while maintaining comparable properties. Bio-based polyurethane can be synthesized by replacing one of the reactants with renewable ones, such as petroleum-based polyol with bio-based polyol. Typically, most of the bio-polyols are produced from castor oil, soybean oil, sunflower oil, and rapeseed oil. Therefore, depending on the bio-based feedstock used, bio content of the polyurethane varies in a wide range [22]–[25].

1.3.1. Polyurethane Synthesis. Polyurethane is prepared by reacting diisocyanate with polyol, known as curing reaction, as shown in Equation (2). This is an exothermic reaction and follows second order kinetics, leads to the formation of urethane linkage spontaneously [26]. Water further reacts with isocyanate to release carbon dioxide, which blows out and leads to rise of foam. This is known as foaming process and shown in Equation (3). Two parts resin mixtures are used for PU foam synthesis. Component A is diisocyanate and component B is a mixture of polyol, catalyst, surfactant and water. Petroleum-based polymeric diphenyl methane diisocyanate (MDI) and polypropylene oxide (PPO) are commonly used precursor for commercially available PUs [22].

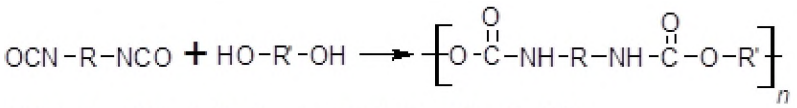

(2)

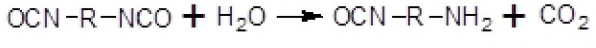

(3)

1.3.2. Polyol. Polyols are mainly of two types: polyether and polyester polyol. Polyol has multiple hydroxyl groups and their reactivity varies depending on position of

hydroxyl groups in the polyol chains. Primary hydroxyl groups react almost three times faster with isocyanate than the secondary hydroxyl groups [27]. Polyols are prepared from vegetables oil, which are essentially triglyceride, i.e. three fatty acids esterified with a glycerol backbone. Hydroformylation, ozonolysis, transesterification and epoxidation-hydroxylations are few reported methods for preparing polyols from vegetable oils [28], [29]. In most common practice, double bonds of these unsaturated fatty acids are usually subjected to epoxidation followed by ring opening to introduce hydroxyl groups, which serve as potential site for crosslinking reaction with isocyanate [30], as shown in Figure 1.5.

Soybean oil contains triglyceride of both saturated (~15%) and unsaturated (~80%) fatty acids. Dominant portion of all these unsaturated fatty acids are oleic acid (C18:1), linoleic acid (C18:2) and linolenic acid (C18:3), as shown in Figure 1.6 [31]. Usually soybean oil has ~4.6 double bonds per molecules and this unsaturation sites serve as reactive sites for polyol synthesis. If triglyceride structure remains unaltered during the polyol formation, it provides network structure making the polyurethane thermosetting in nature [32].

Properties of polyurethane are dependent on polyol functionalities, i.e., number of hydroxyl groups per molecule of polyol; and equivalent weight of polyol, which can be calculated using Equation (4). Polyol functionalities controls the final cross-link density in polyurethane. Polyols are usually characterized by acid number and reported in milligrams of KOH per gram of polyol as defined by Equation (5) [33], [34].

$$Equivalent\ weight\ of\ polyol = \frac{Molecular\ weight}{Functinality} \tag{4}$$

$$Hydroxyl\ Number = \frac{56.1 \times 1000}{Equivalent\ weight\ of\ polyol} (\text{mg KOH/g of polyol}) \tag{5}$$

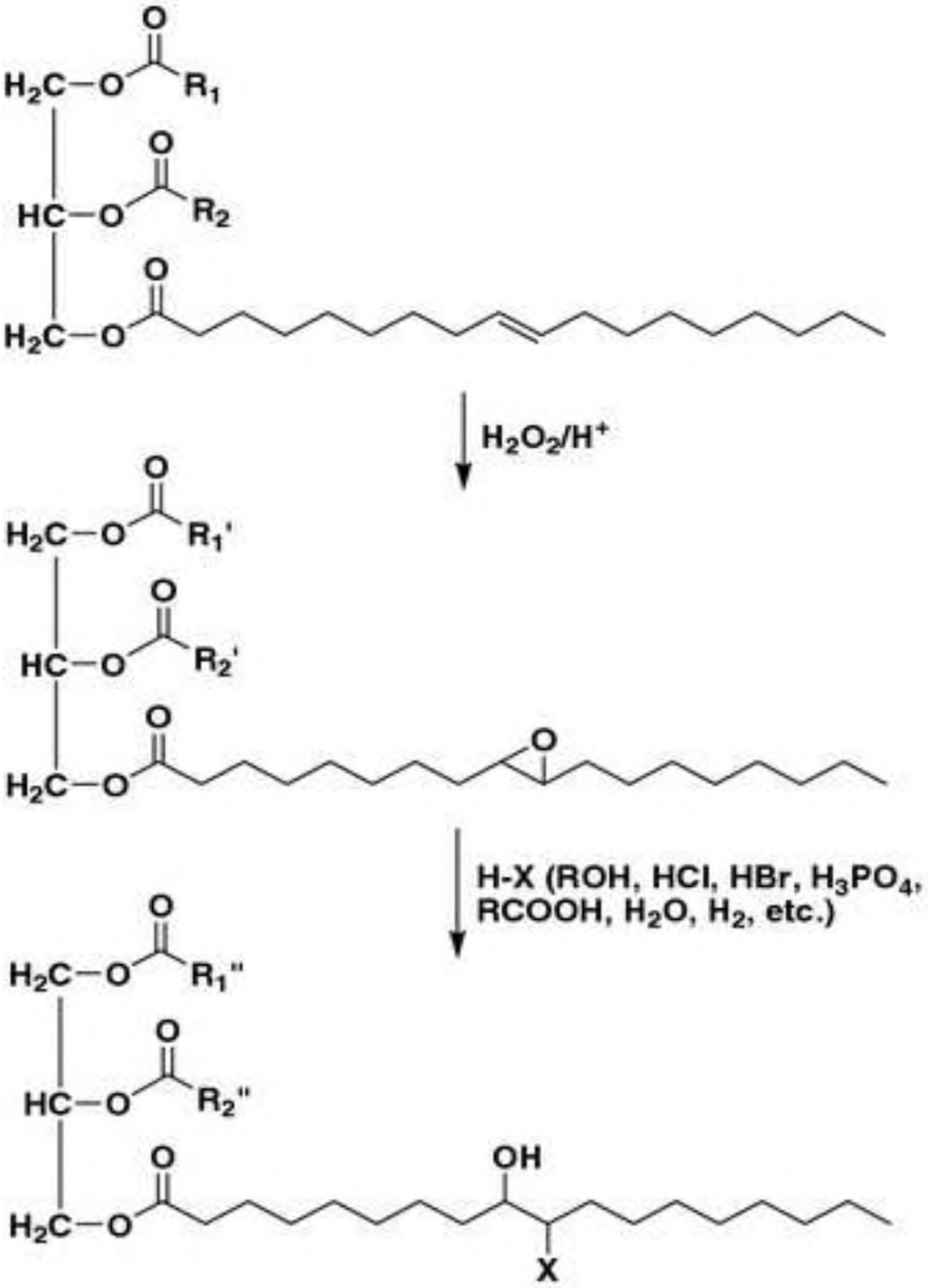

Figure 1.5. Epoxidation followed by ring opening of vegetable oil to obtain polyol [30].

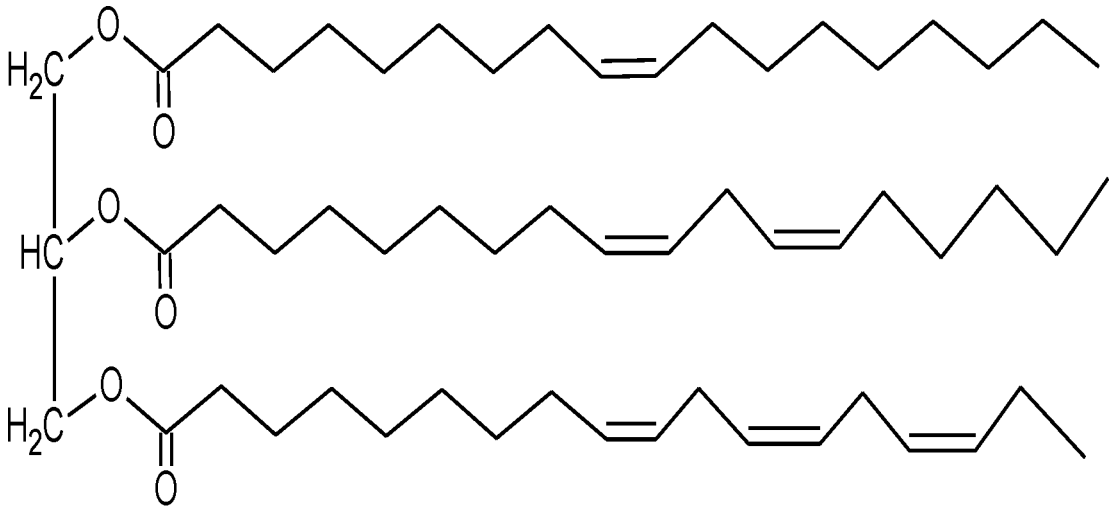

Figure 1.6. Structure of soybean oil.

1.3.3. Isocyanate. Isocyanate is another important component and its -NCO groups react with hydroxyl groups of both polyol and water to generate PU foam, as shown in Equation (2) and (3). Methylene diphenyl diisocyanate (MDI) and toluene diisocyanate (TDI) are two major kinds of aromatic isocyanates consumed globally to synthesize PU, shown in Figure 1.7. These two isocyanates and their derivatives are used for almost 95% of total PU production. All these isocyanates contain at least two -NCO groups per molecule. However, 4,4′ isomer of MDI is preferred for rigid PU production, since it has sterically free isocyanate groups compared to 2,4′ and 2,2′ isomers of MDI. In addition, -NCO groups of 4,4′ MDI are very reactive to polymerize and thus marketed as polymeric MDI (pMDI) blended with monomeric MDI. This also reduces its volatility and hence vapor pressure at ambient temperature, thus minimizes the toxicity problem. It also provides better dimensional stability including high compressive strength [35].

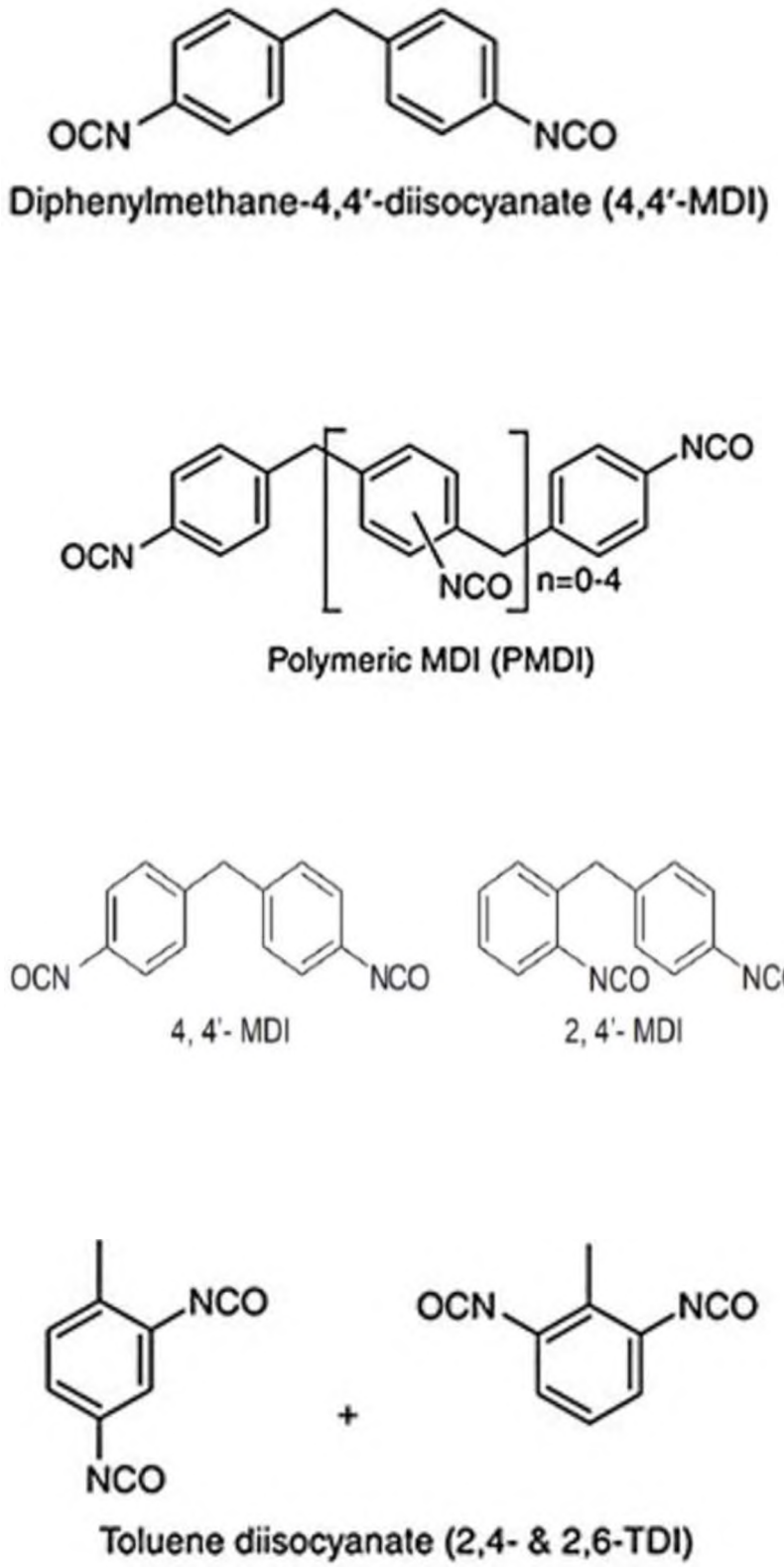

Figure 1.7. Structures of aromatic isocyanates [36].

Amount of isocyanate required for a particular PU formulation is calculated based on the isocyanate index, which is a stoichiometric ratio of moles of isocyanate groups to moles of hydroxyl groups. Properties of PU foam largely depend on isocyanate index used [34].

1.3.4. Blowing Agent. Polyurethane foam production requires a blowing agent to accomplish the foaming process, i.e., rise of the foam. Blowing agent can be of two types: physical blowing agents and chemical blowing agent. Pentane, chloroflurocarbons (CFC) and hydrochloroflurocarbons (HFC) are examples of physical blowing agents, which are low boiling non-reactive liquids and vaporize during the polymerization process. Use of CFC and HFC are forbidden now due to its deteriorating environmental impact. Water is the most commonly used chemical blowing agent. Water reacts with isocyanate and release carbon dioxide, which blows out and leads to rise of the foam, as shown in Equation 3. Water content in the foam formulation has high impact on foam density, and hence on the foam properties. High amount of water leads to higher rise of foam and thus foam volume will increase and so the cell size. But very high water content causes high number of open cell formation, which again adversely affects the desired properties of the rigid foam [37], [38].

1.3.5. Catalyst. Catalysts are often added to accelerate the reaction by reducing cream and gel time. Organo-tin catalysts are generally added to expedite the polymerization reaction and known as gelling catalyst. Sometimes tertiary amines are added to make the foaming process faster and known as blowing catalyst. Proper balance of these two types of catalysts controls the gelling and foaming process, which directly impact the ultimate foam properties [35], [39].

1.3.6. Surfactant. Surfactant plays an important role in mixing of the incompatible reagents. It acts as both emulsifier and foam stabilizer in the polyurethane foaming system. Silicone surfactants, which are commonly used for the foaming system, are non-ionic and non-hydrolysable. Molecular structure of these surfactants usually consists of a non-polar polydimethylsiloxane (PDMS) backbone and polar polyether (polyethylene oxide-co-propylene oxide) grafts, as shown in Figure 1.8. They promote the mixing process by minimizing the surface tension, which again controlled by the siloxane to polyether ratio and ethylene oxide to propylene oxide (EO/PO) ratio in the polyether grafts; represented by ratio of x to y and m to n respectively. During the foaming process surfactant molecules align along the air-polyol interface favoring the bubble generation and cell window stabilization. In absence of surfactants, cells start to coalesce causing complete collapse of foam structure. Surfactant with lower surface tension favors entrapment of high volume of air bubbles during mechanical mixing and these air nuclei slowly grows to form stable closed cells [40]–[42].

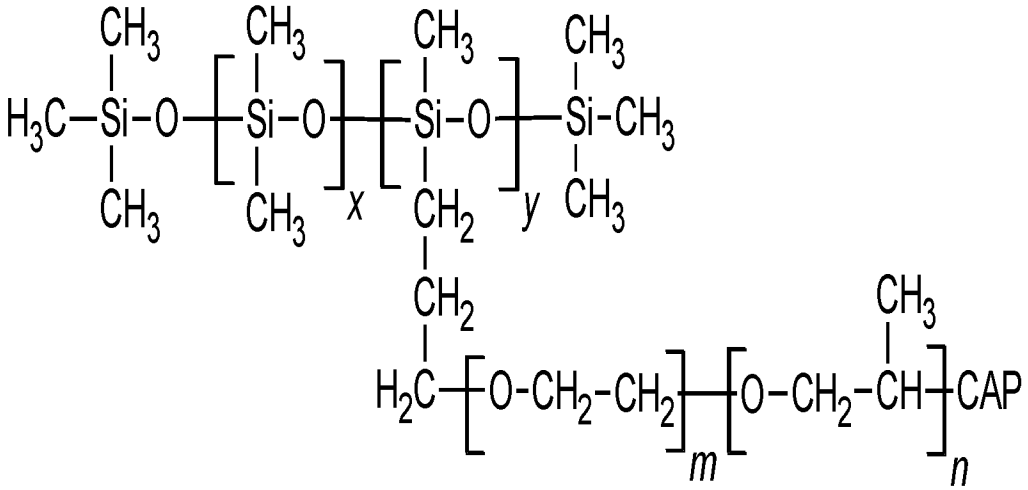

Figure 1.8. Structure of silicone surfactant.

1.4. ENVIRONMENTAL MONITORING OF VOLATILE ORGANIC COMPOUNDS DURING RECYCLING OF POLYMER-BASED MATERIALS USING PORTABLE GAS CHROMATOGRAPHY

Recycling of any polymeric materials, especially when they are subjected to high temperature processing, might be associated with potential environmental risk. For example, recycling of scrap tires as crumb rubber modifier mixed with asphalt pavement materials for road construction can be a suitable reuse of waste rubber. But its high temperature mixing process usually emits hazardous volatile organic compounds (VOCs), which have adverse effects on human health and are associated with potential environmental risk. Among VOCs, benzene, toluene, ethylbenzene and xylenes, named BTEX collectively, are highly carcinogenic chemicals [43], [44]. BTEX emission can also be from variety of materials like any petroleum products, paints, resins, synthetic rubbers, [45]–[47] etc. Therefore, BTEX emission needs to be monitored on-site to maintain healthy environment at the construction site. Gas chromatography (GC) is the most commonly used technique for this purpose [48]. Off-line methods utilize conventional benchtop GCs, but requires time consuming sample preparation step and careful preservation of volatile analytes [49]–[52]. Therefore, demand of on-site or on-line detection techniques are increasing continuously [53]. A light weight portable gas chromatography can be suitable choice for on-site monitoring of the toxic VOC emission during hot-mix asphalt processing containing crumb rubber modifier and used motor oil as processing aids [44], [54]–[56].

Gas chromatography is an analytical technique used for analysis of many small and volatile or semi-volatile compounds. Volatile or semi-volatile compounds are separated in GC based on their boiling points and eluted from GC at different times

detected by a suitable detector [57]. Portable or miniaturized GC consists of mainly four units: injection/sampling, preconcentration, separation and detection, as shown in Figure 1.9.

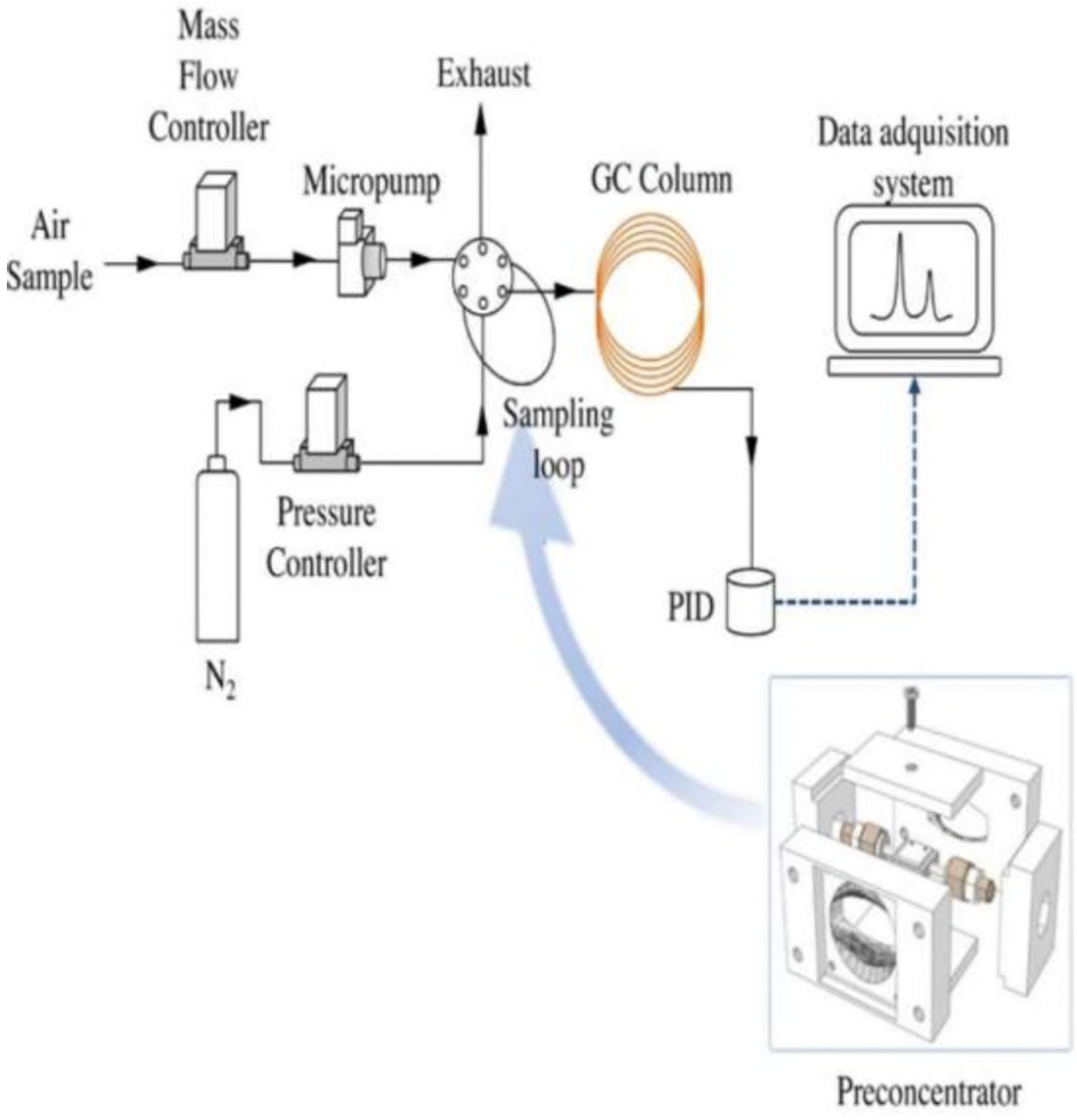

Figure 1.9. Schematic showing different components of a portable GC [58].

1.4.1. Injection. Usually two types of sampling systems are used for GC: (1) gas tight syringe and (2) six ports valve with a sampling loop, which is usually connected with an air pump. Gas tight syringe can be used for variable volume but more prone to error, whereas sampling loop is more accurate but of fixed volume, as shown in Figure 1.10. In loading position, sample flows through the loop to fill it completely. When valve is switched to inject position, carrier gas flows out the fixed volume of sample from the loop to the column [59].

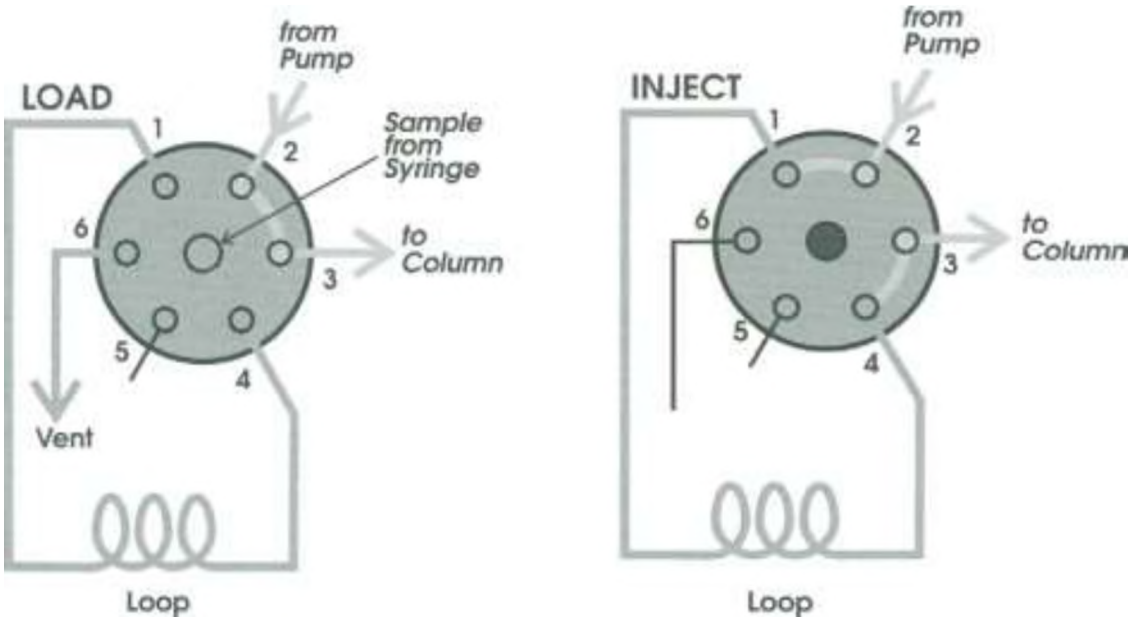

Figure 1.10. Schematic of six ports valve with a fixed sampling loop [60].

1.4.2. Preconcentration. Portable GCs are frequently employed for on-site environmental monitoring, which contain trace amounts of hazardous VOCs (in ppb level), needs some concentrating unit. Hence, most of the miniaturized GCs are attached with a preconcentrator, which is a concentrating device that improves the detection limits

of the trace chemicals significantly. Preconcentrator absorbs the analytes passed through until it gets saturated, then it desorbs the target analytes of high concentration upon heating, shown in Figure 1.11. Conventional preconcentrator is made of trap metal tube, but it is not convenient to use with portable GC since it requires high power due to its larger thermal mass. Other suitable alternative adsorbent materials are activated carbon, carbon nanotube, and molecularly imprinted polymer, etc. But any of these adsorbents should be optimized for selectivity, adsorption capacity, desorption efficiency, integrated cooler and heater for their best performance [46], [61]–[63].

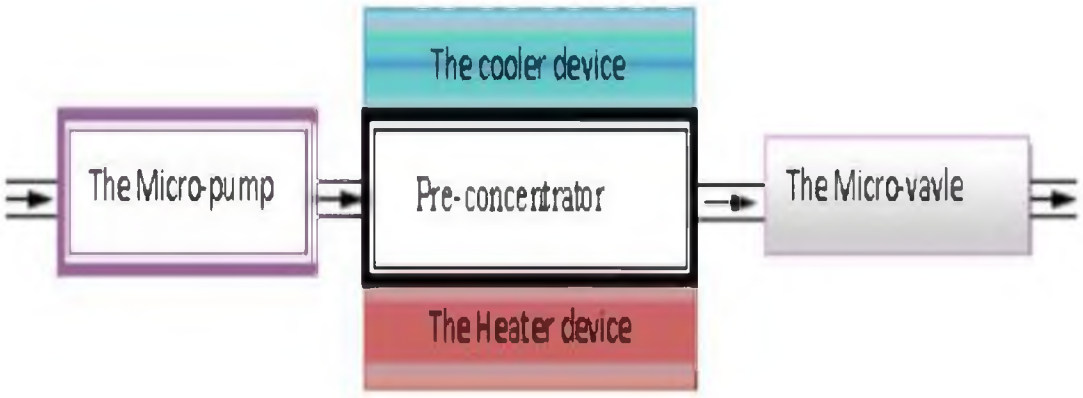

Figure 1.11. Schematic of typical preconcentrator [61].

1.4.3. Separation. Volatile or semi-volatile compounds are separated in GC based on their boiling points. Generally, desorbed analytes from preconcentrator entered the column followed by separation in column and finally eluted by mobile phase at different retention times. Separation takes place based on the affinity of the analytes towards the stationary phase coated on the inner wall of the column and boiling points of the analytes. Stronger interaction between the analyte vapor and coated liquid stationary phase leads to

longer retention time. Capillary column is preferred option for portable GC than packed column since it provides better separation efficiency and sensitivity. Capillary column is basically a fused silica capillary, whose inner wall coated mainly with methyl silicone or methyl phenyl silicone. Use of heated column can further increase the adaptability of this type of device for onsite analysis by providing usable retention time window. Helium or nitrogen is frequently used as mobile phase, they sometimes used as mini cartridge or refillable cylinders [59], [64].

1.4.4. Detection. Eluted compounds from GC column at different retention times transported to detectors. Flame ionization detector (FID), thermal conductivity detector (TCD), photo ionization detector (PID), mass spectroscopy (MS) are commonly used detectors with GC [52], [63], [65]–[68], etc. Most of these detectors such as FID, TCD or MS detector add up extra weight to the system and thus not advantageous for field-monitoring. PID is low-weight, compact, large linear range, highly sensitive and selective for organic compounds. UV lamp in PID provides high energy (~10.6 ev) photon, which can ionize small organic gas vapors of low ionization energy such as aromatic volatile compounds, such as BTEX compounds. Detector signal is equivalent to the current produced by the resulting ions [69], [70].

1.4.5. Sampling. Since portable GC does not have a heated injection port, therefore it requires injection of gaseous sample. Therefore, sample should be gas or vapor at room temperature. Calibration of the analytes can be performed using metal canister or sampling bags. Carrying metal canister onsite with portable GC again adds on extra weight. Use of plastic sampling bags of fixed volumes can be another convenient choice for this purpose. Commercially available standard gas mixtures can be used for

calibration or calibration standards can be prepared by injecting liquid aliquot of analyte mixtures in the bags followed by dilution with carefully measured volume of diluent gas, such as, air or nitrogen [59].

1.5. OBJECTIVES

The objectives of this research are as following:

1. Develop a printable optical oxygen sensor ink to fabricate smart bandage for non-invasive, rapid and sensitive measurement of two-dimensional surface oxygen content.
2. Synthesis of soy polyol-based rigid PU foam to fabricate structural insulated panel (SIP) for energy-efficient and modular building construction. And, to understand the effect of different additives, i.e., catalyst, blowing agent, surfactants, and polyol functionalities on foam properties.
3. Performance evaluation of a newly developed portable gas chromatography employed for environmental monitoring during hot-mix-asphalt processing.

PAPER

I. OPTICAL OXYGEN SENSOR PATCH PRINTED WITH POLYSTYRENE MICROPARTICLES-BASED INK ON FLEXIBLE SUBSTRATE

Mousumi Bose[a], Jason Hagerty[b, c], Jason Boes[a], Chang-Soo Kim[b], William Stoecker[c], Paul Nam[a]

[a]Department of Chemistry, [b]Department of Electrical and Computer Engineering, Missouri University of Science and Technology, Rolla, MO 65409, USA

[C]Stoecker & Associates Technology, Rolla, MO 65401, USA

ABSTRACT

Optical oxygen sensors based on luminescence quenching are gaining attention as a superior technology for continuous monitoring of oxygen in a growing number of applications. A simple and low-cost fabrication technique was developed to produce sensor arrays capable of two-dimensional oxygen tension measurement. Sensor patches were printed on polyvinylidene chloride film using an oxygen-sensitive ink cocktail, prepared by immobilizing Pt(II) meso-tetra(pentafluorophenyl)porphine (PtTFPP) in monodispersed polystyrene microparticles. The dispersion media of the ink cocktail, high molecular weight polyvinyl pyrrolidone suspended in 50% ethanol (v/v in water), allows adhesion promotion and compatibility with most common polymeric substrates. Ink phosphorescence intensity was found to vary primarily with fluorophore concentration and to a lesser extent with polystyrene particle size. The sensor performance was tested as a function of oxygen concentrations using two techniques, a multi-frequency phase

fluorometer and smart phone-based image acquisition. The printed sensor patch showed fast and repeatitive response over 0-21% oxygen concentrations with high linearity (with R^2>0.99) in a Stern-Volmer plot, and sensitivity of I_{N2}/I_{air}>1.5. The optical sensor response on a surface was investigated further using two-dimensional images which were captured and analyzed under different oxygen environment. Printed sensor patch along with imaging read-out technique make an ideal platform for early detection of surface wounds associated with tissue oxygen.

Keywords: Optical sensor; Sensor patch; Photoluminescence; RGB image; Ulcer

1. INTRODUCTION

Oxygen concentration is one the most crucial factors in medical diagnoses, industrial processes and environmental surveillance [1]–[6]. One exemplary area is the tissue oxygen monitoring to prevent ulcers caused by insufficient blood flow over a prolonged period that leads to ischemia and necrosis [7]. The multi-step wound healing process requires adequate oxygen supply at each step [8]. Since, oxygen cannot be stored in the cells, a constant supply of oxygen to the cells is necessary for wound healing as well as for the prevention of ulcer [9]. Hence, real-time monitoring of oxygen concentration is desirable [10].

The Clark electrochemistry-based method is the gold standard to measure partial pressure of oxygen (pO2) [11]. This method incorporates the reduction of oxygen at a platinum cathode under an applied potential of typically 0.7 V. The current generated is related to pO2. The major limitations of this method are that it consumes oxygen (which

can alter the real oxygen level), associated with errors due to interference of the magnetic field and other deposited elements on the electrode, allowing measurements in only a small area [12]. Other available non-invasive, 2D imaging techniques based on radioisotopes (e.g. positron emission tomography) and magnetic resonance (e.g. magnetic resonance oximetry) are expensive and limited to some medical applications [13].

Currently, optical oxygen sensing technology is gaining much attention due to its easy applicability, high sensitivity, and no oxygen consumption [14], [15]. Optical oxygen sensors can be classified based on two operating methods: absorption and luminescence quenching. The absorption method uses the contrast between oxygenated and deoxygenated hemoglobin and serves as the basis for pulse oximetry; this useful clinical tool is applicable for determination of the oxygen level in blood, not in tissue [16]. The photoluminescence detection method is a non-invasive, rapid, real-time, sensitive technique for direct quantitation of oxygen level allowing point measurement and 2D surface monitoring [17]. These attributes make it a desirable technique for wide variety of applications.

The photoluminescence-based optical sensor works through an energy exchange mechanism [13], [18]. Luminescent molecules are excited to a higher energy state on stimulation with light waves and emit light of a longer wavelength when they return to the ground energy state. Dynamic collisions of molecular oxygen with excited molecules quench the luminescent emission, resulting in diminished luminescent intensity. Dynamic quenching is completely reversible and follows the Stern-Volmer equation (Equation 1), where I0 and I are intensity of the fluorophore in absence and presence of oxygen

respectively, Ksv is the Stern-Volmer constant and PO2 represents the partial pressure of oxygen.

$$\frac{I_0}{I} = \frac{\tau_0}{\tau} = 1 + K_{SV} P_{O_2} \quad (1)$$

Metalloporphyrin-based fluorophores are popular due to their intense red phosphorescence with larger Stokes' shift, longer lifetimes, higher chemical stability, etc. Halogen substitution further improves photostability. Fluorine substituted Pt(II) porphyrin (PtTFPP) has become the most frequently used fluorophore for intensity-based sensing systems [19], [20].

Online monitoring of oxygen either in gas or dissolved in liquid requires fluorophores firmly immobilized on a host material. The host polymer should be compatible and inert to fluorophores, provide long-term stability, and have optimum oxygen permeability and diffusion rate to achieve significant sensitivity. Silicone rubber is a commonly used FDA-approved polymer, but it has very high oxygen permeability that leads to a narrow linear dynamic range [21], [22]. Recently, polystyrene particles are widely used as host material to monitor cell metabolism and transcutaneous wound healing status [2], [23], [24]. Polystyrene is an inert, biocompatible material with optimum oxygen permeability in the physiological range of pO_2 (0-21% oxygen), resulting in single exponential calibration curve with a single quenching constant [25], [26]. Dissolving the fluorophore in a polymer/solvent mixture is the most common method of immobilizing it. Sometimes fluorophore dyes are also encapsulated in polymer particles to minimize dye leaching [21]. Polystyrene particles can be synthesized in nano- to micro-particle size and subsequently, luminescent dyes can be immobilized on them utilizing surface adsorption technique [4], [14], [27].

In this work, we report a luminescent polystyrene microparticle-based novel printable optical oxygen sensor ink. Optimum ink composition was determined to prepare a non-invasive, rapid and cost-effective sensor patches to measure oxygen over a surface. The overall sensor performance was characterized with a fluorometer and a smart phone for comparison toward a goal of tissue oxygen monitoring that is the critical signature of early surface wound development such as in ulcers and the subsequent healing process.

2. MATERIALS AND METHODS

2.1. CHEMICALS

Styrene monomer (St, 99%), 2,2'-azobis(2-methylpropio nitrile) (AIBN, 98%) and two types of polyvinyl pyrrolidone (PVP) of molecular weight 360,000 and 40,000 were purchased from Sigma-Aldrich (St. Louis, MO, USA). The inhibitor from styrene was removed by passing it through the basic alumina column. Fluorophore Pt(II) meso-tetra (pentafluorophenyl)porphine (PtTFPP) was procured from Frontier Scientific (Logan, UT, USA). Solvents like tetrahydrofuran (99.9%) and toluene (99.5%) were obtained from Fischer Scientific (Pittsburgh, PA, USA) and ethyl alcohol (99.5%) from Acros Organics (Belgium, WI, USA). Polyvinylidene chloride film (PVDC, thickness 0.033 mm) was purchased from Goodfellow (Coraopolis, PA, USA).

2.2. SYNTHESIS OF POLYSTYRENE MICROPARTICLES

Polystyrene microparticles were prepared using the free radical dispersion polymerization technique. The dispersing agent was prepared in a 3-neck round bottom flask by dissolving 300 mg of PVP (MW 40,000, 5 wt% of styrene) in 12 mL ultrapure

water. 60 mg of AIBN (1 wt% of styrene) was dissolved in 6 g of purified styrene, and 38 mL of ethanol was then poured into the flask. The mixture was stirred at 70 °C for 24 h and after polymerization a white suspension was formed. The suspension was centrifuged at 5000 rpm for 15 min, the supernatant was discarded, and the suspension was washed twice. The particle size was measured using Zetasizer (Malvern Panalytical, Nano ZS90). Polystyrene particles were also synthesized using 450 mg and 600 mg of PVP (7.5 and 10 wt% of styrene) respectively to evaluate the effect of dispersing agent on particle size. Solid particles were suspended in ethanol and particle concentration in the suspension was estimated after drying small portions under vacuum for 24 h.

2.3. PREPARATION OF LUMINESCENCE PRINTING INK

The oxygen-sensitive dye was first encapsulated in polystyrene particles. The suspension containing 100 mg PS particles was centrifuged and re-suspended in 5 mL of 50% ethanol (v/v in water). 1 mg of PtTFPP dye dissolved in 400 μL of THF was added to the mixture and vortexed for 1 min to allow the absorption of dye on the particles. This diffusion and entrapment method allows water-insoluble dyes to diffuse into the polymer matrix and get entrapped in the PS particles [23], [28]. Then the mixture was centrifuged, and the supernatant was discarded. The resultant dyed particles were again suspended in 50% ethanol and fluorescence scans were performed using a Fluoroscence Spectroscope FS5 (Edinburgh Instruments Ltd.).

Printing ink was prepared by suspending dyed PS particles in suitable suspending media i.e., 50% ethanol containing 1 wt% PVP (MW 360,000). In the ink cocktail, PVP plays a dual role: dispersing agent in the liquid phase as well as adhesion promoter for the

PS particles after the ink dries on the printed surface. To evaluate the effect of particle size on intensity, 1 mg dye was loaded in 100 mg PS particles of three different sizes and suspended in 3 mL of suspending solution. To obtain maximum intensity as well as homogeneity of the patch, the dyed polystyrene particle concentration was varied in the ink cocktail. For this purpose 1 mg dye was loaded in 100 mg of PS particles (~1 μm size) and then PtTFPP/PS particles were suspended in 5 ml, 4 ml, 3 ml and 2 ml of suspending media respectively to increase the dye concentration from 0.2 to 0.5 mg/mL of the ink. For both above studies, 10 μL of the ink cocktail was deposited on PVDC film and luminescence intensity of the dried patches was compared.

2.4. PRINTING OF SENSOR PATCH

Initially, a single dot sensor patch was fabricated by manual deposition of 10 μL of ink cocktail on PVDC film and allowed it to dry in a dark place. A sensor patch with an array of sensor dots was also printed on PVDC film using an automated micro-dispensing system suitable for particle-based ink. In the current study, a prototype printer was built using a Nordson EFD (www.nordson.com/, Westlake, Ohio, USA) automated droplet deposition system attached with an AxiDraw V3 2.5D Plotter (www.evilmadscientist.com/, Sunnyvale, California, USA) and a house-built platform, shown in Figure 1. The printer was a low-volume precision dispensing device operated by simple laboratory-scale pneumatic pressure. Size of the printed sensor dots was effectively controlled by dispensed volume of the ink and by means of the needle gauge attached to the printing head as well as the pneumatic pressure utilized. For potential self-calibration, five sensor dots were printed on the opposite side of the film (Figure 2(a))

arranged in a quincunx pattern and always exposed to air, i.e., 21% oxygen to serve as visual reference sensors [29]. These reference sensors will be utilized for compensating the intensity change overtime for long-term application.

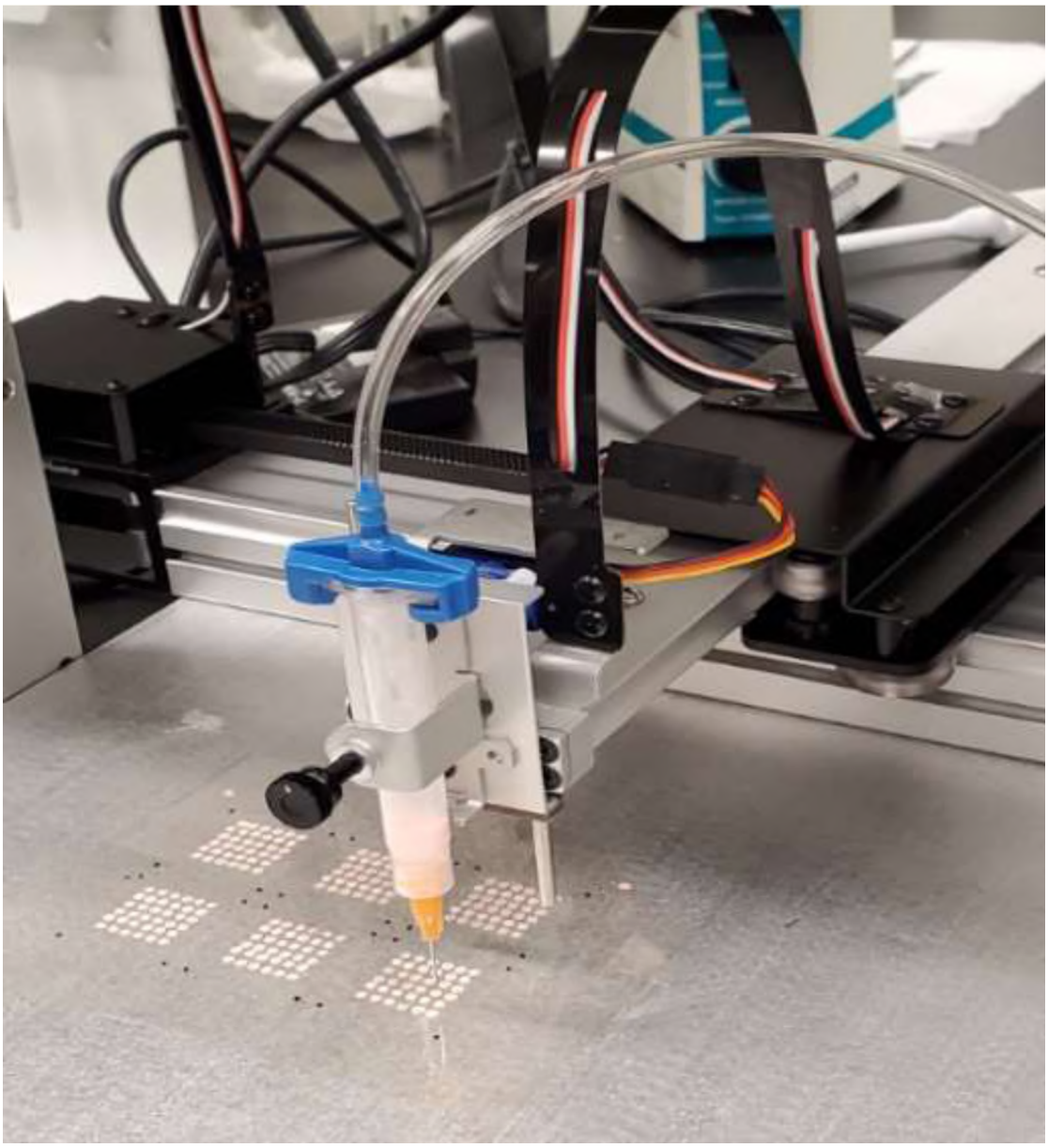

Figure 1. Prototype of printing device.

2.5. SENSOR FILM READOUT TECHNIQUES

The luminescence response of the single-dot sensor patch was measured at different oxygen concentrations in gas phase by a multi-frequency phase fluorometer (MFPF 100, Tau Theta Instruments/Ocean Optics, Inc. www.oceanoptics.com) attached with a built-in 470 nm LED for excitation.

An alternate image acquisition technique was also employed to determine luminescence response from the sensor array using a consumer-grade Android smart phone [30]. The sensor patch was illuminated using 24 405 nm LEDs arranged in a circular layout, magnified using a 10x macro lens assembly and passed through a high pass optical filter with a cut-on wavelength of 600 nm. The entire assembly was externally attached to the smart phone, as shown in Figure 2(b). The 405 nm LEDs were chosen as they have the ideal wavelength to excite the maximum luminescence response. Figure 3(a) to (c) show the luminescence response captured by the smart phone and saved in RAW format. RAW is the industry standard format for serializing image sensor data, i.e., as close as to the silicon sensor response as possible. Typically, the only processing of the sensor data would be based on the Bayer filter, which was used to decode sensor data to RGB image data. The images were further processed using MATLAB® to obtain the luminescence sensor response.

For both the techniques, sensor patches were attached in a calibration chamber, as shown in Figure 2(a). Pure nitrogen and oxygen gases were used, and flow rates were controlled by two mass flow controllers to achieve required oxygen concentration in the chamber. Phosphorescence intensity under different oxygen concentrations (0-21%) were measured and the Stern-Volmer plots were established.

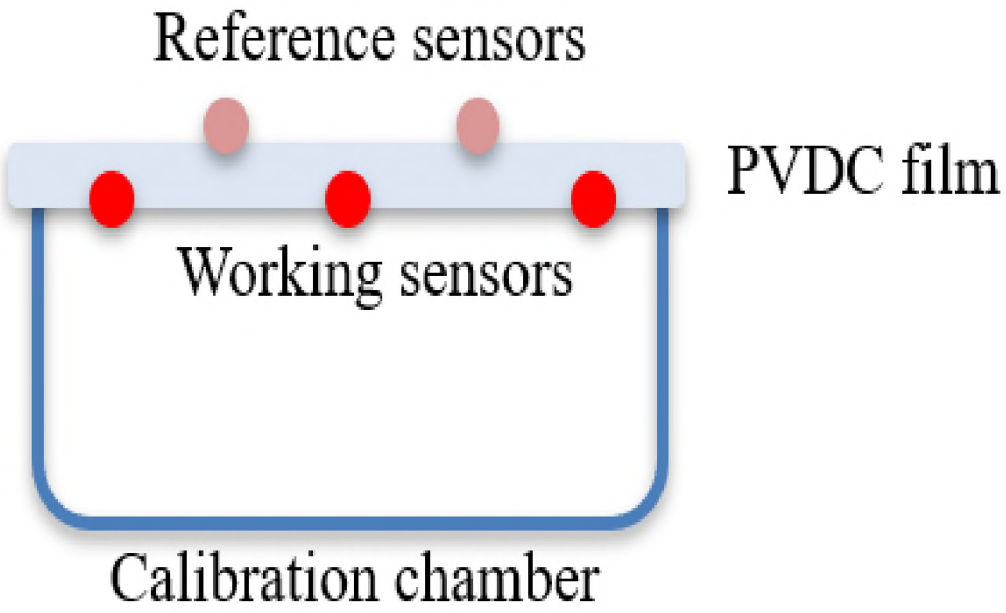

a

b

Figure 2. (a) Schematic of sensor patch attached with calibration chamber and (b) camera setup used for imaging.

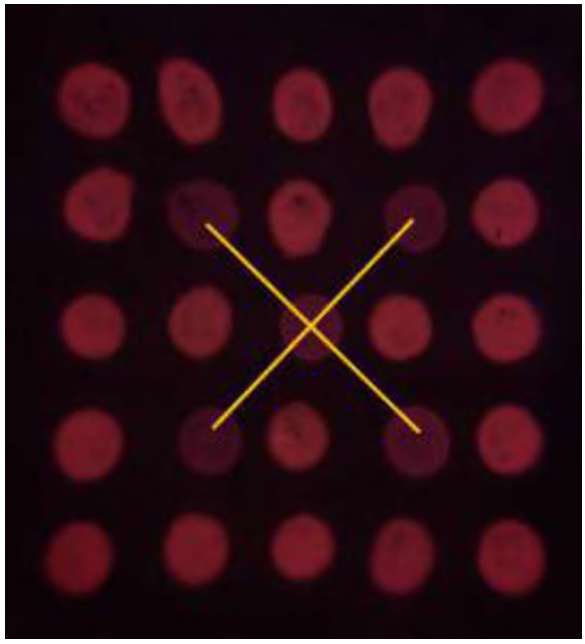

a

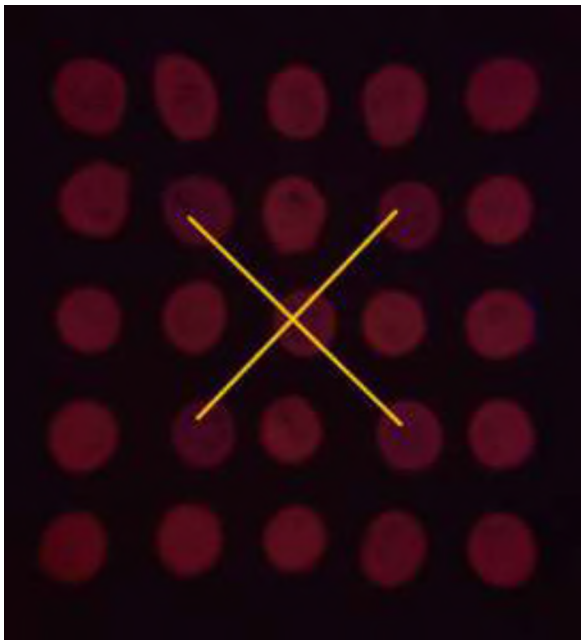

b

Figure 3. Representative images captured using a smart phone to capture the printed sensor patch with reference sensors arranged in a quincunx pattern exposed to air and working sensors exposed to (a) 0%, (b) 4% and (c) 12% oxygen respectively.

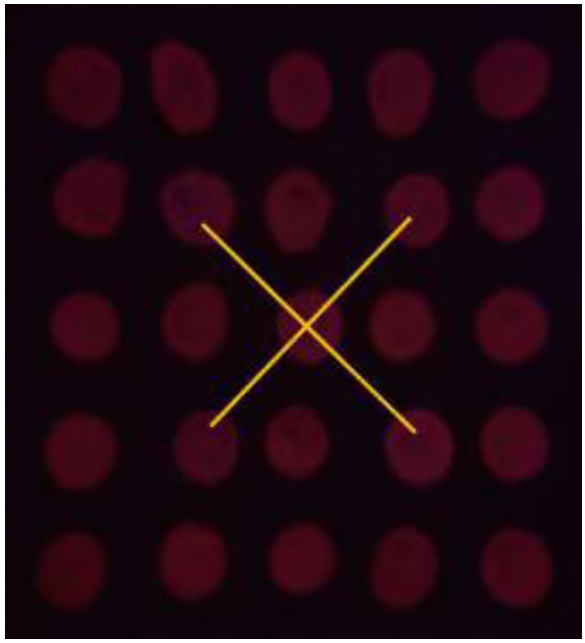

c

Figure 3. Representative images captured using a smart phone to capture the printed sensor patch with reference sensors arranged in a quincunx pattern exposed to air and working sensors exposed to (a) 0%, (b) 4% and (c) 12% oxygen respectively (cont.).

3. RESULTS AND DISCUSSION

3.1. EFFECT OF DISPERSING AGENT ON POLYSTYRENE PARTICLE SIZE

During dispersion polymerization, polystyrene particle size can be controlled by the amount of initiator, monomer, steric stabilizer, and polarity of the reaction media [31]. In this work, particle size was varied by choosing the steric stabilizer amount to alter the reaction condition. Polyvinyl pyrrolidone (PVP) proved to be a suitable steric stabilizer for dispersion polymerization [32]. Figure 4(a) shows the variation of polystyrene particle size with PVP-to-styrene-monomer ratio in the reaction vessel. Resultant polystyrene particles were of three different sizes ranging from ~0.4 to 1.0 μm.

PVP stabilizes polystyrene latex by adsorbing on the particle surface; therefore, average particle size reduces gradually with increasing PVP content. For a lower PVP amount, small polystyrene particles might be generated initially, which aggregate later on to yield larger particles [33]. Size distribution of these three types of particles is shown in Figure 4(b), which demonstrates that a narrow distribution resulted from lower particle size.

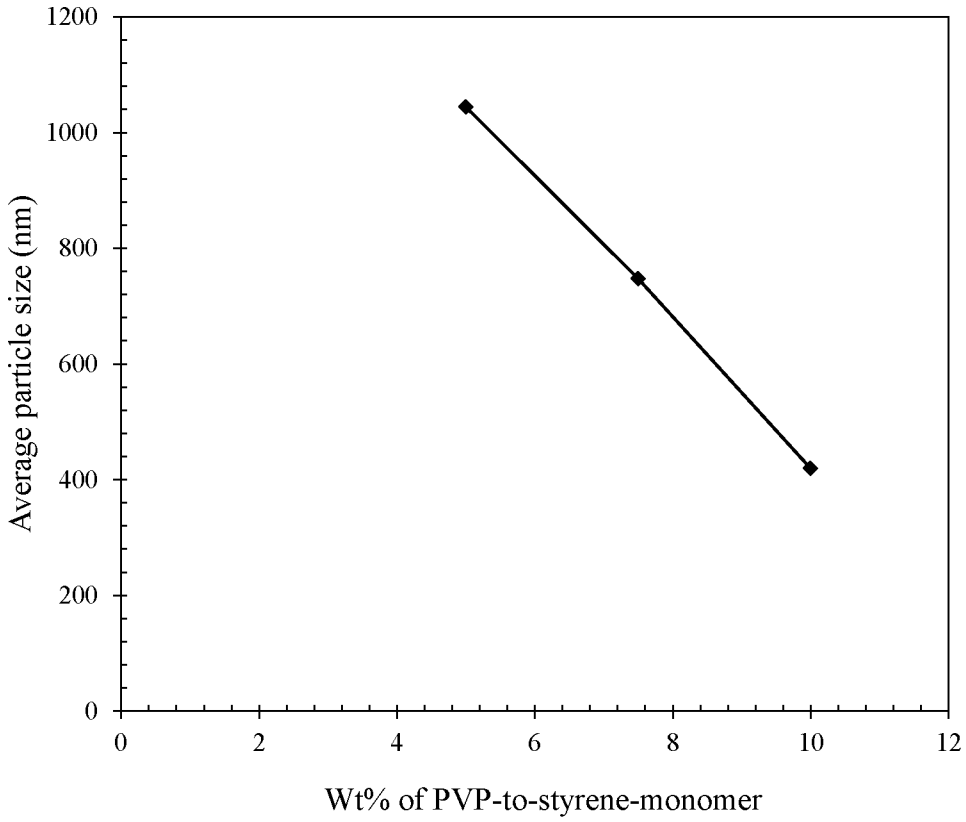

a

Figure 4. (a) Variation of particle size with PVP-to-styrene-monomer ratio and (b) size distribution for three types of polystyrene particles.

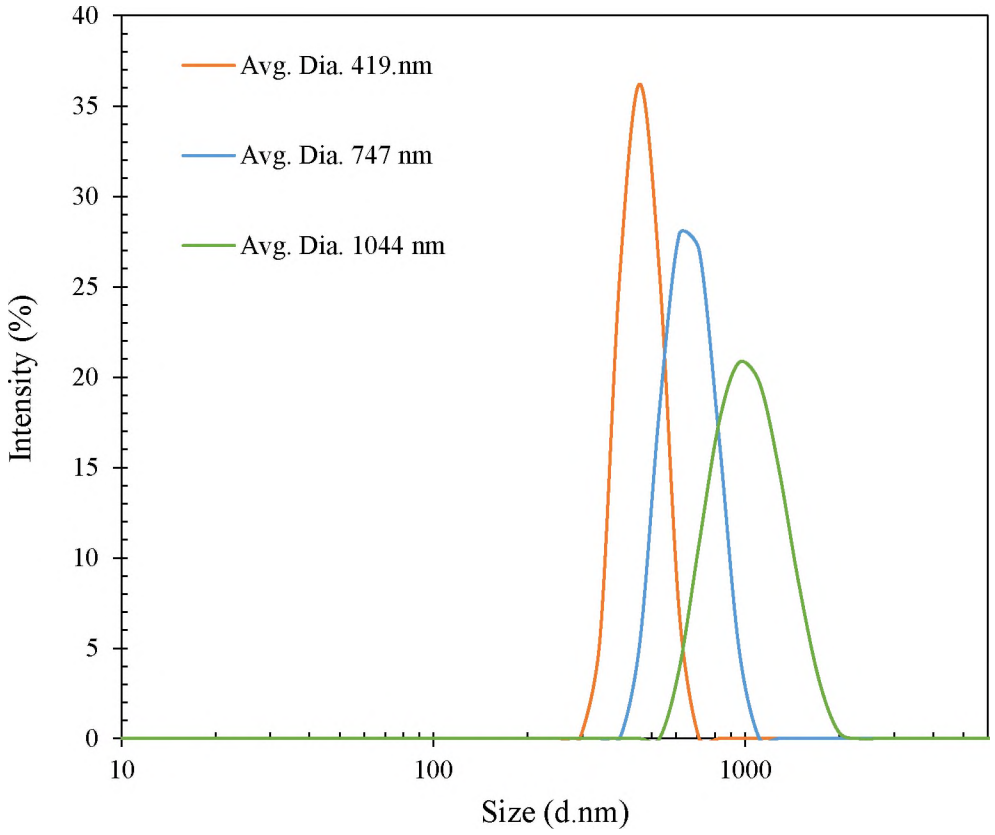

b

Figure 4. (a) Variation of particle size with PVP-to-styrene-monomer ratio and (b) size distribution for three types of polystyrene particles (cont.).

3.2. CHARACTERIZATION OF DYE-LOADED POLYSTYRENE PARTICLES

The dye diffusion and entrapment method allows homogenous distribution of fluorophore into the polystyrene particles without forming any covalent bond on its surface. Figure 5(a) and (b) show the normalized absorption and emission spectra of the PtTFPP dye and dye encapsulated in PS (PtTFPP/PS) particles respectively suspended in 50% ethanol. To minimize the scattering effect from the suspended particles, cuvettes were placed at 45^0 inclined position in the cuvette holder of the Fluoroscence

Spectroscope FS5. Furthermore, spectra for the PtTFPP/PS particle suspension were plotted after subtracting blank PS particle spectra from them to remove the effect of scattering. Figure 5(a) shows that PtTFPP dye has a Soret band at 394 nm followed by two Q bands at 508 nm and 540 nm, respectively. PtTFPP has emission maxima at 650 nm, as seen in Figure 5(b). Absorption and emission maxima for PtTFPP/PS particles were similar to those of the PtTFPP dye alone, which signifies that adsorption of PtTFPP on the PS particles surface did not alter the luminescence characteristics of the fluorophore.

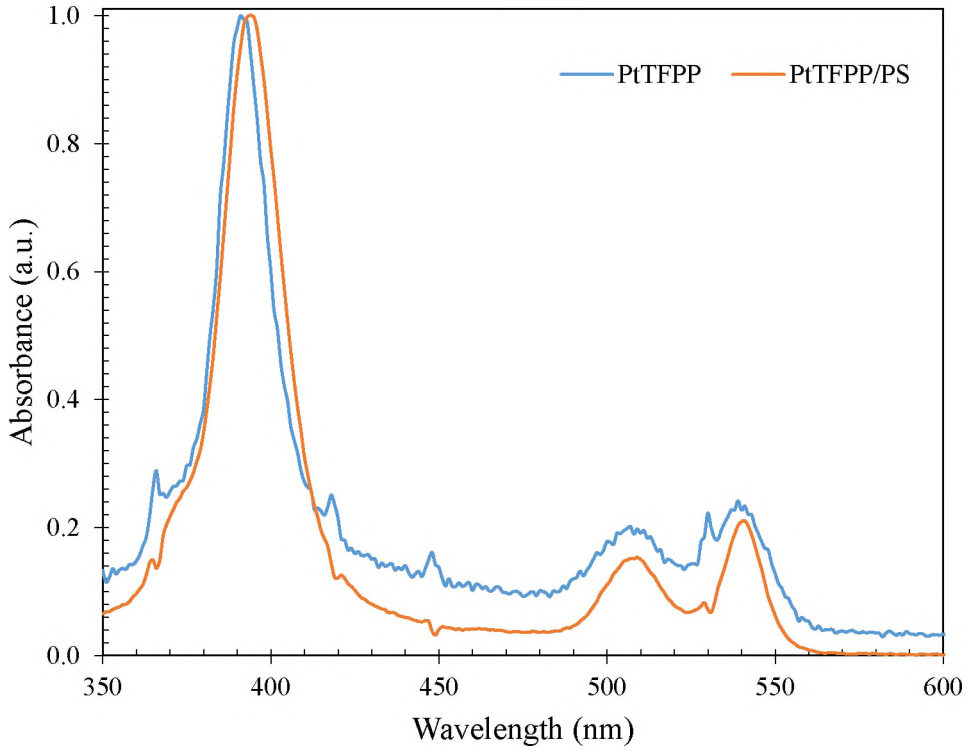

a

Figure 5. (a) Absorption and (b) emission scan of PtTFPP dye and PtTFPP/PS particle suspension.

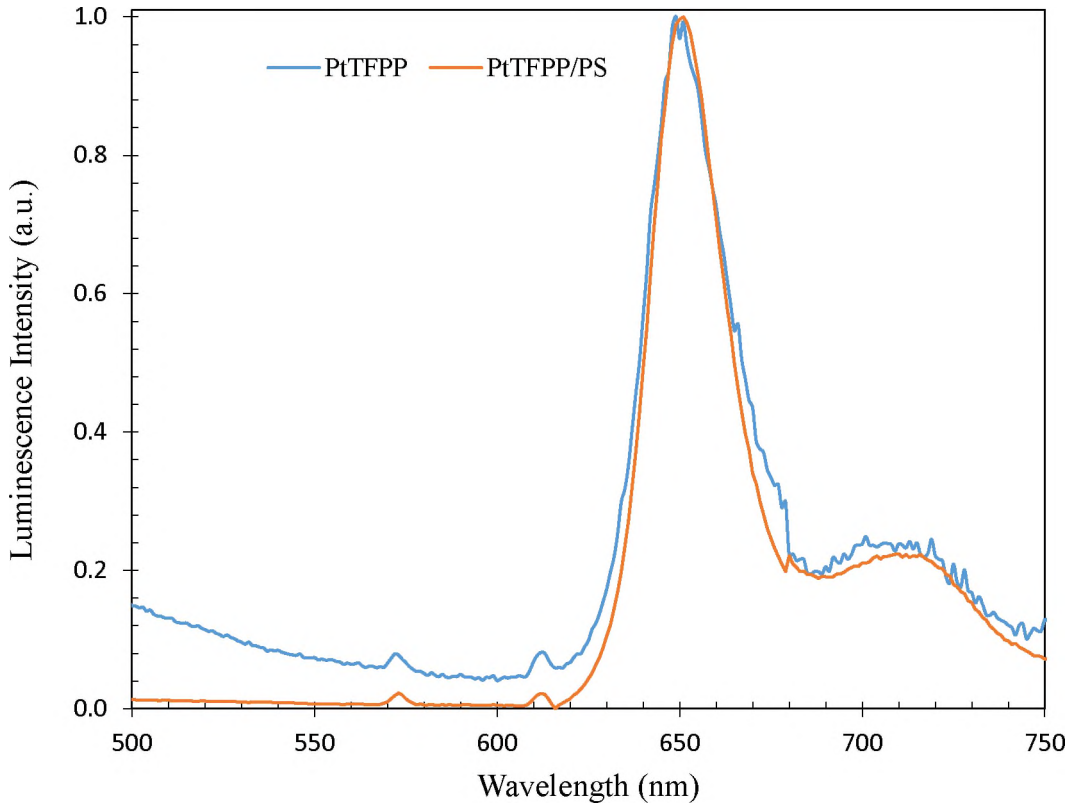

b

Figure 5. (a) Absorption and (b) emission scan of PtTFPP dye and PtTFPP/PS particle suspension (cont.).

3.3. DEPENDENCE OF LUMINESCENCE INTENSITY ON POLYSTYRENE PARTICLE SIZE AND DYE CONCENTRATION

Three types of inks prepared with three different sizes of PS particles were tested for particle size-luminescence intensity correlation. Figure 6(a) represents the fluorescence intensity of the sensor patches measured with MFPF 100; showing that intensity increased somewhat with particle size in both 0% and 21% oxygen environments without altering the sensor performance. This might be due to increased cross section with larger particle size, which leads to more fluorophore being excited.

Our findings are in agreement with previous studies. Konemann *et al.* also reported an increase in fluorescence intensity with PS particle size on a single-particle scale and found that dry vs. wet state did not alter the intensity of dyed particles significantly [34]. According to Hill *et al.* [35] and Sivaprakasam *et al.* [36], fluorescence intensity of bioaerosol also increases with cross sectional area, and hence with particle size. It was found that sensitivity (I0/I21) of the sensors was not altered significantly with particle size, as also reported by Im *et al.* [31]. ~1 μm sized particles emitted maximum fluorescence intensity while maintaining overall homogeneity of the sensor patch.

To determine the fluorophore concentration suitable for optimum intensity, it was varied from 0.2 to 0.5 mg/mL in the ink cocktails, and respective sensor patches were tested with MFPF 100. Figure 6(b) shows the intensity of those patches measured at 0% and 21% oxygen concentrations. Intensity increased linearly with dye concentrations up to 0.33 mg/mL and then leveled off for further higher concentrations, which might be due to self-quenching of the fluorophore. So, 0.33 mg/mL was considered to be optimum dye concentration.

3.4. OXYGEN SENSING PERFORMANCE

Figure 7(a) shows the phosphorescence intensity emitted by single sensor dots when excited with 470 nm light at different oxygen concentration, measured with MFPF 100. Phosphorescence intensity decreased significantly with increase in oxygen concentration. Figure 7(b) represents the Stern-Volmer plot established for the same.

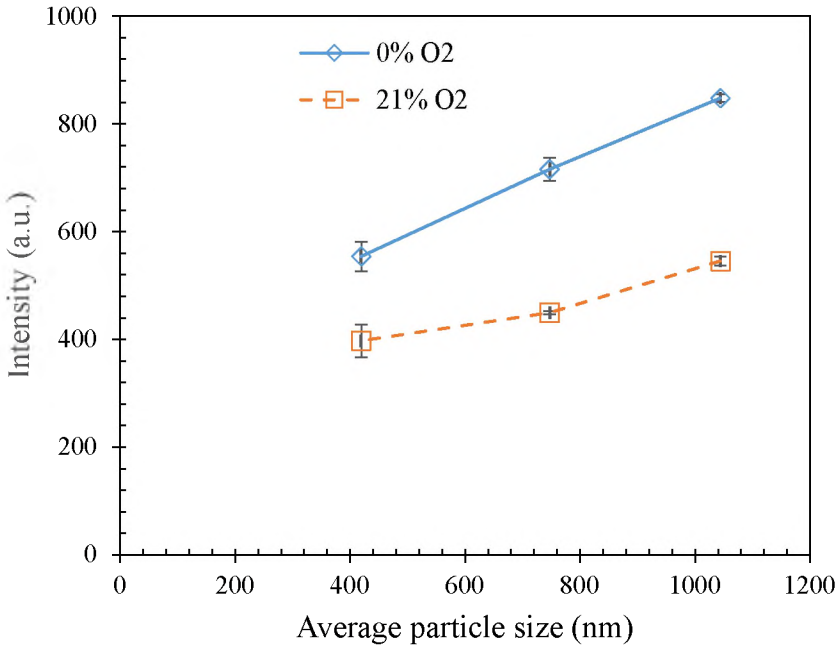

a

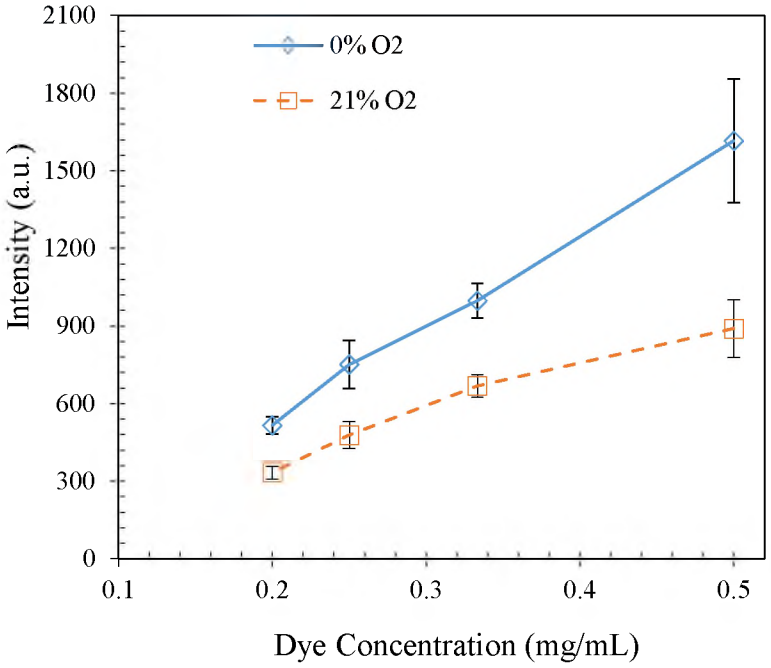

b

Figure 6. Variation of luminescence intensity of sensor patch with (a) polystyrene particle size and (b) dye concentration.

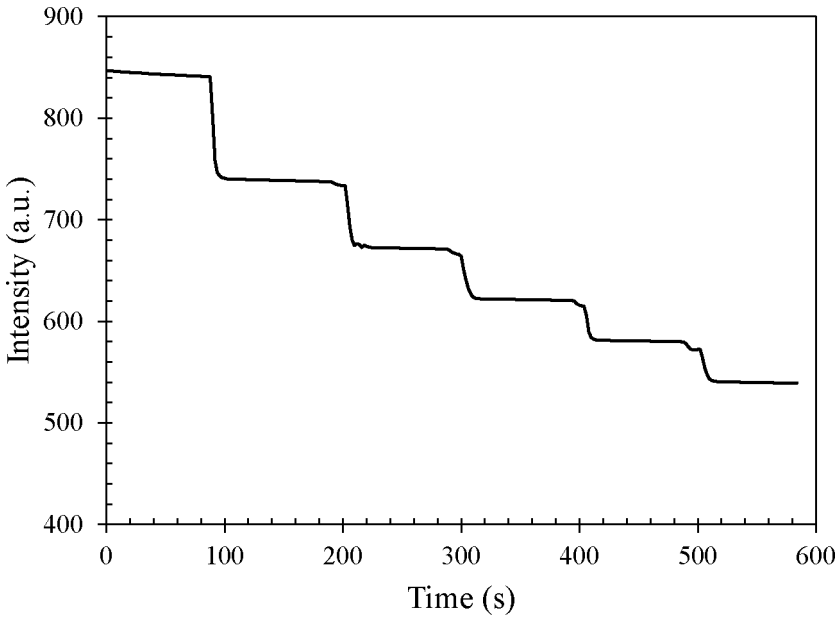

a

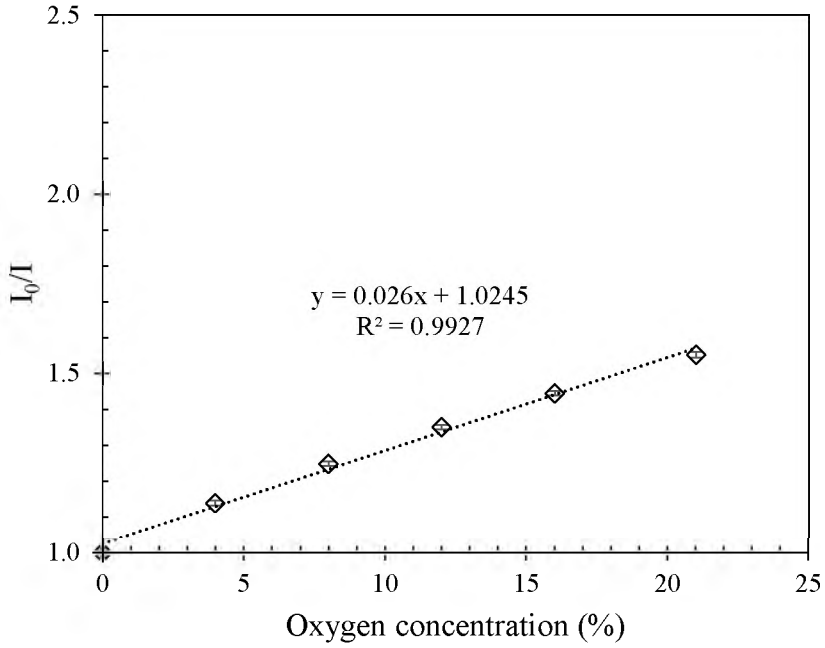

b

Figure 7. (a) Luminescence intensity and (b) Stern-Volmer plot of single sensor dot measured using MFPF 100 at 0, 4, 8, 12, 16 and 21% oxygen concentration using 470 nm excitation.

Figure 8 shows the Stern-Volmer plot for an array of sensors excited with 405 nm light and phosphorescence intensity measured using the image acquisition technique. Each datapoint represents the average of all working sensors in a respective image. Both read-out techniques reported linear response up to 21% oxygen, suitable for most of the common clinical and environmental applications.

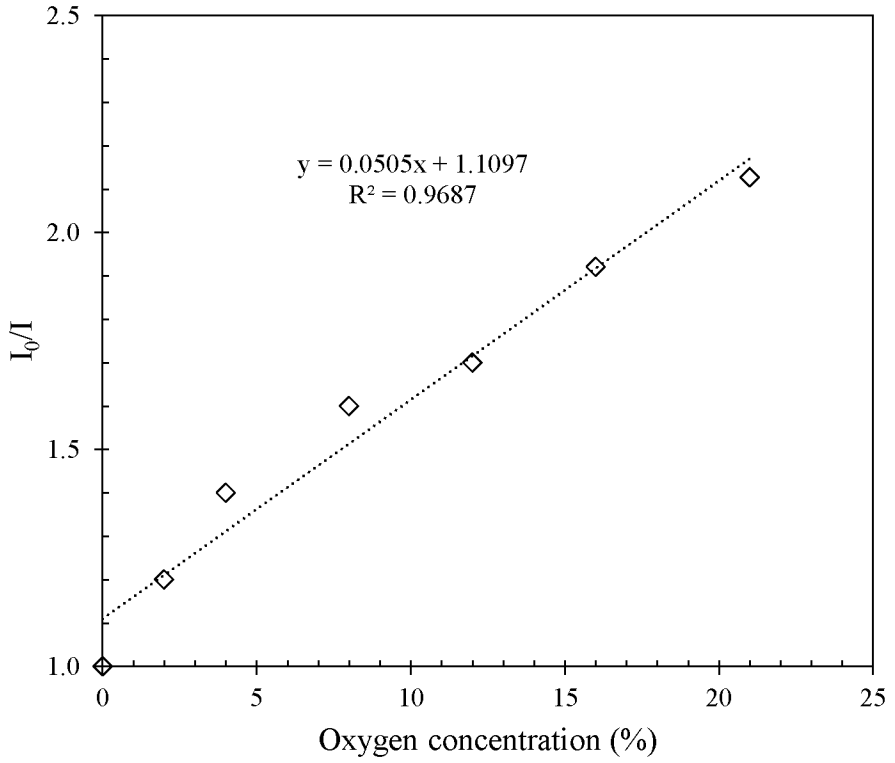

Figure 8. Stern-Volmer plot for sensor array measured using the image acquisition technique excited with 405 nm light.

I_0/I_{21} was used as the measure of sensor sensitivity, where I_0 and I_{21} represents the phosphorescence intensity of the sensors exposed to 0% and 21% oxygen respectively. Sensitivity between 0-21% obtained for the sensor array was 2.13, which was higher than

the sensitivity of single sensor dots, i.e., 1.55. This lower sensitivity was expected since sensor dots were excited with 470 nm light (the only wavelength available from MFPF), whereas the sensor array was illuminated with 405 nm light, which is much closer to the Soret band of the PtTFPP dye. The sensor response was very fast and reproducible with relative standard deviation of less than 1.5%.

Figure 9 represents the operational stability of the sensor patch excited with 470 nm light. It was observed that the sensor response was very stable and reproducible when switching between fully oxygenated to fully deoxygenated atmosphere.

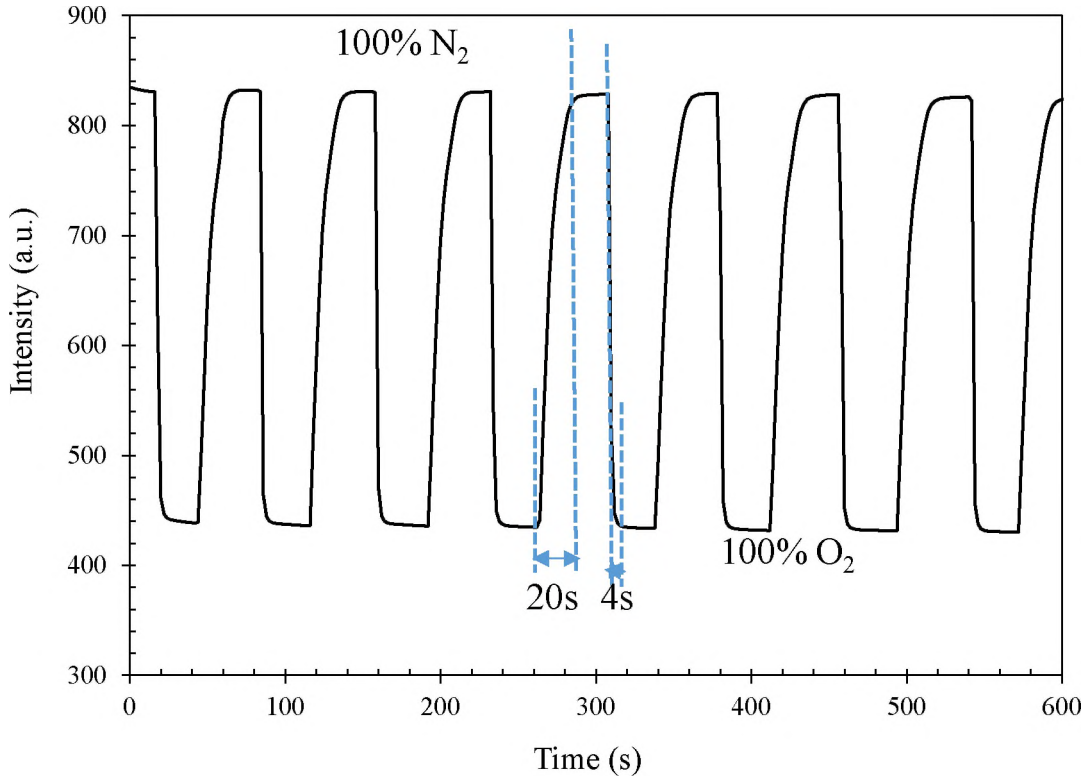

Figure 9. Operational stability and response time of the sensor patch when switching alternately between 100% nitrogen and 100% oxygen environment.

Response time and recovery time of the sensor were evaluated based on t_{95} i.e. time required to achieve 95% of the total intensity change when switching between oxygen and nitrogen environments [14], [15]. Response time of the sensor to fully oxygenated condition was 4 s, whereas recovery time to fully deoxygenated condition was 20 s. The short response time makes it suitable for rapid detection of gaseous oxygen concentration in many practical applications.

4. CONCLUSIONS

An optical oxygen sensor patch was fabricated using a PtTFPP fluorophore immobilized in polystyrene microparticle-based ink. Polystyrene particle size and its distribution were decreased with higher amount of low molecular weight polyvinyl pyrrolidone, which served as a steric stabilizer in polymerization of styrene. Phosphorescence intensity was found to be increased with fluorophore concentration and polystyrene particle size without any notable change of the sensor performance. A prototype printing technique was developed suitable to print particle-based ink. An Android smart phone-based image acquisition technique was also established to quantify the phosphorescence intensity response as a function of oxygen concentration.

Printed sensor patches along with imaging read-out technique made the system suitable for simple, cost-effective monitoring of oxygen on a surface. Wide dynamic linear range (0-21% oxygen) of the sensors covers the physiological range. Future research will determine potential usefulness of the sensor patches in clinical applications.

It is expected that the proposed sensor is an ideal platform for early detection and timely intervention of surface wounds associated with tissue oxygen.

ACKNOWLEDGEMENTS

This work was supported in part by the National Institutes of Health (NIH) under Grant STTR 1R41NR018126-01 of the NIH. Its contents are solely the responsibility of the authors and do not necessarily represent the official views of the NIH.

REFERENCES

[1] M.A. Regan, R.W. Teasell, D.L. Wolfe, D. Keast, W.B. Mortenson, J.A.L. Aubut, A systematic review of therapeutic interventions for pressure ulcers after spinal cord injury, Arch. Phys. Med. Rehabil. 90 (2009) 213–231.

[2] S. Schreml, R.J. Meier, O.S. Wolfbeis, T. Maisch, R.-M. Szeimies, M. Landthaler, J. Regensburger, F. Santarelli, I. Klimant, P. Babilas, 2D luminescence imaging of physiological wound oxygenation, Exp. Dermatol. 20 (2011) 550–554.

[3] X.-H. Wang, H.-S. Peng, L. Yang, F.-T. You, F. Teng, L.-L. Hou, O.S. Wolfbeis, Targetable phosphorescent oxygen nanosensors for the assessment of tumor mitochondrial dysfunction by monitoring the respiratory activity, Angew. Chemie Int. Ed. 53 (2014) 12471–12475.

[4] J. Napp, T. Behnke, L. Fischer, C. Würth, M. Wottawa, D.M. Katschinski, F. Alves, U. Resch-Genger, M. Schäferling, Targeted luminescent near-infrared polymer-nanoprobes for in vivo imaging of tumor hypoxia, Anal. Chem. 83 (2011) 9039–9046.

[5] M. Fitzgerald, D.B. Papkovsky, M. Smiddy, J.P. Kerry, C.K. O'Sullivan, D.J. Buckley, G.G. Guilbault, Nondestructive monitoring of oxygen profiles in packaged foods using phase-fluorimetric oxygen sensor, J. Food Sci. 66 (2001) 105–110.

[6] C. McDonagh, C. Kolle, A.K. McEvoy, D.L. Dowling, A.A. Cafolla, S.J. Cullen, B.D. MacCraith, Phase fluorometric dissolved oxygen sensor, Sensors Actuators B Chem. 74 (2001) 124–130.

[7] J. Azimian, N. Dehghan Nayeri, E. Pourkhaleghi, M. Ansari, Transdermal wound oxygen therapy on pressure ulcer healing: a single-blind multi-center randomized controlled trial, Iran. Red Crescent Med. J. 17 (2015) e20211.

[8] S. Schreml, R.M. Szeimies, L. Prantl, S. Karrer, M. Landthaler, P. Babilas, Oxygen in acute and chronic wound healing, Br. J. Dermatol. 163 (2010) 257–268.

[9] C.K. Sen, Wound healing essentials: let there be oxygen, Wound Repair Regen. 17 (2009) 1–18. https://doi.org/10.1111/j.1524-475X.2008.00436.x.

[10] Z. Li, E. Roussakis, P.G.L. Koolen, A.M.S. Ibrahim, K. Kim, L.F. Rose, J. Wu, A.J. Nichols, Y. Baek, R. Birngruber, G. Apiou-Sbirlea, R. Matyal, T. Huang, R. Chan, S.J. Lin, C.L. Evans, Non-invasive transdermal two-dimensional mapping of cutaneous oxygenation with a rapid-drying liquid bandage, Biomed. Opt. Express. 5 (2014) 3748–3764. https://doi.org/10.1364/BOE.5.003748.

[11] L.C. Clark, R. Wolf, D. Granger, Z. Taylor, Continuous recording of blood oxygen tensions by polarography, J. Appl. Physiol. 6 (1953) 189–193. https://doi.org/10.1152/jappl.1953.6.3.189.

[12] O.S. Wolfbeis, Luminescent sensing and imaging of oxygen: fierce competition to the Clark electrode, Bioessays. 37 (2015) 921–928. https://doi.org/10.1002/bies.201500002.

[13] E. Roussakis, Z. Li, A.J. Nichols, C.L. Evans, Oxygen-sensing methods in biomedicine from the macroscale to the microscale, Angew. Chemie Int. Ed. 54 (2015) 8340–8362. https://doi.org/10.1002/anie.201410646.

[14] L. Liang, G. Li, Z. Mei, J. Shi, Y. Mao, T. Pan, C. Liao, J. Zhang, Y. Tian, Preparation and application of ratiometric polystyrene-based microspheres as oxygen sensors, Anal. Chim. Acta. 1030 (2018) 194–201. https://doi.org/https://doi.org/10.1016/j.aca.2018.05.017.

[15] C.-S. Chu, Optical fiber oxygen sensor based on Pd(II) complex embedded in sol–gel matrix, J. Lumin. 135 (2013) 5–9. https://doi.org/https://doi.org/10.1016/j.jlumin.2012.10.006.

[16] J.E. Sinex, Pulse oximetry: principles and limitations, Am. J. Emerg. Med. 17 (1999) 59–66. https://doi.org/https://doi.org/10.1016/S0735-6757(99)90019-0.

[17] S. Medina-Rodríguez, M. Marín-Suárez, J.F. Fernández-Sánchez, Á. de la Torre-Vega, E. Baranoff, A. Fernández-Gutiérrez, High performance optical sensing nanocomposites for low and ultra-low oxygen concentrations using phase-shift measurements, Analyst. 138 (2013) 4607–4617. https://doi.org/10.1039/C3AN00239J.

[18] W.L. Rumsey, J.M. Vanderkooi, D.F. Wilson, Imaging of phosphorescence: a novel method for measuring oxygen distribution in perfused tissue, Science (80-.). 241 (1988) 1649–1651. https://doi.org/10.1126/science.3420417.

[19] M. Quaranta, S.M. Borisov, I. Klimant, Indicators for optical oxygen sensors, Bioanal. Rev. 4 (2012) 115–157. https://doi.org/10.1007/s12566-012-0032-y.

[20] Y. Mao, Y. Gao, S. Wu, S. Wu, J. Shi, B. Zhou, Y. Tian, Highly enhanced sensitivity of optical oxygen sensors using microstructured PtTFPP/PDMS-pillar arrays sensing layer, Sensors Actuators B Chem. 251 (2017) 495–502. https://doi.org/https://doi.org/10.1016/j.snb.2017.05.081.

[21] X. Wang, O.S. Wolfbeis, Optical methods for sensing and imaging oxygen: materials, spectroscopies and applications, Chem. Soc. Rev. 43 (2014) 3666–3761. https://doi.org/10.1039/C4CS00039K.

[22] B. Adhikari, S. Majumdar, Polymers in sensor applications, Prog. Polym. Sci. 29 (2004) 699–766. https://doi.org/https://doi.org/10.1016/j.progpolymsci.2004.03.002.

[23] E. Schmälzlin, J.T. van Dongen, I. Klimant, B. Marmodée, M. Steup, J. Fisahn, P. Geigenberger, H.-G. Löhmannsröben, An optical multifrequency phase-modulation method using microbeads for measuring intracellular oxygen concentrations in plants, Biophys. J. 89 (2005) 1339–1345. https://doi.org/10.1529/biophysj.105.063453.

[24] E. Schmälzlin, B. Walz, I. Klimant, B. Schewe, H.-G. Löhmannsröben, Monitoring hormone-induced oxygen consumption in the salivary glands of the blowfly, Calliphora vicina, by use of luminescent microbeads, Sensors Actuators B Chem. 119 (2006) 251–254. https://doi.org/https://doi.org/10.1016/j.snb.2005.12.024.

[25] D.B. Papkovsky, G. V Ponomarev, W. Trettnak, P. O'Leary, Phosphorescent complexes of porphyrin ketones: optical properties and application to oxygen sensing, Anal. Chem. 67 (1995) 4112–4117. https://doi.org/10.1021/ac00118a013.

[26] S.-K. Lee, I. Okura, Photostable optical oxygen sensing material: platinum tetrakis(pentafluorophenyl)porphyrin immobilized in polystyrene, Anal. Commun. 34 (1997) 185–188. https://doi.org/10.1039/A701130J.

[27] T. Behnke, C. Würth, K. Hoffmann, M. Hübner, U. Panne, U. Resch-Genger, Encapsulation of hydrophobic dyes in polystyrene micro- and nanoparticles via swelling procedures, J. Fluoresc. 21 (2011) 937–944. https://doi.org/10.1007/s10895-010-0632-2.

[28] E. Eftekhari, I.S. Cole, Q. Li, The effect of fluorophore incorporation on fluorescence enhancement in colloidal photonic crystals, Phys. Chem. Chem. Phys. 18 (2016) 1743–1749. https://doi.org/10.1039/C5CP06489A.

[29] A.J. Palma, J. López-González, L.J. Asensio, M.D. Fernández-Ramos, L.F. Capitán-Vallvey, Open air calibration with temperature compensation of a luminescence quenching-based oxygen sensor for portable instrumentation, Anal. Chem. 79 (2007) 3173–3179. https://doi.org/10.1021/ac062246d.

[30] N. López-Ruiz et al., "Determination of O2 using colour sensing from image processing with mobile devices," Sensors Actuators B Chem., vol. 171–172, pp. 938–945, 2012, doi: https://doi.org/10.1016/j.snb.2012.06.007.

[31] S.H. Im, G.E. Khalil, J. Callis, B.H. Ahn, M. Gouterman, Y. Xia, Synthesis of polystyrene beads loaded with dual luminophors for self-referenced oxygen sensing, Talanta. 67 (2005) 492—497. https://doi.org/10.1016/j.talanta.2005.06.046.

[32] A.J. Paine, W. Luymes, J. McNulty, Dispersion polymerization of styrene in polar solvents. 6. Influence of reaction parameters on particle size and molecular weight in poly(N-vinylpyrrolidone)-stabilized reactions, Macromolecules. 23 (1990) 3104–3109. https://doi.org/10.1021/ma00214a012.

[33] Y.-S. Cho, C.H. Shin, S. Han, Dispersion polymerization of polystyrene particles using alcohol as reaction medium, Nanoscale Res. Lett. 11 (2016) 46. https://doi.org/10.1186/s11671-016-1261-8.

[34] T. Könemann, N.J. Savage, J.A. Huffman, C. Pöhlker, Characterization of steady-state fluorescence properties of polystyrene latex spheres using off- and online spectroscopic methods, Atmos. Meas. Tech. 11 (2018) 3987–4003. https://doi.org/10.5194/amt-11-3987-2018.

[35] S.C. Hill, C.C. Williamson, D.C. Doughty, Y.-L. Pan, J.L. Santarpia, H.H. Hill, Size-dependent fluorescence of bioaerosols: Mathematical model using fluorescing and absorbing molecules in bacteria, J. Quant. Spectrosc. Radiat. Transf. 157 (2015) 54–70. https://doi.org/https://doi.org/10.1016/j.jqsrt.2015.01.011.

[36] V. Sivaprakasam, H.-B. Lin, A.L. Huston, J.D. Eversole, Spectral characterization of biological aerosol particles using two-wavelength excited laser-induced fluorescence and elastic scattering measurements, Opt. Express. 19 (2011) 6191–6208.

II. ROLE OF ADDITIVES IN FABRICATION OF SOY-BASED RIGID POLYURETHANE FOAM FOR STRUCTURAL AND THERMAL INSULATION APPLICATIONS

Mousumi Bose[a], Gurjot Dhaliwal[b], K. Chandrashekhara[c], Paul Nam[a]

[a] Department of Chemistry, Missouri University of Science and Technology, Rolla, MO, 65409, USA

[b] Intertribal Research and Resource Center, United Tribes Technical College, Bismarck, ND, 58504, USA

[c] Department of Mechanical and Aerospace Engineering, Missouri University of Science and Technology, Rolla, MO, 65409, USA

ABSTRACT

Recently environmental concerns triggered the challenge to replace petroleum-based products with renewable ones completely or at least partially while maintaining comparable properties. Herein, rigid polyurethane foams were prepared using soy-based polyol for thermal insulation applications. Cell size, density, thermal resistivity and compression force deflection (CFD) values were evaluated and compared with that of petroleum-based polyurethane foam Baydur 683. The role of different additives, i.e., catalyst, blowing agent, surfactants, and different functionalities of polyol on determining these foam properties were also investigated. For this study, dibutyltin dilaurate (DBTL) was employed as catalyst and water was used as environment friendly blowing agent. Their competitive effect on density and cell size of the foams were evaluated. Five different silicone-based surfactants were employed to study the effect of surface tension on cell size of foam. It was also found that 5g of surfactant per 100g of polyol

demonstrated minimum surface tension and highest thermal resistivity (R value: 26.11 m.K/W). However, CFD values were compromised for higher surfactant loading. Additionally, blending of 5g of higher functionality soy-based polyol improved the CFD values to 328.19 kpa, comparable to that of petroleum-based foam Baydur 683.

1. INTRODUCTION

Polyurethane (PU) foam is widely used material in construction, automobile and packaging industries due to its high strength to weight ratio and high thermal insulation property. It can be synthesized as both flexible and rigid foam depending on its density and cell size. Rigid PU foam is about 23% of all types of PU production and is a versatile material with easily tunable properties [1], [2]. Polyurethane foams are usually synthesized by reacting diisocyanate with polyol in presence of catalyst, blowing agent and surfactant to achieve the desired morphology. Foam properties are direct consequence of its chemical structure and cross-link density. Both functionalities of isocyanate and hydroxyl number of polyol can alter the cross-link density of polymer network, and higher number of functionalities lead to more rigid structure [3]. Petroleum-based polymeric diphenyl methane diisocyanate (MDI) and polypropylene oxide (PPO) are commonly used precursor for commercially available PU [4]. There is a recent urge to replace petroleum-based products with environment-friendly renewable ones. Current approach to achieve this goal is to replace the conventional polyol with renewable polyols derived from different vegetable oils such as castor oil, safflower oil, palm oil, rapeseed oil and soybean oil [4]–[7]. Only castor oil shows reactivity towards isocyanate

as it contains ~90% of ricinoleic acid with secondary hydroxyl group attached to it [8]. Other vegetable oils must be modified to incorporate enough hydroxyl groups in the carbon chains, necessary to react with isocyanate groups. Hydroformylation, ozonolysis, transesterification and epoxidation-hydroxylations are the most commonly reported methods for preparing polyols from vegetable oils [9], [10].

The major challenges in synthesizing vegetable oil-based PU foams are to achieve mechanical and thermal properties comparable to that of commercial petroleum-based foam. Guo et al. prepared soybean oil-based rigid polyurethane foam cross-linked with glycerin and reported comparable compressive strength and thermal insulation with that of petroleum-based PU foams [4]. Hu et al. synthesized rigid polyurethane foam using rape seed oil-based polyol and the foams found to have relatively low compression strength compared to the petroleum-based foam. They reported this polyol started to solidify after one month of storage due to extensive hydrogen bonding and also exhibited slower reaction rate with isocyanate due to presence of secondary hydroxyl groups [6]. Javni et al. reported vegetable oil-based polyurethane exhibited higher initial thermal stability (below 10% weight loss during thermogravimetric analysis) in air compared to PPO-based [7]. Tu et al. compared fifty vegetable oil-based polyols to substitute 50% of petroleum-based polyol and found soybean oil-based polyol substituted foam has better compressive strength and thermal resistivity than only petroleum-based foam [11]. Rigid PU foam containing 20-30% of soy-based polyol reported in literature with thermal conductivity (0.022-0.026 w/mK) and compressive strength (15-20 psi), in the range of commercial PUs [12].

Soybean oil is an environment friendly, renewable material combined with high stability and relatively low price. It has triglyceride structure containing both saturated (~15%) and unsaturated (~80%) fatty acids [13]. Usually soybean oil has ~4.6 double bonds per molecules and this unsaturation sites serve as reactive sites for polyol synthesis [14]. Introduced hydroxyl groups are mainly secondary in nature, which reacts slowly with isocyanate groups. Primary hydroxyl groups react almost three times faster with phenyl isocyanate than the secondary hydroxyl groups [15]. Polarity of soy-based polyols is much less compared to the petroleum based one. The hydrophobicity of such polyols increases thermal and weather stability of soy-based polyurethanes [16].

Different additives such as catalyst, water, surfactant etc. control the reaction rate, cross-link density, cell size, close to open cell ratio; thus, have great influence on density, morphology, mechanical and thermal properties of the foams. Previous studies have shown feasibility for synthesis of soy-based polyurethane foams, but there is still challenge remaining to evaluate proper formulation for fabrication of such PUs commercially with adequate properties. In this current study, soy based rigid polyurethane foam was synthesized, and their structural, thermal and mechanical properties were compared with that of petroleum-based rigid commercial foam. The focus of this work was to understand the effect of chemistry of different additives in determining the foam properties.

2. EXPERIMENTALS

2.1. MATERIALS

Diisocyanate was obtained as a blend of diphenylmethane diisocyanate (MDI) and polymeric methylene diphenyl diisocyanate (pMDI) from Covestro LLC (Pittsburgh, PA, USA). Soy-based polyols HB230 and HB530 with functionality approximately 2 and 6 respectively were obtained from MCPU Polymer Engineering (Pittsburg, KS, USA). Catalyst dibutyltin dilaurate (DBTL) was purchased from Sigma-Aldrich (St. Louis, MO, USA). Surfactants Xiameter OFX 0193, Dow Corning 2937 and 2938 were obtained from Dow Corning (Midland, MI, USA), Tegostab B 8466 and 8870 from Evonik Industries (Richmond, VA, USA). Distilled water was used as chemical blowing agent. Petroleum-based conventional two parts polyurethane system Baydur 683 was obtained from Covestro LLC (Pittsburgh, PA, USA).

2.2. FOAM SYNTHESIS

Two parts resin mixture was used to synthesize polyurethane foams. Component A was diisocyanate and component B was a mixture of polyol, catalyst, surfactant and water. Typical composition of foam is listed in Table 1. Amount of catalyst (0.08g, 0.32g and 0.45g), water (0.75g, 0.90g, 1.20g and 1.50g) and surfactant (0.5g. 2.0g and 5.0g) were then varied to study their effects on different properties of foam and discussed in the representative sections. Polyols of two different functionalities HB230 and HB530 were also blended in ratio of 95:5 to 85:15 to verify their effects on thermal resistivity and CFD values of foam. All parts of component B were blended in a cup at 1200 rpm for 40s

using an overhead mixer. Required amount of diisocyanate was added to component B and mixed for another 10s at the same speed. The mixture then poured quickly into a rectangular mold (213.4 mm x 111.8 mm x 63.5 mm) and prepared foams were conditioned at ambient atmosphere for at least 24 h before performing any characterization.

Table 1. General formulation of polyurethane foam.

Chemicals	Amount (g)
Polyol (HB230)	100.00
Catalyst (DBTL)	0.08
Water	1.50
Surfactant (Xiameter OFX 0193)	5.00
Isocyanate index	1.14

2.3. EVALUATION OF FOAM PROPERTIES

To measure the density, foams were cut in a specific size (25.4 mm x 25.4 mm x 25.4 mm) of known volume followed by precise weight measurement, according to ASTM D1622. Foam morphology images were captured using field emission scanning electron microscope (Hitachi S4700, Tokyo, Japan). To avoid the image drift due to static charge build up on foam sample surface, samples were sputter coated with Au/Pd alloy and accelerating voltage was 10 kV. Cell sizes were measured from these images using Image J software. Surface tension of component B was measured with a stalagmometer,

using drop weight technique. Thermal conductivity was measured by a QuickLine-30 Thermal property analyzer (Anter Corp., Pittsburgh, PA, USA). Compression force deflection (CFD) of foam samples (dimension: 50.8 mm x 50.8 mm x 25.4 mm) was measured in accordance to ASTM D3574-Test C, using a universal testing machine Instron 5985. Average results are reported based on measurements of five specimens from each category.

3. RESULTS AND DISCUSSION

3.1. COMPETITIVE EFFECT OF CATALYST AND BLOWING AGENT ON FOAM

Properties and performance of foams are controlled by different competitive reactions, which are direct consequence of activities of different additives used during foam synthesis. Reaction of hydroxyl group with isocyanate is exothermic and follows second order kinetics, leads to the formation of urethane linkage spontaneously. Since the vegetable oil-based polyols mostly contain secondary or tertiary hydroxyl groups, react very slowly with isocyanate. Therefore, catalyst is often added to accelerate the reaction by reducing cream and gel time. Water is used frequently as environment friendly chemical blowing agent in polyurethane foam formulation. Water reacts with isocyanate groups and produces amine with release of carbon-di-oxide (CO_2), which blows out and leads to rise of foam. However, amine further reacts with isocyanate and produces substituted urea [17]. Above mentioned reactions are summarized in scheme 1. Organotin based catalyst e.g. DBTL exhibits high catalytic activity towards the reaction of isocyanate with polyol compared to that of isocyanate with water [18].

Scheme 1. Chemical reactions involved in polyurethane foam synthesis.

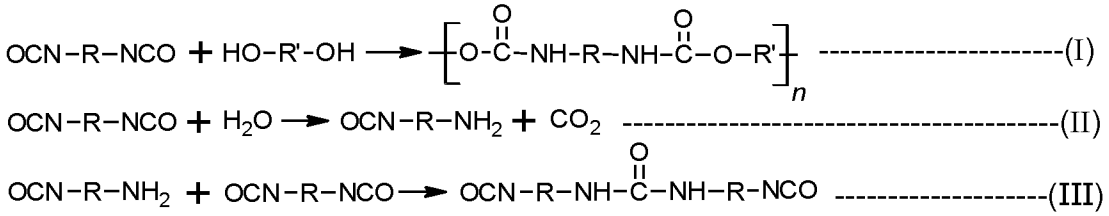

Reaction I and II in scheme 1 are competitive with each other and controlled by the amounts of catalyst and blowing agent respectively. Table 2 summarizes different formulations of foams synthesized to study the effect of distinct amounts of catalyst and water per 100g of soy-based polyol (HB230). 5g of surfactant i.e. Xiameter OFX 0193 was used for all the formulations. Density, cell size, thermal resistivity and CFD values of these foams were evaluated.

Rate of reaction I (curing rate in scheme 1) gets accelerated to a great extent in presence of higher amount of catalyst, resulting high density rigid foam structure. This effect was evident in formulation I to III, where catalyst amount increased without altering water amount, and density increased significantly, as shown in Figure 1(a). On higher amount of water addition, rate of reaction II (CO_2 production rate in scheme 1) exceeds the curing rate and produces expanded foams of low density. As seen in Figure 1(b), the density dropped very rapidly as water content increased. Cell size is the direct evidence of the competitive reaction effect. Cell size decreased with higher addition of catalyst amount, as shown in Figure 1(a). But, more than 0.32g catalyst did not alter cell size and density effectively. Even addition of 0.45g catalyst made the gelling process too rapid to allow sufficient mixing and transfer the reaction mixture completely into the mold. Cell size increased significantly in expanded foams with higher amount of water

added in it, as shown in Figure 1(b). Further increase in water content more than 1.50g produced foams with irregular cell structures and broken cell walls, as shown in Figure 2 (a) and (b). High water content leads to generation of high amount of CO_2 formation in the foam system and negative pressure gradient generated by high diffusion rate of produced CO_2 results in cell rupture [19]. Higher amount of water also produces amines and subsequently higher amount of substituted urea (reaction III in scheme 1) [13]. Since urea has rigid structure, these foams were very brittle and could not be tested.

Table 2. Effect of catalyst and water amount on soy-based PU foam samples.

Formulation	Catalyst (g)	Water (g)	Density (kg/m^3)	Cell size (mm^2)	R-value (m.K/W)	CFD (kPa)
I	0.08	0.75	77.60±2.11	0.16±0.06	25.06±0.06	111.70±1.53
II	0.32	0.75	95.65±1.03	0.08±0.03	25.19±0.02	75.20±2.28
III	0.45	0.75	95.50±1.70	0.09±0.03	25.32±0.06	137.11±3.20
IV	0.08	0.90	65.45±1.20	0.49±0.04	25.42±0.04	86.23±2.37
V	0.08	1.20	60.45±1.91	0.57±0.03	25.64±0.04	79.89±2.51
VI	0.08	1.50	55.95±2.33	0.69±0.07	26.32±0.03	74.61±2.44
Baydur 683	-	-	79.75±1.24	0.63±0.08	28.44±0.02	366.90±4.70

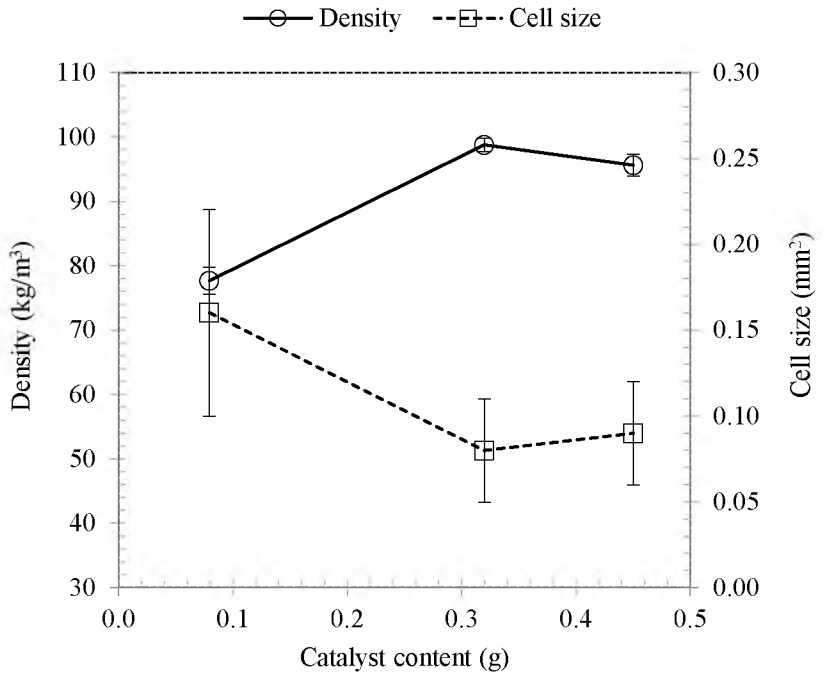

a

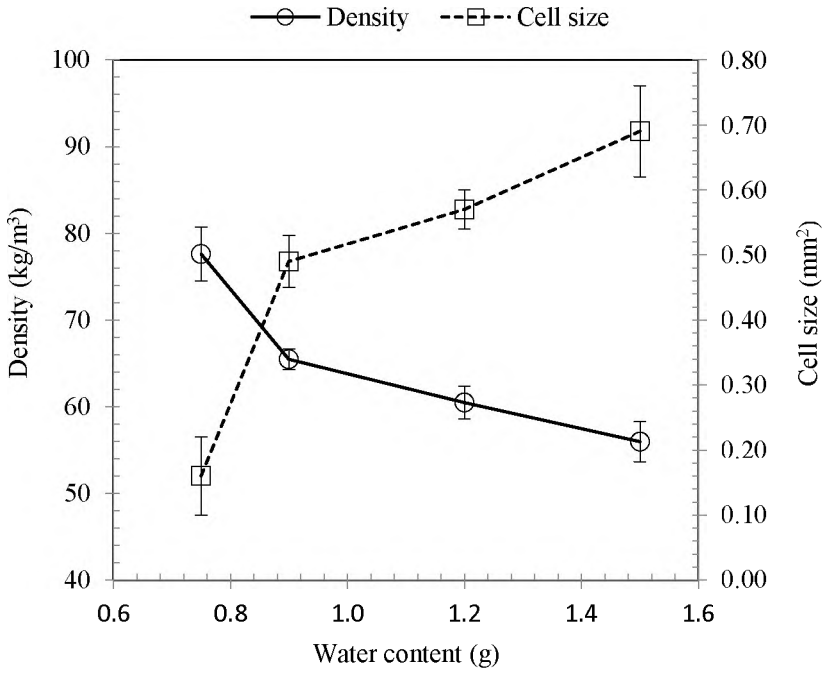

b

Figure 1. Variation of density and cell size of foam with (a) catalyst and (b) water content

a

b

Figure 2. Cross-section of polyurethane foams with (a) regular, medium sized cell structure (1.50g water) and (b) big, irregular, broken cell structure (1.80g water).

For polyurethane insulation panel, thermal resistance or R-value is the most important property to measure. It is controlled by foam density, cell size, and thermal conductivity of the blowing agents, etc. Gas entrapped cells in polyurethane foam along with poor thermal conductivity of polymer surface itself provide the ultimate insulation effect to the foam structure. Variation in catalyst amount did not alter R-value significantly, as shown in Figure 3(a). However, increasing water content leads to bigger cells, which allow higher gas entrapment and retard heat flow through the walls. This effect was evident in R-value, which increased for higher water content, as can be seen in Figure 3(b). Thirumal et al. also found that cell size increased, and density decreased with increased water content due to release of higher quantity of blowing agent [20]. Guo et al. reported increase in R-value with decrease in density due to poor thermal conductivity of blowing agent compared to polymer matrix. They also found that R-values remained unchanged for more than 1g of catalyst addition per 100g of polyol [4]. Change in catalyst amount in our system also did not alter thermal resistivity effectively. So, 0.08g catalyst and 1.50g of water added in 100g of soy-based polyol was evaluated as best for optimally expanded foam with high thermal resistivity close to that of Baydur 683.

Compression force deflection (CFD) is the required force to compress the sample 50% of its thickness. CFD values of all these foams are incomparable with that of petroleum-based foam, summarized in Table 2. As shown in Fig. 3(a), CFD values initially dropped but then increased with increase in catalyst amount. Fig. 3(b) shows that CFD value decreased with higher water content, which is apparently due to increased cell size. Choe et al. studied effect of gelling and blowing catalyst separately and observed

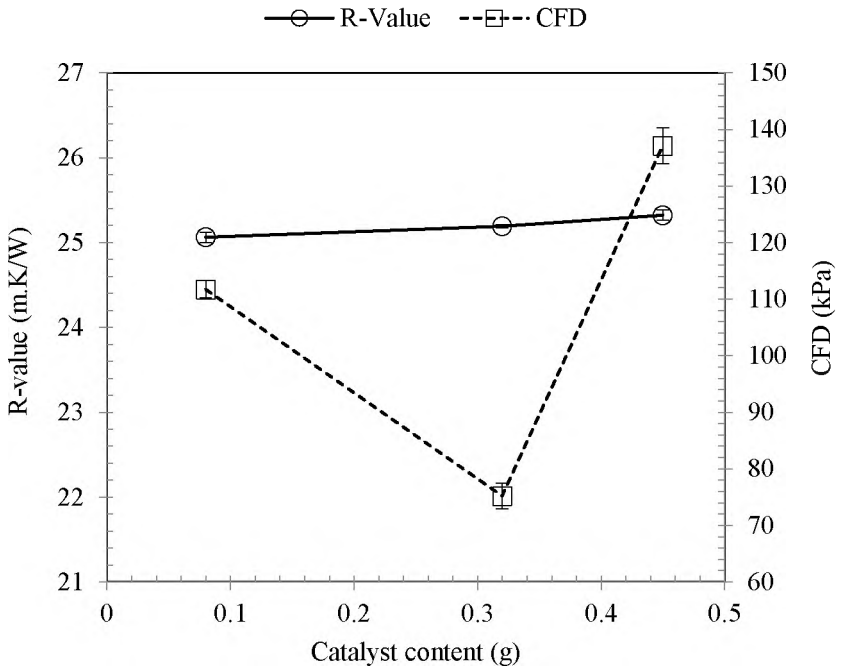

a

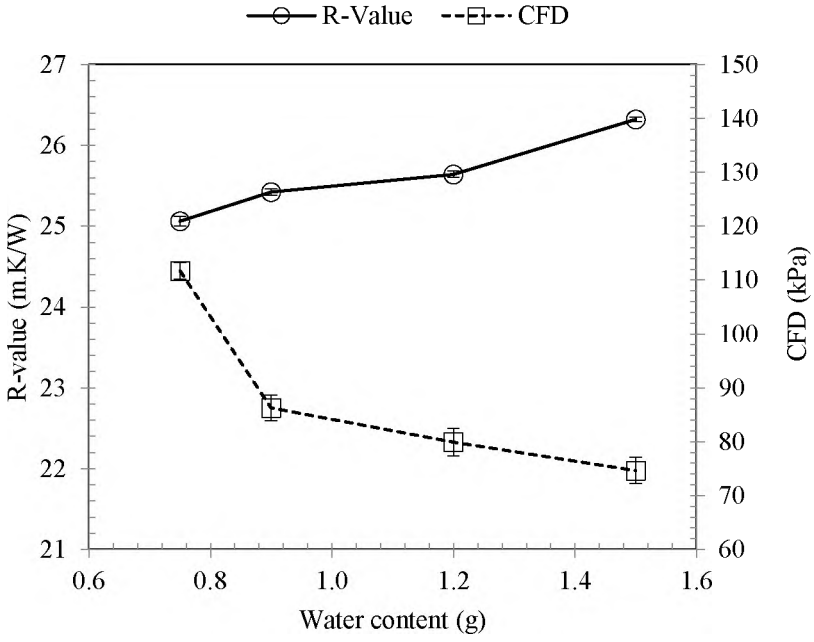

b

Figure 3. Variation of R-value and CFD of foam with (a) catalyst and (b) water content.

minimum influence of catalyst amount on compressive strength for completely water blown rigid PU foam. They also observed that kinetic rate of PU formation increased with water content, which might be due to temperature rise by heat evolution during reaction of water with isocyanate [21]. Different studies reported in literature stated the significant decrease of the density and compressive strength for water blown PU foam with the increase in water content [22], [23].

3.2. EFFECT OF SURFACTANT ON FOAM

Silicone surfactant plays dual role of emulsifier and foam stabilizer in the polyurethane foaming system without altering reaction kinetics. Silicone surfactants used for the foaming system are non-ionic and non-hydrolysable [24]. Molecular structure of these surfactants usually consists of a non-polar polydimethylsiloxane (PDMS) backbone and polar polyether (polyethylene oxide-co-propylene oxide) grafts, shown in Figure 4. Five commercial surfactants used for this study and all were of above type differing in their additive content, listed in Table 3. Presence of large number of methyl groups in these surfactants cause low intermolecular attraction between the siloxane moieties. This results in very high surface activity or low surface tension in both aqueous and organic phase. Low cohesive force and difference in polarity in the same molecule allow its favorable orientation. Therefore, during the mixing of surfactants with polyol in component B surfactant molecules align at the interface of different reactants and promote mixing.

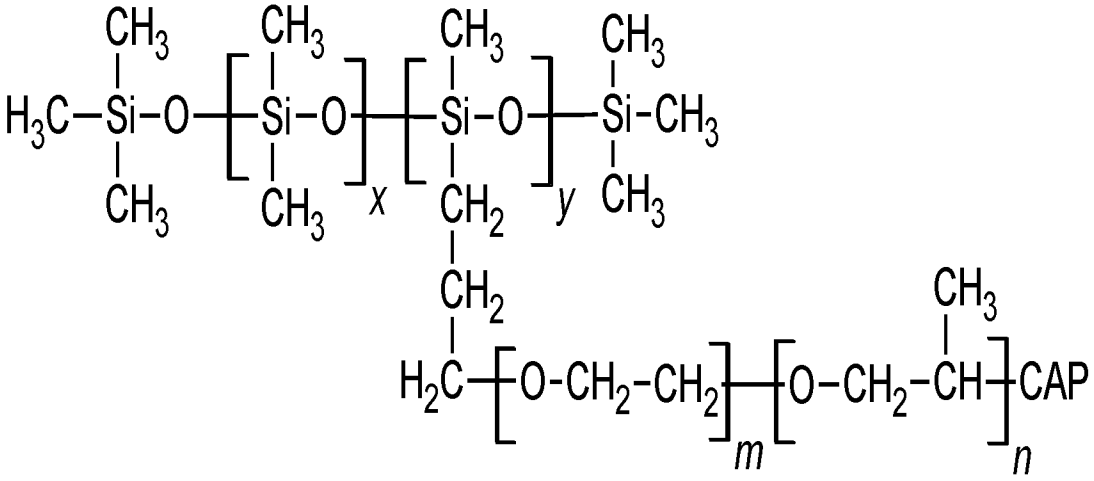

Figure 4. Molecular structure of silicone surfactant.

Table 3. List of five commercial surfactants.

Surfactant	Additive	Viscosity (mPa.s)	Surface tension (mN/m)
Xiameter OFX 0193	Polyethylene glycol (5-10%)	260	38.08±0.30
Dow Corning 2937	Octamethyl cyclotetrasiloxane (1-5%) Decamethyl cyclopentasiloxane (1-5%)	700	31.21±0.63
Dow Corning 2938	Octamethyl cyclotetrasiloxane (0.1-1%)	400	30.23±0.52
Tegostab B 8466	1,1',1"-nitrilotris-2-propanol (<0.5%) 1,2-propanediol (<5%)	450-650	36.35±0.27
Tegostab B 8870	1,1',1"-nitrilotris-2-propanol (<0.1%) Oxybispropanol (<5%)	2000-3000	40.31±0.65

Table 3 summarizes viscosities of the five different surfactants (obtained from company data sheet) and surface tension of component B with 5g of each surfactant mixed in it (measured in lab). Surface tension is directly dependent on the siloxane to polyether ratio and ethylene oxide to propylene oxide (EO/PO) ratio in polyether grafts; represented by ratio of x to y and m to n respectively in Figure 4. Therefore, similar surface tension imparted by different surfactants might have similar ratios of chain lengths in their molecular structures. Although, the difference in viscosity might be a direct attribute of their molecular weights. High polyether percentage increases the surface tension significantly, whereas high siloxane percentage decreases the surface tension and provides better emulsification. Higher EO/PO ratio and higher polyether percentage increase polarity of the molecule and hence the water solubility. But surfactant molecule should align more at the interface of the dissimilar compounds, therefore water blown system requires less polar surfactants [25]. Therefore, surfactant composition is very important parameter to obtain better miscibility of the chemical reactants and stable cells in the PU foam system.

During the foaming process surfactant molecules also align along the air-polyol interface favoring the bubble generation and cell window stabilization. In absence of surfactants, cells start to coalesce causing complete collapse of foam structure. Surfactant with lower surface tension favors entrapment of high volume of air bubbles during mechanical mixing and these air nuclei slowly grows. Surfactant molecules, adsorbed at air-polyol interface, stabilize the air bubbles inside the cells without getting permeated or coalesced to very big bubbles until cell walls get cured completely. As the bubble grows capillary pressure generates, which results in liquid drainage from the cell window to the

struts. This drainage is very fast in absence of surfactant causing cell rupture. Gradient of surface tension generated at air-polyol interface due to adsorption of surfactant results in surface elasticity, which in turn slows down the drainage process and increase the cell stability [26]. Figure 5 demonstrates the effect of surface tension imparted by five different surfactants on the cell size of foam. Lower surface tension helped to generate finer cells, except Tegostab B 8870. Very high viscosity, which is a result of high molecular weight of the surfactant, might be the reason to stabilize the smaller cells.

Increase in surfactant content in component B significantly lowers the surface tension, which again leads to better mixing and smaller cell size. In this study, Xiameter OFX 0193 content was varied from 0.5g to 5g for 100g of polyol and isocyanate index was used as 1.40. 2g surfactant significantly decreased the surface tension and also the cell size, as shown in Figure 6. On further increase of surfactant content from 2 to 5g, the reduction in surface tension and cell size was not very significant. Lim et al. also reported similar trend, where surface tension decreased rapidly about 2/3 of the surfactant-free value on addition 2g of surfactant and thereafter it remains almost same up to 5g of surfactant [19]. It is also suggested in most of the datasheet of surfactants to use 1.5-2g for 100g of polyol for rigid polyurethane foam.

Higher amount of surfactant usually helps to stabilize the cell window and increase closed cell content. Thermal resistivity increases linearly as the closed cell content increases and cell size gets smaller [27]. As seen in Figure 7, thermal resistivity increased with surfactant content and maximum thermal resistivity was observed for the foam with 5g of surfactant. Compression strength also depends on closed cell content and dimensional stability of foam structure. Figure 7 shows that CFD increased with addition

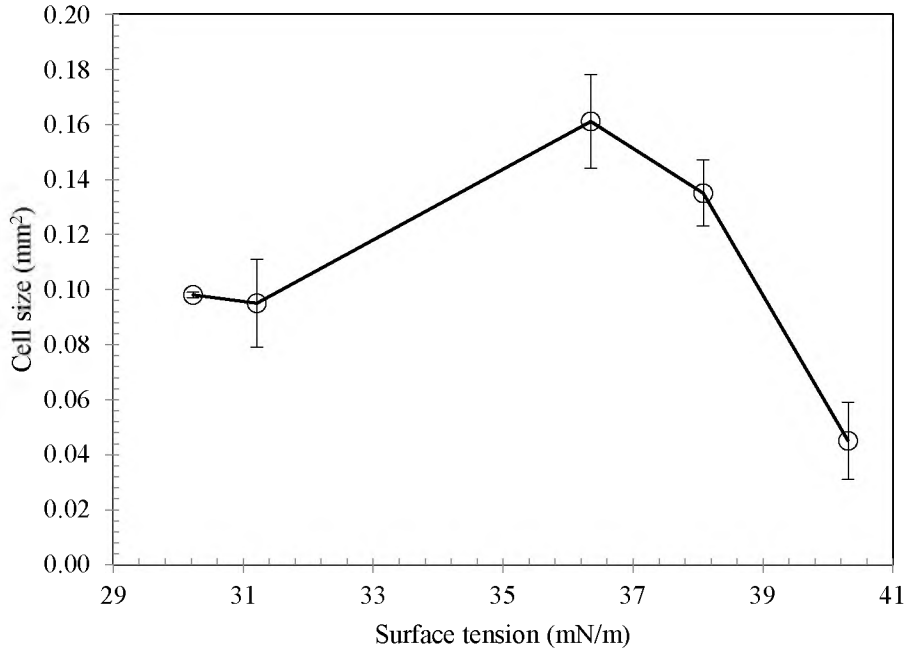

Figure 5. Effect of surface tension imparted by five different surfactants on cell size of foam.

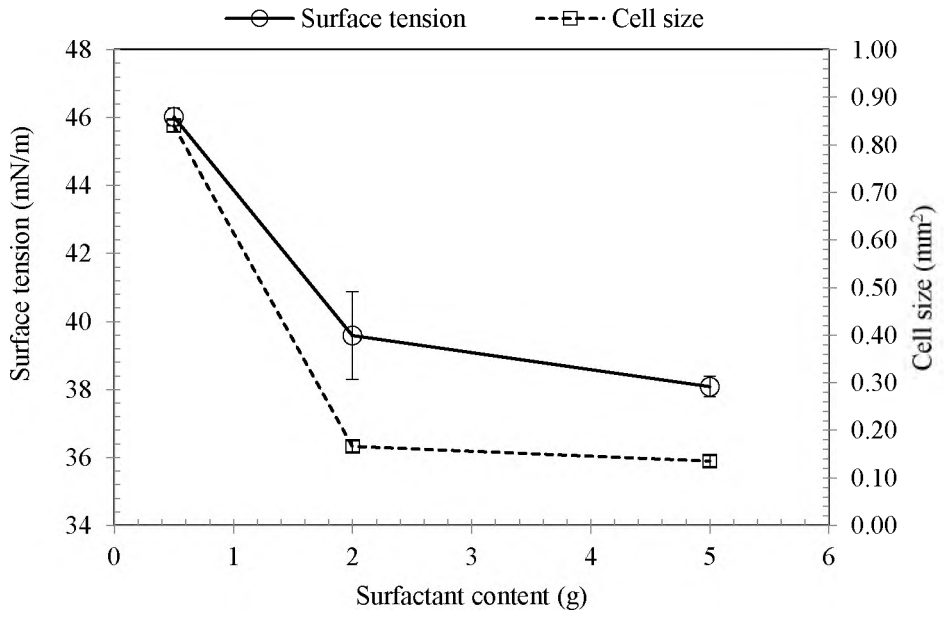

Figure 6. Effect of surfactant (Xiameter OFX 0193) content on surface tension and cell size.

of 2g surfactant, further addition of surfactant reduced CFD considerably. Seo et al. also reported similar trend and explained that plasticizing effect of surfactants on PU foam system might be responsible for reduction of compression strength of foam with higher surfactant content [28].

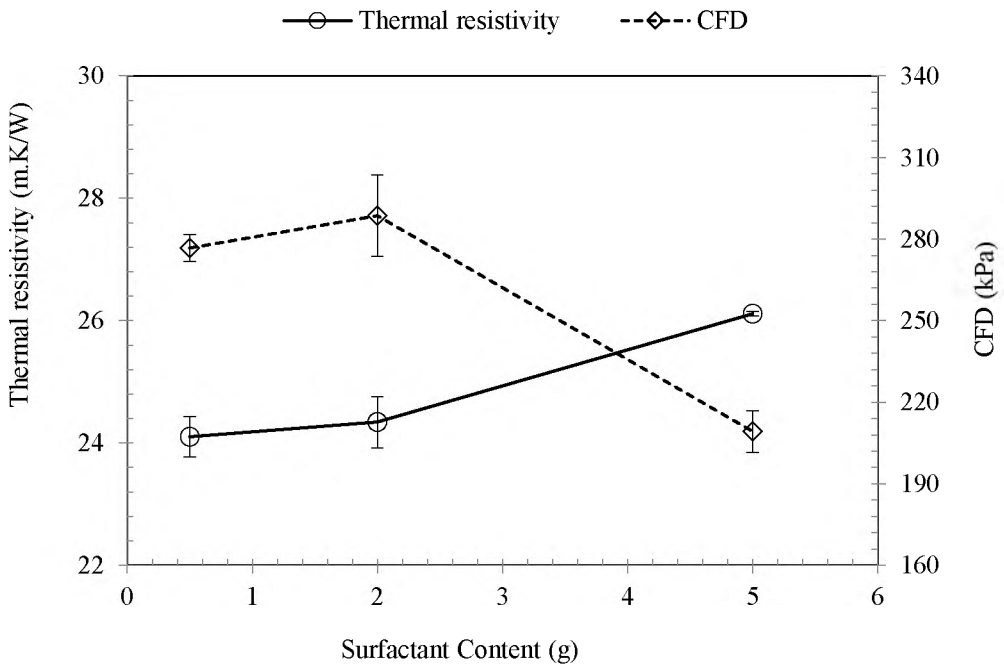

Figure 7. Effect of surfactant (Xiameter OFX 0193) content on thermal resistivity and CFD.

3.3. EFFECT OF HYDROXYL GROUP ACTIVITY ON FOAM

Soybean oil contains triglyceride of both saturated and unsaturated fatty acids. Dominant portion of all these unsaturated fatty acids are oleic acid (C18:1), linoleic acid (C18:2) and linolenic acid (C18:3), as shown in Figure 8. Double bonds of these unsaturated fatty acids are usually subjected to epoxidation followed by ring opening to introduce hydroxyl groups, which serve as potential site for crosslinking reaction with

isocyanate. If triglyceride structure remains unaltered during the polyol formation, it provides network structure making the polyurethane thermosetting in nature.

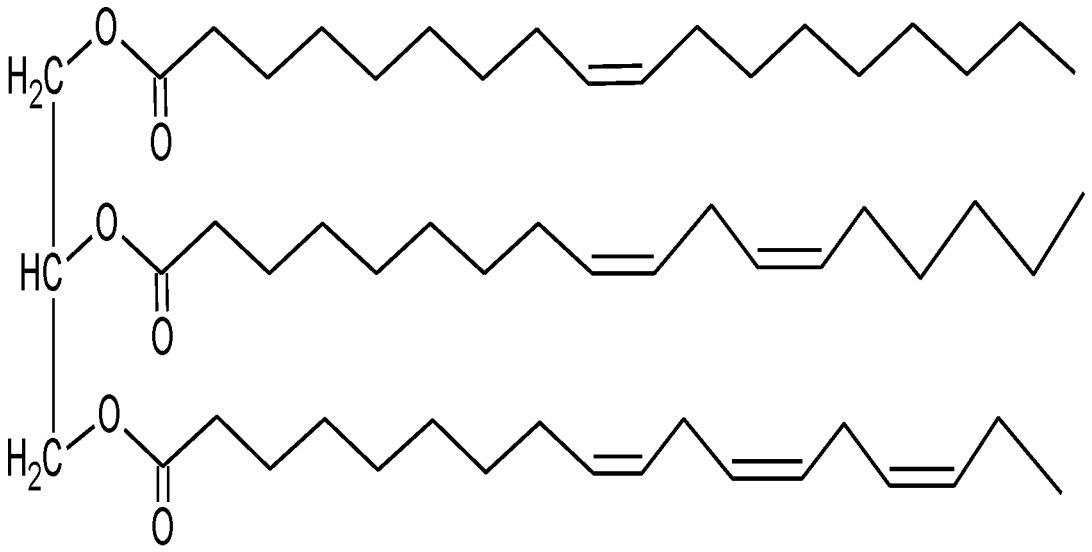

Figure 8. Structure of soybean oil.

Performance of the polyurethane network depends on composition of the soybean oil, i.e., position and distribution of double bonds in the fatty acid molecules, crosslinking density, etc. Double bond position decides the hydroxyl group position in the polyol and therefore, the dangling chain length in the polyurethane structure. Uncrosslinked chain ends of polyol or saturated fatty acid chains from the oil can behave as dangling chains, which do not support elastic stress of the network under applied load and acts as plasticizer [29]. Crosslinking density depends on the functionality i.e. number of hydroxyl groups in polyol, which is a direct consequence of number of double bonds presents in the fatty acid chains and on its degree of conversion. Insertion of hydroxyl

group in the double bond always increases the viscosity and therefore, polyol with higher functionality has higher viscosity [13].

In this study, two types of polyol HB230 and HB530 were used and their properties are listed in Table 4. Higher viscosity of HB530 is attributed to its higher functionality or hydroxyl number compared to HB230. Since HB530 has functionality ~6, it results fewer dangling chains upon crosslinking and acts as crosslinking agent. HB530 content was varied from 0 to 15g while HB230 content was also altered to make total polyol content of 100g. Figure 9 shows the change in density and cell size of foam with HB530 content. Addition of 5g of HB530 caused an initial drop of foam density but further addition resulted in higher density. Higher amounts of HB530 increased crosslinking density and minimized plasticizing effect of dangling chains; therefore, produce more dense and rigid network. Cell size slowly decreased with HB530 content but was not altered significantly.

Table 4. Properties of HB230 and HB530 mentioned in technical datasheet.

Properties	HB230	HB530
Functionality	~2	~6
Hydroxyl no. (mg KOH/g)	220-240	510-550
Acid no. (mg KOH/g)	≤3	≤3
Viscosity at 25 °C (mPa.s)	375	54,000

Thermal resistivity usually varies inversely with density, while compressive strength increases with increment of density [4]. As seen in Figure. 10, thermal resistivity increased initially, but then decreased with further addition of HB530. However, CFD values increased almost linearly with HB530 content. For thermal insulation application higher thermal resistivity along with greater CFD values are preferred conditions, which can be obtained by blending of HB230 with HB530 in 95:5 w/w ratio. Thermal resistivity and CFD values of this foam were comparable with that of the Baydur 683.

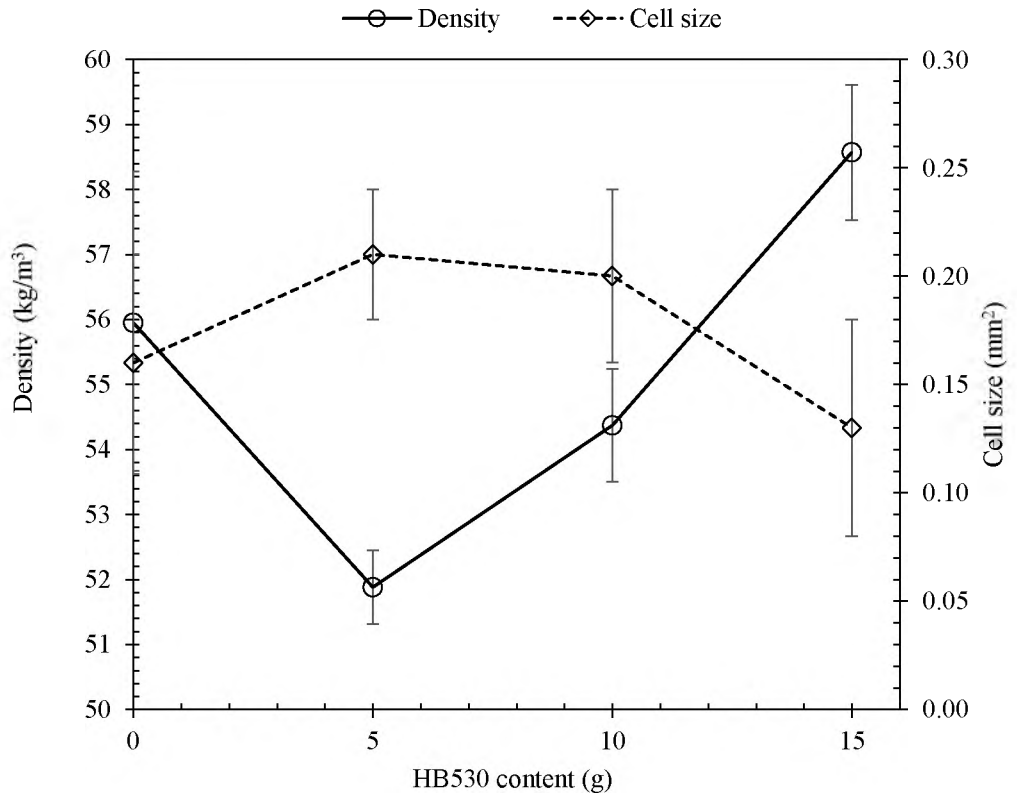

Figure 9. Effect of HB530 on foam density and cell size.

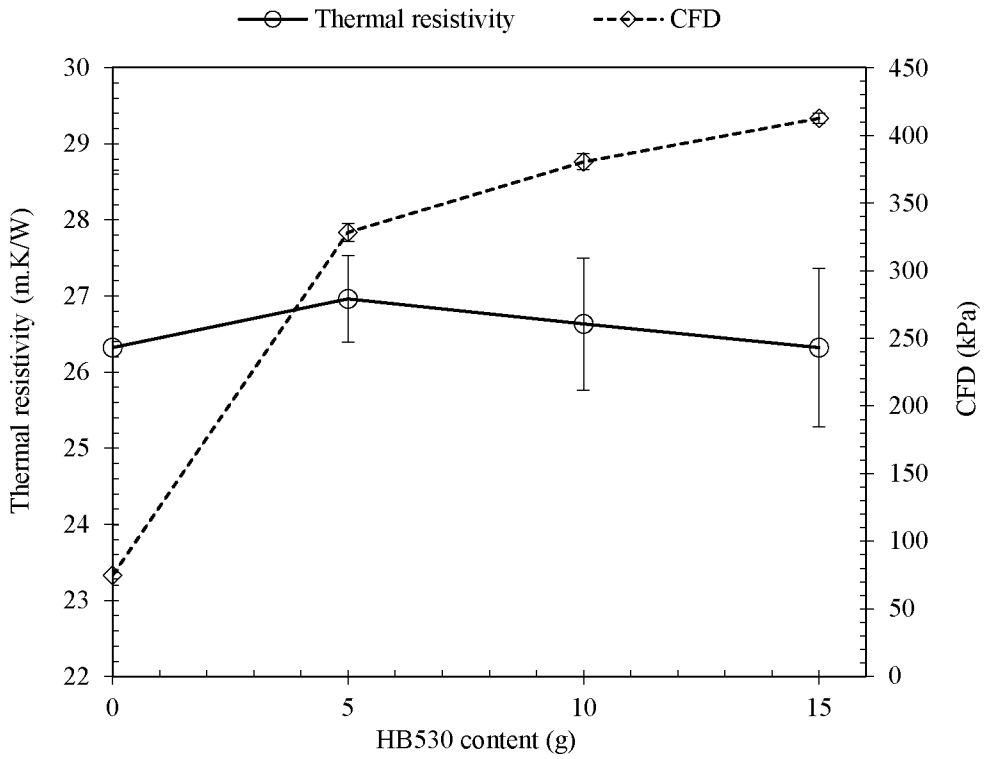

Figure 10. Variation of thermal resistivity and CFD of foam with HB530 content.

4. CONCLUSIONS

Soy-polyol based polyurethane foams were synthesized for thermal insulation applications. The aim of this study was to investigate the effect of different additives on the structural and thermal insulation properties of soy-based foam. It was observed that higher catalyst content increased the foam density by increasing the curing rate; whereas higher water content enhanced the blowing rate and produced low density foam. However, very high amount of water addition produced foams with irregular cell structures and broken cell walls. Addition of surfactant improved the miscibility of the reactants as well as stabilized the foam structure. Therefore, thermal resistivity values

were improved for higher surfactant content, but CFD values decreased due to the plasticizing effect of it. It was observed that 100% soy polyol-based PU foam has comparable thermal resistivity but poor CFD values with that of the petroleum-based foam Baydur 683. However, blending of HB530 with HB230 improved CFD values significantly. It was found that mixing of 5g of HB530 with 95g of HB230 along with 0.08g catalyst, 1.50g of water and 5g of surfactant can produce soy-based foam with CFD and R-value similar to that of Baydur 683.

ACKNOWLEDGEMENTS

Support for this research was provided by Missouri Soybean Merchandising Council (Jefferson City, MO, USA) and US Department of Agriculture. The author would like to thank Covestro LLC (Pittsburgh, PA, USA) for providing isocyanate and MCPU Polymer Engineering LLC (Pittsburg, KS, USA) for providing the polyol used in this study.

REFERENCES

[1] S. Tan, T. Abraham, D. Ference, and C. W. Macosko, "Rigid polyurethane foams from a soybean oil-based polyol," *Polymer (Guildf).*, vol. 52, no. 13, pp. 2840–2846, 2011, doi: https://doi.org/10.1016/j.polymer.2011.04.040.

[2] A. A. Abdel Hakim, M. Nassar, A. Emam, and M. Sultan, "Preparation and characterization of rigid polyurethane foam prepared from sugar-cane bagasse polyol," *Mater. Chem. Phys.*, vol. 129, no. 1, pp. 301–307, 2011, doi: https://doi.org/10.1016/j.matchemphys.2011.04.008.

[3] I. Javni, W. Zhang, and Z. S. Petrović, "Effect of different isocyanates on the properties of soy-based polyurethanes," *J. Appl. Polym. Sci.*, vol. 88, no. 13, pp. 2912–2916, Jun. 2003, doi: 10.1002/app.11966.

[4] A. Guo, I. Javni, and Z. Petrovic, "Rigid polyurethane foams based on soybean oil," *J. Appl. Polym. Sci.*, vol. 77, no. 2, pp. 467–473, Jul. 2000, doi: 10.1002/(SICI)1097-4628(20000711)77:2<467::AID-APP25>3.0.CO;2-F.

[5] K. S. Chian and L. H. Gan, "Development of a rigid polyurethane foam from palm oil," *J. Appl. Polym. Sci.*, vol. 68, no. 3, pp. 509–515, Apr. 1998, doi: 10.1002/(SICI)1097-4628(19980418)68:3<509::AID-APP17>3.0.CO;2-P.

[6] Y. H. Hu *et al.*, "Rigid polyurethane foam prepared from a rape seed oil based polyol," *J. Appl. Polym. Sci.*, vol. 84, no. 3, pp. 591–597, Apr. 2002, doi: 10.1002/app.10311.

[7] I. Javni, Z. S. Petrović, A. Guo, and R. Fuller, "Thermal stability of polyurethanes based on vegetable oils," *J. Appl. Polym. Sci.*, vol. 77, no. 8, pp. 1723–1734, Aug. 2000, doi: 10.1002/1097-4628(20000822)77:8<1723::AID-APP9>3.0.CO;2-K.

[8] M. Heinen, A. E. Gerbase, and C. L. Petzhold, "Vegetable oil-based rigid polyurethanes and phosphorylated flame-retardants derived from epoxydized soybean oil," *Polym. Degrad. Stab.*, vol. 108, pp. 76–86, 2014, doi: https://doi.org/10.1016/j.polymdegradstab.2014.05.024.

[9] D. Ji *et al.*, "Polyurethane rigid foams formed from different soy-based polyols by the ring opening of epoxidised soybean oil with methanol, phenol, and cyclohexanol," *Ind. Crops Prod.*, vol. 74, pp. 76–82, 2015, doi: https://doi.org/10.1016/j.indcrop.2015.04.041.

[10] C. Zhang and M. R. Kessler, "Bio-based polyurethane foam made from compatible blends of vegetable-oil-based polyol and petroleum-based polyol," *ACS Sustain. Chem. Eng.*, vol. 3, no. 4, pp. 743–749, Apr. 2015, doi: 10.1021/acssuschemeng.5b00049.

[11] Y.-C. Tu, P. Kiatsimkul, G. Suppes, and F.-H. Hsieh, "Physical properties of water-blown rigid polyurethane foams from vegetable oil-based polyols," *J. Appl. Polym. Sci.*, vol. 105, no. 2, pp. 453–459, Jul. 2007, doi: 10.1002/app.26060.

[12] A. A. Beltran and L. A. Boyaca, "Production of rigid polyurethane foams from soy-based polols," *Lat. Am. Appl. Res.*, vol. 41, no. 1, pp. 75–80, 2011.

[13] J. John, M. Bhattacharya, and R. B. Turner, "Characterization of polyurethane foams from soybean oil," *J. Appl. Polym. Sci.*, vol. 86, no. 12, pp. 3097–3107, Dec. 2002, doi: 10.1002/app.11322.

[14] A. Guo, Y. Cho, and Z. S. Petrović, "Structure and properties of halogenated and nonhalogenated soy-based polyols," *J. Polym. Sci. Part A Polym. Chem.*, vol. 38, no. 21, pp. 3900–3910, Nov. 2000, doi: 10.1002/1099-0518(20001101)38:21<3900::AID-POLA70>3.0.CO;2-E.

[15] L.-T. Yang, C.-S. Zhao, C.-L. Dai, L.-Y. Fu, and S.-Q. Lin, "Thermal and mechanical properties of polyurethane rigid foam based on epoxidized soybean oil," *J. Polym. Environ.*, vol. 20, no. 1, pp. 230–236, 2012, doi: 10.1007/s10924-011-0381-6.

[16] S. Husić, I. Javni, and Z. S. Petrović, "Thermal and mechanical properties of glass reinforced soy-based polyurethane composites," *Compos. Sci. Technol.*, vol. 65, no. 1, pp. 19–25, 2005, doi: https://doi.org/10.1016/j.compscitech.2004.05.020.

[17] A. Campanella, L. M. Bonnaillie, and R. P. Wool, "Polyurethane foams from soyoil-based polyols," *J. Appl. Polym. Sci.*, vol. 112, no. 4, pp. 2567–2578, May 2009, doi: 10.1002/app.29898.

[18] Q. Zhang, X.-M. Hu, M.-Y. Wu, Y.-Y. Zhao, and C. Yu, "Effects of different catalysts on the structure and properties of polyurethane/water glass grouting materials," *J. Appl. Polym. Sci.*, vol. 135, no. 27, p. 46460, Jul. 2018, doi: 10.1002/app.46460.

[19] H. Lim, S. H. Kim, and B. K. Kim, "Effects of silicon surfactant in rigid polyurethane foams," *xpress Polym. Lett.*, vol. 2, no. 3, pp. 194–200, 2008.

[20] M. Thirumal, D. Khastgir, N. K. Singha, B. S. Manjunath, and Y. P. Naik, "Effect of foam density on the properties of water blown rigid polyurethane foam," *J. Appl. Polym. Sci.*, vol. 108, no. 3, pp. 1810–1817, May 2008, doi: 10.1002/app.27712.

[21] K. H. Choe, D. S. Lee, W. J. Seo, and W. N. Kim, "Properties of rigid polyurethane foams with blowing agents and catalysts," *Polym. J.*, vol. 36, no. 5, pp. 368–373, 2004, doi: 10.1295/polymj.36.368.

[22] W. J. Seo, J. H. Park, Y. T. Sung, D. H. Hwang, W. N. Kim, and H. S. Lee, "Properties of water-blown rigid polyurethane foams with reactivity of raw materials," *J. Appl. Polym. Sci.*, vol. 93, no. 5, pp. 2334–2342, Sep. 2004, doi: 10.1002/app.20717.

[23] Y. Yan, H. Pang, X. Yang, R. Zhang, and B. Liao, "Preparation and characterization of water-blown polyurethane foams from liquefied cornstalk polyol," *J. Appl. Polym. Sci.*, vol. 110, no. 2, pp. 1099–1111, Oct. 2008, doi: 10.1002/app.28692.

[24] D. Perry, "Silicone surface active agents," in *Additives in Water-Borne Coatings*, G. Davison and B. Lane, Eds. Cambridge: The Royal Society of Chemistry, 2003, pp. 77–84.

[25] J. Grimminger and K. Muha, "Silicone surfactants for pentane blown rigid foam," *J. Cell. Plast.*, vol. 31, no. 1, pp. 48–72, Jan. 1995, doi: 10.1177/0021955X9503100104.

[26] X. D. Zhang, C. W. Macosko, H. T. Davis, A. D. Nikolov, and D. T. Wasan, "Role of silicone surfactant in flexible polyurethane foam," *J. Colloid Interface Sci.*, vol. 215, no. 2, pp. 270–279, 1999, doi: https://doi.org/10.1006/jcis.1999.6233.

[27] J.-W. Wu, W.-F. Sung, and H.-S. Chu, "Thermal conductivity of polyurethane foams," *Int. J. Heat Mass Transf.*, vol. 42, no. 12, pp. 2211–2217, 1999, doi: https://doi.org/10.1016/S0017-9310(98)00315-9.

[28] W. J. Seo *et al.*, "Mechanical, morphological, and thermal properties of rigid polyurethane foams blown by distilled water," *J. Appl. Polym. Sci.*, vol. 90, no. 1, pp. 12–21, Oct. 2003, doi: 10.1002/app.12238.

[29] A. Zlatanić, C. Lava, W. Zhang, and Z. S. Petrović, "Effect of structure on properties of polyols and polyurethanes based on different vegetable oils," *J. Polym. Sci. Part B Polym. Phys.*, vol. 42, no. 5, pp. 809–819, Mar. 2004, doi: 10.1002/polb.10737.

III. A RAPID AND SENSITIVE METHOD FOR ON-SITE REAL-TIME MONITORING OF AIRBORNE BTEX USING A NEWLY DEVELOPED PORTABLE GC

Mousumi Bose[a], Xiaolong He[a], Honglan Shi[a, b], Paul Nam[a, b]

[a]Deparment of Chemistry, Missouri University of Science and Technology, Rolla, MO, 65409 USA

[b]Center of Research for Energy and Environment, Missouri University of Science and Technology, Rolla, MO, 65409 USA

ABSTRACT

Rapid onsite monitoring of toxic volatile organic compounds with high sensitivity is in great demand from many government agencies and industries to assess human health impacts. In this study, a high throughput, sensitive and accurate method for onsite real-time analysis of benzene, toluene, ethylbenzene, and xylenes (BTEX) in ambient air was developed. A new portable gas chromatography – photoionization detector (GC-PID) system which has a patented on-line preconcentrator and a short capillary GC column with novel at-column heater configuration was used. GC separation and detection of all BTEX compounds were completed in only 2 min, with excellent retention time reproducibility (<1% RSD) and peak area reproducibility (<6% RSD) from multiple days of measurements. The detection limits were 14 pg for benzene and toluene, and 28 pg for ethylbenzene and xylenes. Good linearity (R^2>0.99) was achieved for the calibration range of 10^3 for all BTEX compounds. The results demonstrated the faster and higher sensitivity when compared to other commercial portable GC. This method was successfully employed for on-line, real-time monitoring of BTEX emission during the

production of asphalt pavement cement with recycled materials. This portable GC based analytical method can be a very useful tool for onsite environmental monitoring of various VOC emission sources such as synthetic material shop floors, emission from car exhaust, gasoline spill in the gas stations, etc. due to the ultra-fast and highly portable nature of the system.

Keywords: Environmental monitoring; Portable GC; VOC; BTEX; Real-time; On-site; Air

1. INTRODUCTION

Volatile organic compounds (VOC) have adverse effects on human health. Among VOCs, benzene, toluene, ethylbenzene and xylenes, named BTEX collectively, are hazardous even at trace level [1]. BTEX emission can be from variety of materials like petroleum products, paints, resins, synthetic rubbers, [2], [3] etc. BTEX are carcinogenic and neurotoxic chemicals. Long time exposure to specially benzene may cause leukemia and classified as a Group A-human carcinogenic material by US Environmental Protection Agency (EPA) [4]. EPA regulated inhalation reference concentration for benzene of 0.03 mg/m3 (9.3 parts per billion by volume (ppbv)) [5]. Rapid and highly sensitive analysis of BTEX is critically important.

Among the different techniques available to detect BTEX, gas chromatography (GC) is the most commonly used method. Both off-line and on-line measurement techniques are available now-a-days. Off-line methods able to detect multiple analytes with very low detection limit but require time consuming sample preparation step prior to

analysis. Additionally, BTEX are very volatile compounds, hence sometimes it is difficult to preserve for long-time without losing of analytes. Therefore, demand of on-site or on-line detection techniques are increasing continuously. On-line detection of BTEX requires light weight transportable GC with high selectivity and accuracy [1], [6], [7]. Portable GC is an extremely valuable tool for on-site measurement of VOC in indoor air [8], synthetic material processing shop floor, emission from car exhaust [9], gasoline spill in the gas station from underground storage tank [10], [11], and in petroleum refineries [6], etc. Most commonly used detectors for GC are flame ionization detector (FID), thermal conductivity detector (TCD), photo ionization detector (PID), mass spectroscopy (MS) [12]–[16], etc. Use of FID, TCD or MS detector for field-monitoring has the disadvantage of adding up extra weight to the system and/or safety risks. Sometimes sensitivity is also an issue for TCD and FID. PID is low-weight, compact, cheap, requiring low maintenance, highly sensitive and selective for BTEX compounds detection. UV lamp in PID provides energy of 10.6 eV, which can support ionization of aromatic volatile compounds. Hence PID is ideal for on-line monitoring of BTEX compounds by portable GC. Varieties of miniaturized GC have been developed throughout the years with different levels of detection limits and response times. Benzene is the most harmful compound among BTEX, requiring to be monitored in sub-ppbv level and hence efficiency of portable GC are mostly compared based on detection limit of benzene [3]. Detection limit in sub-ppbv level for benzene has reported with compact GC-PID [15].

The goal of this study is to develop a novel high throughput and highly sensitive method for analysis of BTEX for field and on-line applications. A newly developed

portable GC-PID with patented online pre-concentration has been developed. This portable GC-PID weighs only 7 kg including carrier gas cylinder and everything. The method has been applied for rapid on-site real-time measurement of BTEX emitting from lab-scale processing of hot-mix-asphalt (HMA) pavement. Since hot mixing of these recycled materials is very likely to emit hazardous volatile materials, careful evaluation of emitted VOC is highly desirable to ensure environmental safety [17], [18].

2. MATERIALS AND METHODS

2.1. CHEMICALS AND MATERIALS

Benzene (99%) was obtained from Acros Organics (Belgium, WI, USA). Toluene (99.9%) and ethylbenzene (99%) were purchased from Fisher Scientific (Pittsburgh, PA, USA). o-Xylene (95%) was product of Eastman Organic Chemicals (Rochester, NY, USA) while m-xylene (99%) and p-xylenes (99%) were from Sigma-Aldrich (St. Louis, MO, USA). Optima grade hexane was purchased from Fisher Scientific (Pittsburgh, PA, USA) and used as solvent. Helium gas (99.5%), in 95 mL cylinders, was obtained from Leland Gas Technologies (South Plainfield, NJ, USA). 5-L size Tedlar® bags (made of polyvinyl fluoride film with single polypropylene septum fitting) were purchased from SKC Inc. (Eighty Four, PA, USA). For hot-mix-asphalt experiment, neat asphalt PG 52-28 was obtained from Philips 66 Company (Granite, IL, USA), CRM from Liberty Tire Recycling Company (Montgomery, IL, USA) and UMO from a local auto repair shop.

2.2. ANALYTICAL INSTRUMENT AND METHOD PARAMETERS

A newly developed NovaTest™ P100 portable GC-PID provided by Nanova Environmental, Inc. (Columbia, MO, USA) was used for this study. The GC-PID equipped with a patented automatic online sampling/preconcentrator and a short 6 m (0.25 mm i.d. and 1.40 μm d_f) Rtx-VMS™ capillary GC column (Restek Corp, Bellefonte, PA, USA) and at-column heater configuration [19]. Online preconcentrator was made of a stainless steel tube packed with Carboxen 1018 beads as adsorbent material, wrapped with an insulated copper wire for thermal desorption at 300 °C and a thermocouple placed at the center to monitor its real-time temperature. Gas sample was introduced by a vacuum and passed through the preconcentrator at a flow rate 10 mL/min for a selected time. After the valve switching connection to the column, the analytes in the preconcentrator were thermally desorbed at 300 °C directly into the column for separation and detection. GC carrier gas was helium from a 95 mL disposable helium gas cylinder. The head pressure of the column was set at 10 psi. The separation was processed with a temperature gradient from 50 to 80 °C at 15 °C/min rate. Total run time required to separate BTEX was 2 min.

2.3. EVALUATING SUITABILITY OF TEDLAR® BAGS FOR CALIBRATION STANDARD PREPARATION

Diffusion and adsorption of analytes in the Tedlar® bag may affect its suitability to be used as sampling bag for standard preparation and storage. It has been reported that recovery of BTEX from Tedlar® bags was more than 90% for up to 10 h of storage [20], [21]. For appropriate response it is very important to establish equilibrium time and storage time by complete volatilization after injecting the analytes into the bags. This can

be achieved quickly by heating the bags at a higher temperature for short time period or set the bags at room temperature for comparatively longer time after injecting BTEX standard into the bags. A concentrated BTEX stock mixture (~0.145 g/mL each) was prepared by combining 1.0 mL of each benzene, toluene, ethylbenzene, o-xylene, m-xylene and p-xylene (BTEX) in a glass vial. Varying concentration of BTEX solutions were prepared by serial dilution of the BTEX stock mixture in hexane. To study the effect of temperature, the Tedlar® bags were pre-cleaned five times (bags were filled with high purity nitrogen gas and then emptied; this cleaning process was repeated for 5 times), then filled with high purity (99.99%) nitrogen gas. A selected concentration of the BTEX mixture (1 μL using 1 μL size syringe) was injected into each bag. The bags were heated at 40 °C, 50 °C and 60 °C in an oven for 20 min separately, then cooled to room temperature in 20 min before being analyzed by GC-PID method, and the results were compared. To evaluate the optimum equilibrium time required at room temperature, storing time was tested from 10 min to 5 h. At the selected time intervals, BTEX standard was analyzed by the GC-PID method with the portable GC for 5 min sampling time.

2.4. BTEX STANDARDS PREPARATION AND CALIBRATION METHOD

Gas phase BTEX calibration standards were prepared in 5-liter Tedlar® bags. All the bags were cleaned five times by pure nitrogen gas as described in the earlier section prior to be used for calibration standard preparation. The bags were filled with high purity nitrogen gas before injecting 1 μL (using 1 μL size syringe) of the prepared BTEX standard solution into each to prepare 0.9, 9, 90 and 900 ppbv calibration standards. The mass per volume (μg/L) unit value was subsequently converted to ppbv unit value using

the EPA on-line tools for indoor air unit conversion [22]. Each standard bag was allowed to equilibrate for 30 mins at room temperature (22 °C) as optimized in the earlier section, and then sampled at different times from 0.5 to 5.0 min. Variable sampling time in combination with different concentrations of BTEX standards allowed introducing a wide range amount of BTEX for calibration curves. Analysis was performed in triplicate for each sampling. Reproducibility of the test method was evaluated by retention times and peak areas of different samples.

2.5. DETERMINATION OF BTEX EMISSION ON-LINE DURING HOT-MIX-ASPHALT PROCESSING

Recycling of waste materials in different applications is current urge for better waste management, but it triggers the potential environmental risks. As an application of the developed novel GC-PID method, on-line monitoring of BTEX emission from CRM and UMO recycled with asphalt was conducted using the new GC method. In the previous studies of asphalt binder mix containing CRM and UMO as rejuvenator, both air test and batch leaching test were reported to verify the amount of BTEX released during and post processing respectively [17], [23]. Both methods were very time consuming (take several hours for each sample) and did not allow the on-site monitoring of BTEX. Here in this study, we used the portable GC to monitor BTEX emission on-line during HMA processing. The experiment was conducted by mixing 1600 g asphalt cement with 15% CRM with/without 2.5% UMO by continuously stirring at 170 °C for 75 min in a vessel. GC was placed near the processing vessel and fume above the vessel was sampled for 1 min via a 2-feet long Teflon tubing connected to the sampling port of the portable GC-PID. BTEX content in the fume was analyzed at every 10 min intervals during the

mixing. The performance of the GC was checked on-site prior to real-time analysis by performing a quick calibration test with 90 ppbv BTEX standard prepared in a Tedlar® bag. Similar response was obtained for on-site calibration test with that of in-lab test performed using the same calibration standard in the bag (prepared and checked 20 h prior to this on-site test).

3. RESULTS AND DISCUSSION

3.1. METHOD VALIDATION

Establishment of a proper method and its validation is utmost important for any analysis. Using portable GC for field analysis requires a thorough evaluation of its method parameters. Actual calibration curve for the target compounds with linear regression equation, detection limit and dynamic linear range should be established. In addition, a simple yet reliable on-site calibration method is necessary to check proper functioning of the instrument prior to real-time application. To fulfill the requirement while maintaining the simplicity of the procedure, sampling bags filled with gaseous analytes in high purity nitrogen were used for calibration of the GC. Although metal canisters are widely used for volatile samples, for on-site calibration carrying metal canister with portable GC is not convenient in addition of more costly. To maintain the coherency, 5-L sampling bags were used for both in-lab and on-site calibration. A representative chromatogram for BTEX standard generated by the portable GC is shown in Figure 1. First big peak is solvent hexane peak. All BTEX compounds were completely resolved except m and p-xylenes co-eluted as a single peak.

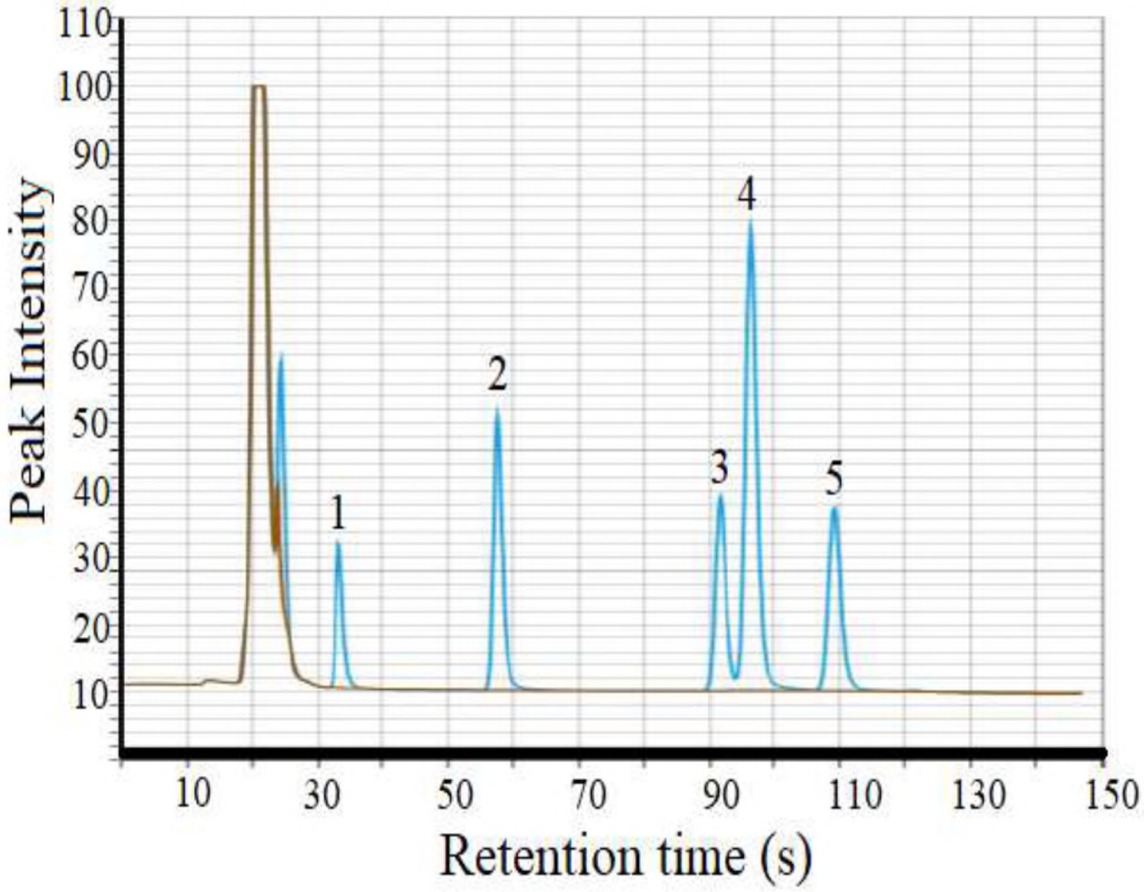

Figure 1. Representative chromatogram of BTEX standards (90 ppbv, sampled for 5 min); peak 1: benzene, 2: toluene, 3: ethylbenzene, 4: m & p - xylene and 5: o - xylene. Unnumbered peak represents hexane.

3.1.1. Conditions of Standard Preparation. For accuracy of calibration, complete volatilization of the analytes and equilibration must be achieved in the sampling bags prior to the analysis. Equilibrium can be achieved either by heating the bags at a certain temperature for short time or storing the filled bags at room temperature for longer time. To check the effect of heating, nitrogen filled Tedlar® bags were heated to 40 °C, 50 °C and 60 °C in an oven for 20 min separately and then analyzed after cooling them to room temperature. As seen in Figure 2, a noticeable rise in baseline with humps at higher retention time was observed for all the heated sampling bags. The rising of

baseline was a result of the PID response to thermal degradation or off-gas volatile products generated at higher temperature in the sampling bags and humps at higher retention time indicated that the volatiles were high boiling compounds. In contrary, the response baseline was completely flat (Figure 2A) when bags were equilibrated at room temperature only. Thus, all the subsequent calibration was prepared and equilibrated at room temperature.

To determine the minimum time for complete volatilization and equilibration of the analytes in the bag, 90 ppbv BTEX standard was injected in the Tedlar® bag and standing time was varied from 10 min to 5 h at room temperature before analysis. Peak area response was compared to estimate the minimum time required to achieve the equilibrium, shown in Figure 3. It was observed that BTEX peak area was stabilized after 30 min equilibration and was constant within 5 h tested. Therefore, all calibrations for this study were carried out at least after 30 min from injection of the standards into the bags.

3.1.2. Method Performance. Reproducibility of the retention time and peak area of the BTEX standards was evaluated. To introduce a wide range of sample concentration, 0.9 to 900 ppbv BTEX standards were prepared and tested for different sampling times from 0.5 to 5.0 min. Since retention time is the key parameter to identify the different compounds for all chromatographic techniques, certified reproducibility of retention times of compounds is mandatory. The experimental results performed for multiple days with standard concentrations indicated excellent reproducibility of the method, with relative standard deviation (RSD) 0.9% or less (Table 1).

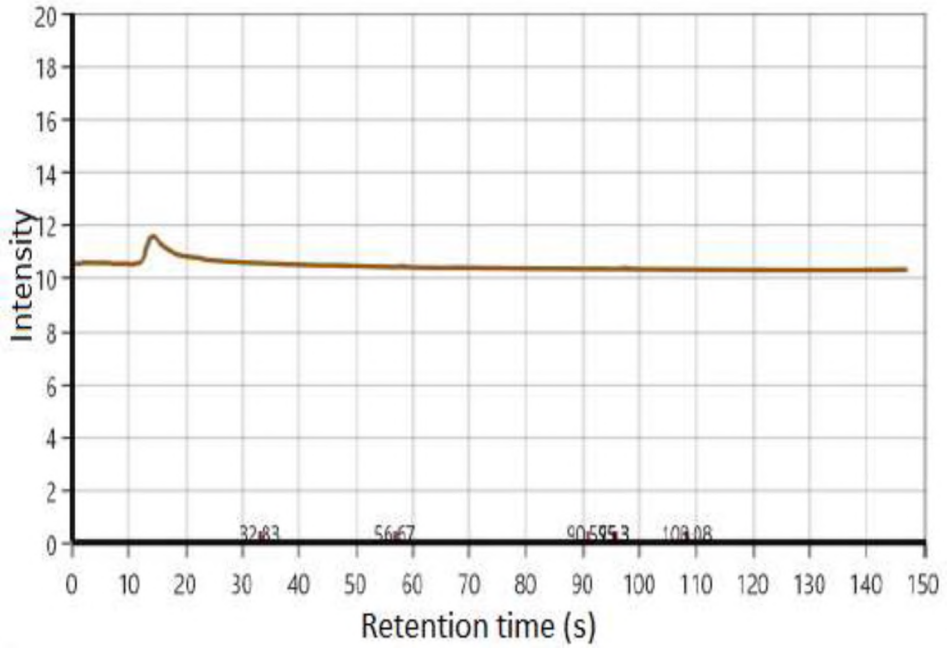

a

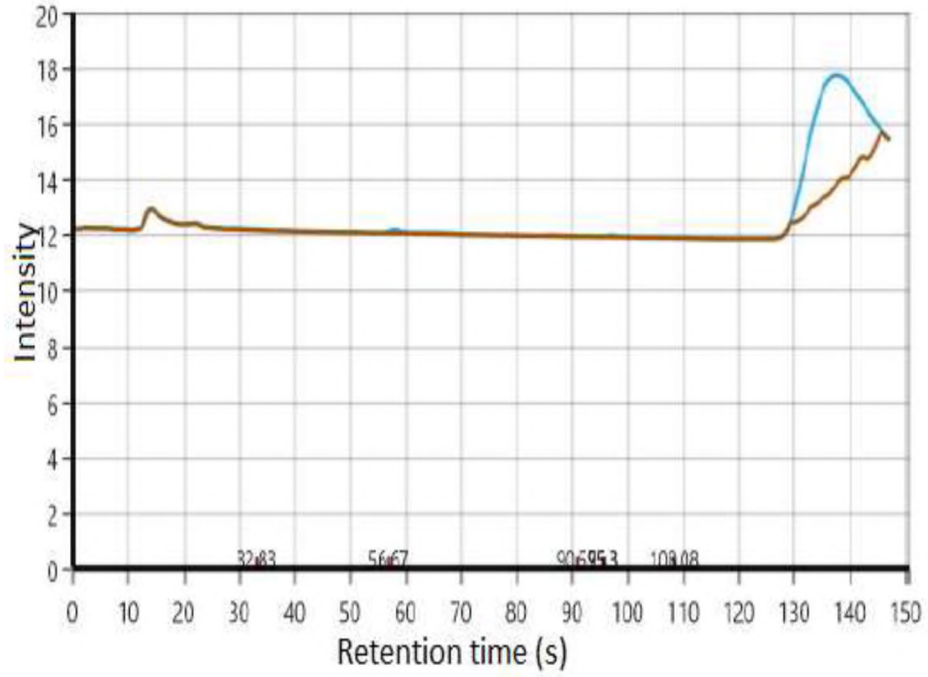

b

Figure 2. Chromatograms of nitrogen gas filled blank Tedlar® bags (no BTEX in the bags) at different temperatures: (a) room temperature (22 °C), heated at (b) 40 °C, (c) 50 °C and (d) 60 °C prior to analysis.

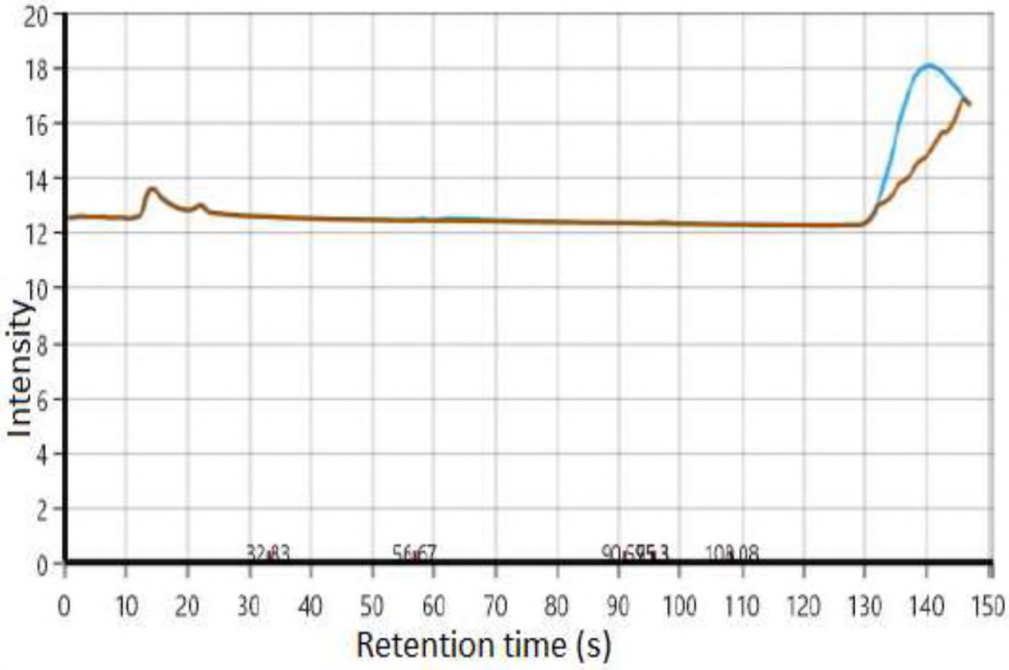

c

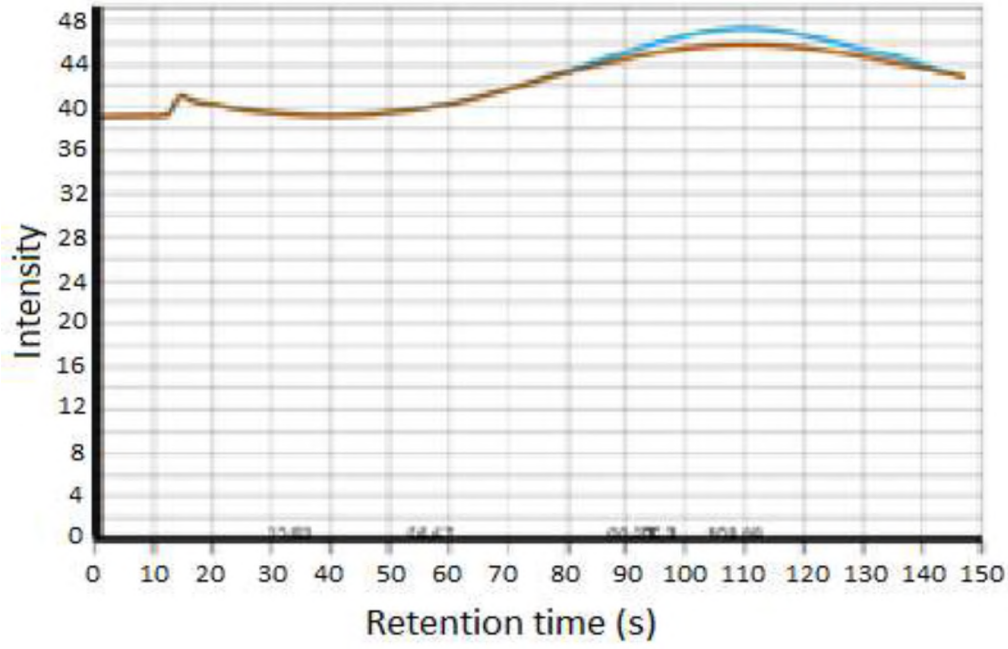

d

Figure 2. Chromatograms of nitrogen gas filled blank Tedlar® bags (no BTEX in the bags) at different temperatures: (a) room temperature (22 °C), heated at (b) 40 °C, (c) 50 °C and (d) 60 °C prior to analysis (cont.).

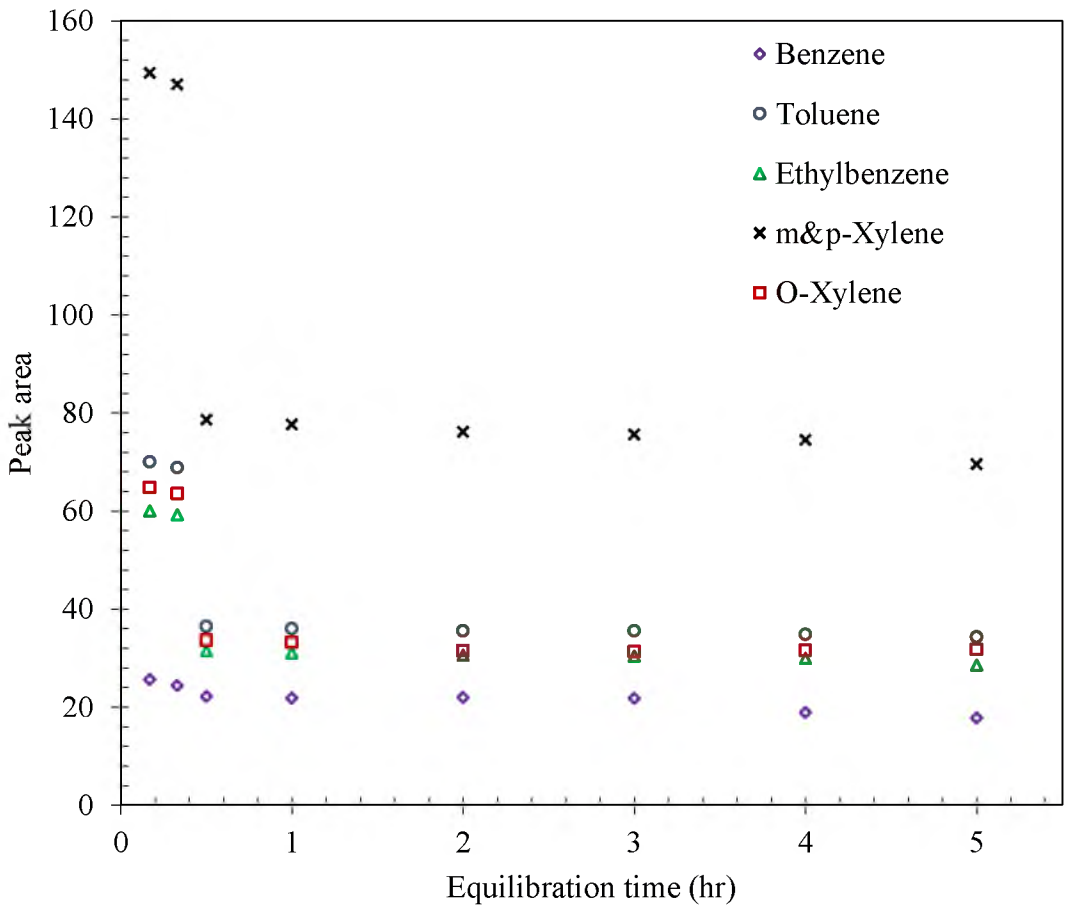

Figure 3. Peak area response of 90 ppbv BTEX standard for different equilibration and storage times at room temperature (22 °C).

Linear increase in peak area with increasing sampling time and standard concentration was observed for all the analytes. Only peak area of benzene corresponding to 5 min sampling time was levelled. It was assumed that due to low boiling point, benzene showed a breakthrough from the preconcentrator for 5 min sampling time and corresponding response were considered as outlier. RSD for peak area was up to 5.5% representing a satisfactory precision of the method. The peak area responses of all the compounds with 0.9 to 90 ppbv concentrations were linear for all sampling times except

for benzene, which was linear up to 3 min. Amount of BTEX compounds was calculated as product of sampling time, flow rate and concentration of BTEX standards used. Calibration curves of peak area vs. amount of BTEX were established and very good linearity (R^2>0.99) were obtained for all the compounds. The method is highly sensitive for BTEX with detection limits (LOD) in the range of 14.4 pg to 29.3 pg (Table 1). LOD was also calculated in ppbv unit using EPA on-line tools for indoor air unit conversion [22]. Since m and p-xylene could not be separated by this method, their combined LOD was reported.

Table 1. Method performance parameters.

Compounds	Retention time (s)		Peak Area	R^2	LOD (pg)	LOD (ppbv)	Linear range (ng)
	AVG	% RSD	% RSD				
Benzene	32.86	0.81	5.56	0.9997	14.6	0.9	0.014-27.8
Toluene	57.04	0.89	3.81	0.9999	14.4	0.7	0.014-27.5
Ethylbenzene	91.05	0.56	4.11	0.9985	28.7	0.6	0.029-54.6
m and p-xylene	95.62	0.59	2.81	0.9910	28.8	1.3	0.029-54.9
o-xylene	108.69	0.88	4.86	0.9982	29.3	0.6	0.029-55.8

Over the years several brands of portable miniaturized instruments have been reported in literature to measure VOC. Some of them need longer sampling and analysis time along with high carrier gas consumption rate requires heavier gas cylinder attached to GC and as a result overall weight of the machine increases, making it moderately

portable. Total weight of the instruments is reported sometimes to confirm its portability. Weight of NovaTestTM P100 portable GC-PID (7 kg) used in this study are comparable with that of other miniaturized portable systems, which mostly weigh between 2 to 14 kg [12], [15], [24]–[26]. Single or multistage preconcentration step sometimes used to achieve lower detection limit. Detection limit of benzene achieved by NovaTest^{TM} P100 was 14.6 pg, which is much lower compared to other preconcentration based miniaturized GC systems (37.8 to 880 pg) [15], [24], [26], [27]. Most of these reported systems could not separate three isomers of xylenes; even ethylbenzene sometimes coelutes with xylene due to their very close boiling point [25], [28]. All BTEX compounds can be separated by NovaTest^{TM} P100, except m and p–xylenes. The method was very rapid (2 min), which was much shorter compared to the analysis time (5 to 15 min) reported in literatures [3], [12], [25]–[27], [29]. For multiple injections, reproducibility of peak area or measured concentrations by NovaTest^{TM} P100 was also comparable or superior to the other reported systems [24], [25], [27].

3.2. ON-LINE MEASUREMENT OF BTEX EMISSION DURING HOT-MIX-ASPHALT PROCESSING

As a field application, real-time BTEX emission was monitored on-line during processing of HMA with and without CRM and UMO addition. CRM is made from scrap tires and a prospective source of releasing VOC. To increase the low temperature behavior and flexibility, UMO was further blended with asphalt pavement material. UMO was also proved to be a potential candidate to release VOC at high temperature processing condition [17], [18]. For comparative study two batches of asphalt/CRM were processed with/without UMO and BTEX emission was evaluated at every 10 min

intervals during processing. Chromatogram in Figure 4 represents the headspace emission gas analysis of HMA with 1 min sampling time. All six BTEX compounds were detected during HMA processing.

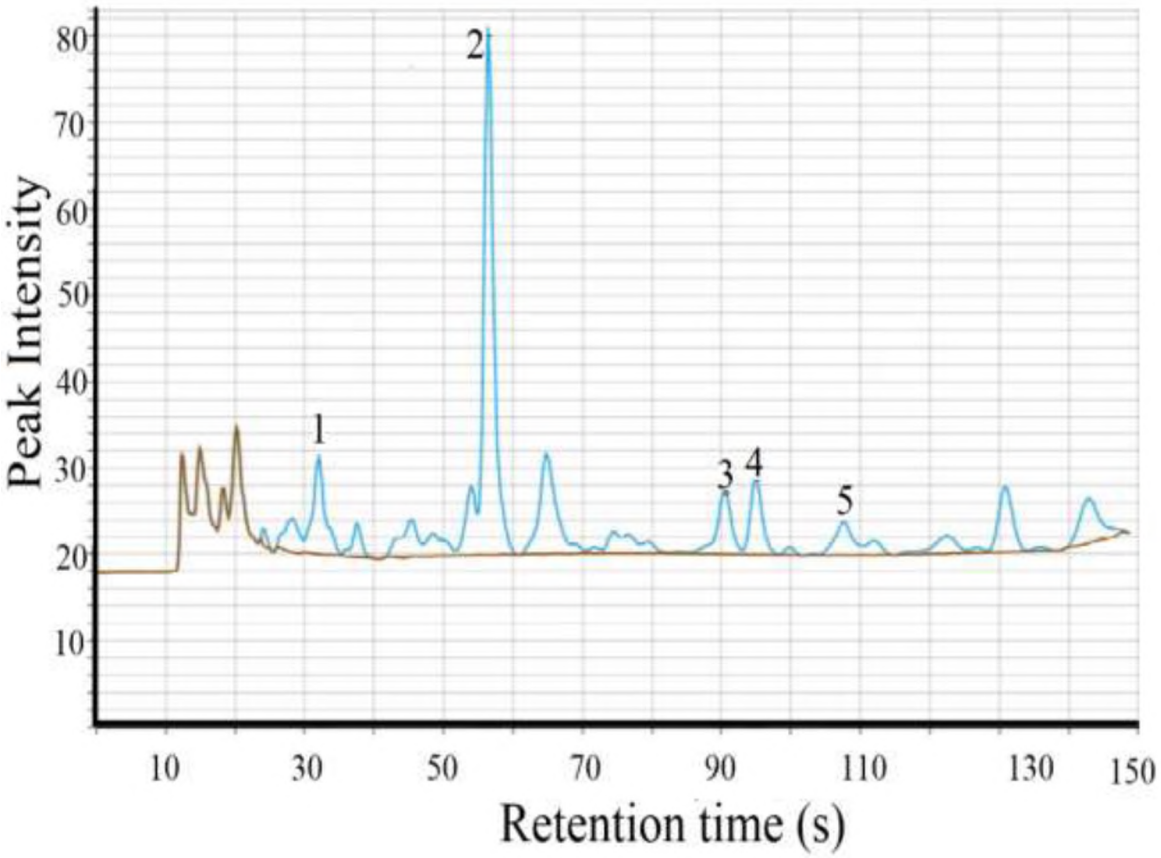

Figure 4. Representative chromatogram of BTEX in the fume of hot-mix-asphalt sampled for 1 min; peak 1: benzene, 2: toluene, 3: ethylbenzene, 4; m & p - xylene, 5; o-xylene. Unnumbered peaks are VOCs other than BTEX emitted from HMA.

Peak area at specific time interval was used to calculate the amount of emitted BTEX using linear regression equation. Finally, BTEX concentration in part-per-billion-volume (ppbv) was determined, shown in Figure 5. It was observed that addition of UMO in hot-mix-asphalt resulted in higher release of all BTEX compounds. Among the

released BTEX compounds, toluene emission was highest around 600 ppbv initially and was subsequently decreased with increasing processing time. Same trend was observed for benzene, ethylbenzene and o-xylene. In contrast, m and p-xylene initial emission concentration was lower than benzene, toluene and ethylbenzene, but its emission rate became higher with progress of processing time. Same trend was observed for both types of HMA.

3.3. ON-LINE VS. OFF-LINE DETECTION OF BTEX EMISSION DURING HMA PROCESSING

In the previous study of asphalt pavement material, BTEX emission during processing of hot-mix-asphalt was measured off-line by conventional GC-MS [23]. Both the air test and batch leaching test showed toluene as the most abundant compound of BTEX present in HMA, while benzene level was found above the national drinking water standard. It was also reported that the UMO content has the positive effect on BTEX emission rate, which again decreased steeply with interaction time. The off-line air sample collection required more complicated set up and was very time-consuming process, whereas on-line experiment with portable GC in this study allowed measuring transient BTEX emission rate with a very simple direct sampling and detection. On-line monitoring results also showed the same negative trend for the analytes with interaction time, but only m and p-xylene showed increasing emission rate. Xylene emission rate could not be compared directly with the emission gas test from off-line GC-MS results since emission of three isomers of xylene could not be separated in of-line method. The on-line test results in this study agree with the off-line GC-MS test results confirming toluene as the most prevalent toxic compound during waste material recycling process.

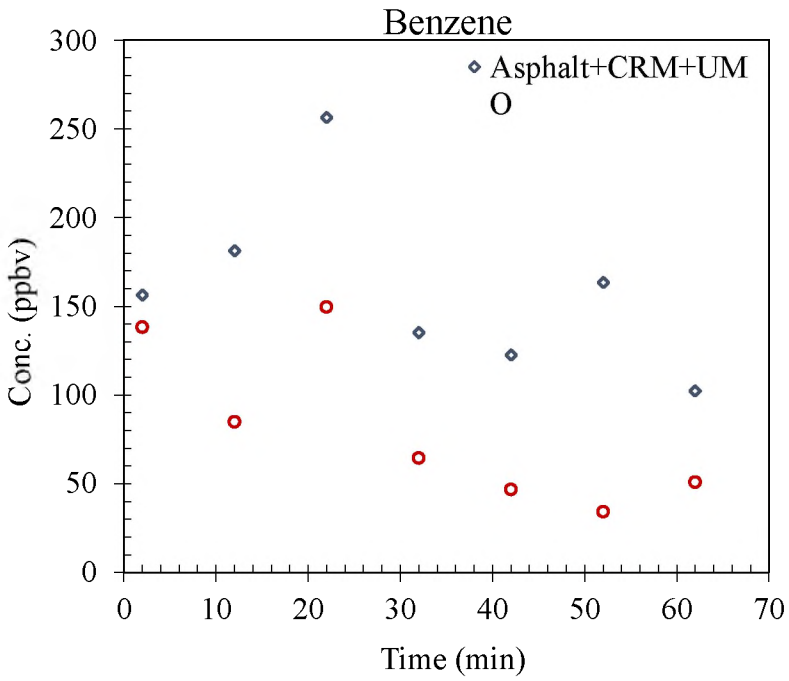

a

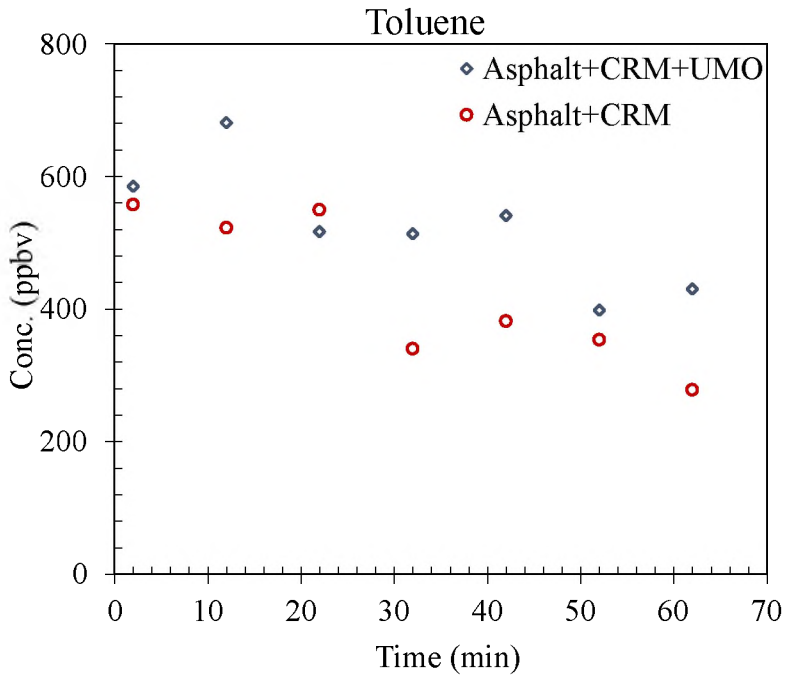

b

Figure 5. BTEX emission during processing of hot-mix-asphalt.

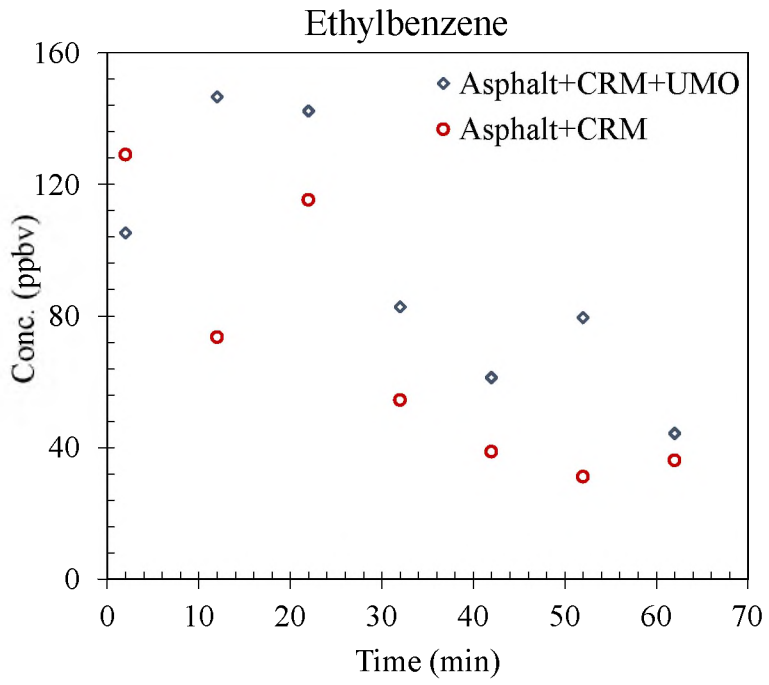

c

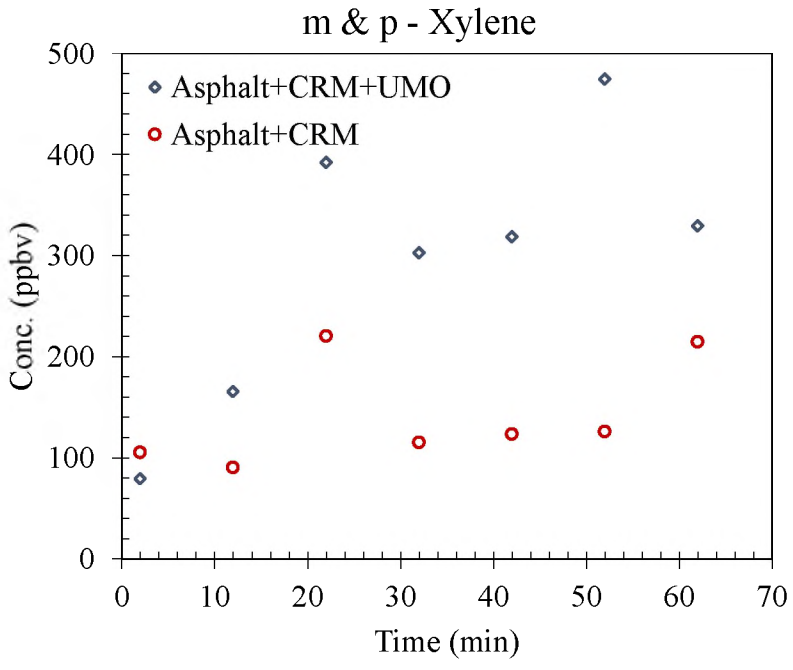

d

Figure 5. BTEX emission during processing of hot-mix-asphalt (cont.).

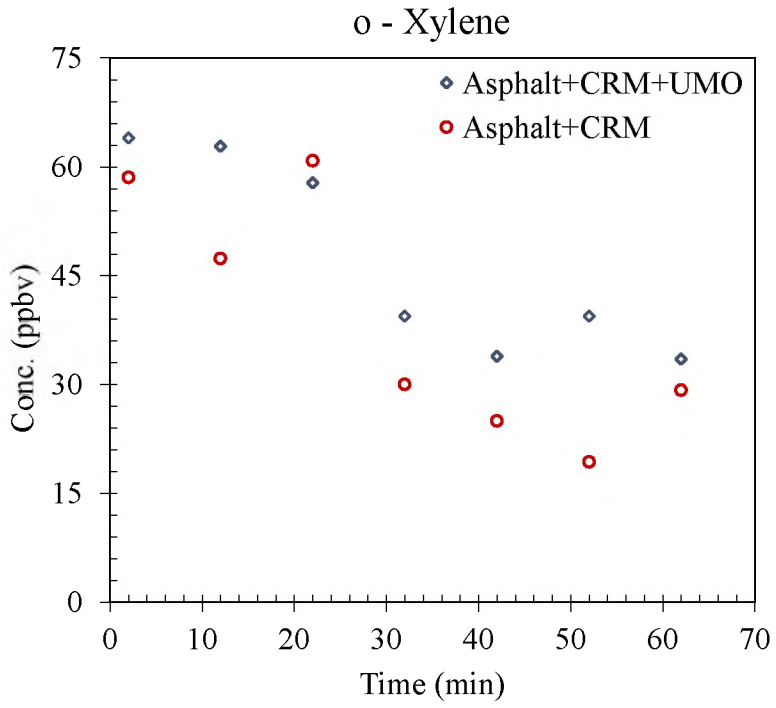

e

Figure 5. BTEX emission during processing of hot-mix-asphalt (cont.).

Another major advantage of this on-line monitoring method using the portable GC-PID is that BTEX emission profiles of all the BTEX with processing time were obtained simultaneously, whereas off-line measurement reported average BTEX emission.

4. CONCLUSIONS

In this study, a rapid, highly sensitive and selective analytical method utilizing a portable GC-PID was developed for the on-site and on-line analysis of VOC emission. PID is well known to be highly sensitive and selective for aromatic volatile compounds

with low ionization energy. The patented on-line preconcentration capability also allowed the detection limit for benzene, as a standard for comparison, much lower than any current commercially available or reported transportable GC of similar type. Analysis time of the method for BTEX analysis was very short (2 min) with excellent retention time and peak response reproducibility. The specific at-column heater configuration of the portable GC also makes the heating and cooling extremely fast for column temperature equilibration and gradient, resulting in very short overall analysis time. The system is easily portable due to its light weight (7 kg) and low gas consumption, which requires only small helium cylinder. Longer sampling time, if needed, may further lower the detection limit. The method was successfully applied for on-line analysis of BTEX emission during hot-mix-asphalt processing. Therefore, this new method using the portable GC is a powerful tool for rapid field-monitoring of BTEX in air.

ACKNOWLEDGEMENT

This work was supported by Nanova Environmental, Inc. (Columbia, MO, USA). The authors would like to acknowledge Dr. Mark Fitch and Dr. Magdy Abdelrahman for helping in hot-mix-asphalt processing experiments.

REFERENCES

[1] Y. Ueno, T. Horiuchi, T. Morimoto, and O. Niwa, "Microfluidic device for airborne BTEX detection," *Anal. Chem.*, vol. 73, no. 19, pp. 4688–4693, Oct. 2001, doi: 10.1021/ac010210+.

[2] R. E. Dodson, J. I. Levy, J. D. Spengler, J. P. Shine, and D. H. Bennett, "Influence of basements, garages, and common hallways on indoor residential volatile organic compound concentrations," *Atmos. Environ.*, vol. 42, no. 7, pp. 1569–1581, 2008, doi: https://doi.org/10.1016/j.atmosenv.2007.10.088.

[3] R. Nasreddine, V. Person, C. A. Serra, and S. Le Calvé, "Development of a novel portable miniaturized GC for near real-time low level detection of BTEX," *Sensors Actuators B Chem.*, vol. 224, pp. 159–169, 2016, doi: https://doi.org/10.1016/j.snb.2015.09.077.

[4] D. W. R. Bleyl, "IARC monographs on the evaluation of carcinogenic risks to humans. Overall evaluations of carcinogenicity: an updating of IARC monographs vol. 1 to 42. Supplement 7. 440 Seiten. International Agency for Research on Cancer, Lyon 1987. Preis: 65, – s.Fr," *Food / Nahrung*, vol. 33, no. 5, p. 462, Jan. 1989, doi: 10.1002/food.19890330516.

[5] "Toxicological profile for benzene - Agency for Toxic Substances and Disease Registry (ATSDR)," Atlanta, GA, 2007.

[6] T. Horiuchi, Y. Ueno, S. Camou, T. Haga, and A. Tate, "Portable aromatic VOC gas sensor for onsite continuous air monitoring with 10-ppb benzene detection capability," *NTT Tech. Rev.*, vol. 4, no. 1, pp. 30–37, 2006.

[7] A. Allouch, S. Le Calvé, and C. A. Serra, "Portable, miniature, fast and high sensitive real-time analyzers: BTEX detection," *Sensors Actuators B Chem.*, vol. 182, pp. 446–452, 2013, doi: https://doi.org/10.1016/j.snb.2013.03.010.

[8] J.-H. Lee, S.-M. Hwang, D.-W. Lee, and G.-S. Heo, "Determination of volatile organic compounds (VOCs) using Tedlar bag/solid-phase microextraction/gas chromatography/mass spectrometry (SPME/GC/MS) in ambient and workplace air," *Bull. Korean Chem. Soc.*, vol. 23, no. 3, pp. 488–496, 2002, [Online]. Available: http://dx.doi.org/10.5012/bkcs.2002.23.3.488.

[9] C. Martines, M. Longo, D. Lerda, G. Ceroni, and A. Cavalláro, "A GC method for the quantitative determination of BTEX in gasoline," *J. Chromatogr. Sci.*, vol. 34, no. 9, pp. 413–417, Sep. 1996, doi: 10.1093/chromsci/34.9.413.

[10] L. Zwank, T. C. Schmidt, S. B. Haderlein, and M. Berg, "Simultaneous determination of fuel oxygenates and BTEX using direct aqueous injection gas chromatography mass spectrometry (DAI-GC/MS)," *Environ. Sci. Technol.*, vol. 36, no. 9, pp. 2054–2059, May 2002, doi: 10.1021/es010270x.

[11] I. Arambarri, M. Lasa, R. Garcia, and E. Millán, "Determination of fuel dialkyl ethers and BTEX in water using headspace solid-phase microextraction and gas chromatography–flame ionization detection," *J. Chromatogr. A*, vol. 1033, no. 2, pp. 193–203, 2004, doi: https://doi.org/10.1016/j.chroma.2004.01.046.

[12] C. Liaud, N. T. Nguyen, R. Nasreddine, and S. Le Calvé, "Experimental performances study of a transportable GC-PID and two thermo-desorption based methods coupled to FID and MS detection to assess BTEX exposure at sub-ppb level in air," *Talanta*, vol. 127, pp. 33–42, 2014, doi: https://doi.org/10.1016/j.talanta.2014.04.001.

[13] A. Sarafraz-Yazdi, A. H. Amiri, and Z. Es'haghi, "Separation and determination of benzene, toluene, ethylbenzene and o-xylene compounds in water using directly suspended droplet microextraction coupled with gas chromatography-flame ionization detector," *Talanta*, vol. 78, no. 3, pp. 936–941, 2009, doi: https://doi.org/10.1016/j.talanta.2008.12.069.

[14] J. A. Dziuban *et al.*, "Portable gas chromatograph with integrated components," *Sensors Actuators A Phys.*, vol. 115, no. 2, pp. 318–330, 2004, doi: https://doi.org/10.1016/j.sna.2004.04.028.

[15] R.-S. Jian, Y.-S. Huang, S.-L. Lai, L.-Y. Sung, and C.-J. Lu, "Compact instrumentation of a μ-GC for real time analysis of sub-ppb VOC mixtures," *Microchem. J.*, vol. 108, pp. 161–167, 2013, doi: https://doi.org/10.1016/j.microc.2012.10.016.

[16] B. A. Eckenrode, "Environmental and forensic applications of field-portable GC-MS: an overview," *J. Am. Soc. Mass Spectrom.*, vol. 12, no. 6, pp. 683–693, 2001, doi: 10.1016/S1044-0305(01)00251-3.

[17] D. Bergerson, M. Abdelrahman, and M. Ragab, "Environmental study of the release of BTEX from asphalt modified with used motor oil and crumb rubber modifier," *Int. J. Waste Resour.*, vol. 4, no. 4, p. 165, 2014, [Online]. Available: https://www.longdom.org/open-access/environmental-study-of-the-release-of-btex-2252-5211-4-165.

[18] M. Abdelrahman, Magdy Ragab and D. Bergerson, "Effect of used motor oil on the macro and micromechanical properties of crumb rubber modified asphalt," *Int. J. Waste Resour.*, vol. 5, no. 3, p. 180, 2015, [Online]. Available: https://www.longdom.org/open-access/effect-of-used-motor-oil-on-the-macro-and-micromechanical-properties-of-crumb-rubber-modified-asphalt-2252-5211-1000180.

[19] X. Fan, Y. B. Gianchandani, and J. Liu, "Device and methods for adaptive micro-gas chromatography," US9341604, 2016.

[20] J. Beauchamp, J. Herbig, R. Gutmann, and A. Hansel, "On the use of Tedlar® bags for breath-gas sampling and analysis," *J. Breath Res.*, vol. 2, no. 4, p. 46001, Dec. 2008, doi: 10.1088/1752-7155/2/4/046001.

[21] P. Mochalski, J. King, K. Unterkofler, and A. Amann, "Stability of selected volatile breath constituents in Tedlar, Kynar and Flexfilm sampling bags," *Analyst*, vol. 138, no. 5, pp. 1405–1418, Mar. 2013, doi: 10.1039/c2an36193k.

[22] EPA, "Indoor air unit conversion," 2016. https://www3.epa.gov/ceampubl/learn2model/part-two/onsite/ia_unit_conversion.html.

[23] E. Deef-Allah, M. Abdelrahman, M. Fitch, M. Ragab, M. Bose, and X. He, "Balancing the performance and environmental concerns of used motor oil as rejuvenator in asphalt mixes," *Recycling*, vol. 4, no. 1, p. 11, 2019, [Online]. Available: https://doi.org/10.3390/recycling4010011.

[24] A. Garg *et al.*, "Zebra GC: A mini gas chromatography system for trace-level determination of hazardous air pollutants," *Sensors Actuators B Chem.*, vol. 212, pp. 145–154, 2015, doi: https://doi.org/10.1016/j.snb.2014.12.136.

[25] W. Zhang *et al.*, "Fast Determination of Monocyclic Aromatic Hydrocarbons in Ambient Air Using a Portable Gas Chromatography–Photoionization Detector," *Chromatographia*, vol. 80, no. 8, pp. 1233–1247, 2017, doi: 10.1007/s10337-017-3331-1.

[26] D.-W. You, Y.-S. Seon, Y. Jang, J. Bang, J.-S. Oh, and K.-W. Jung, "A portable gas chromatograph for real-time monitoring of aromatic volatile organic compounds in air samples," *J. Chromatogr. A*, vol. 1625, p. 461267, 2020, doi: https://doi.org/10.1016/j.chroma.2020.461267.

[27] S. Zampolli *et al.*, "Real-time monitoring of sub-ppb concentrations of aromatic volatiles with a MEMS-enabled miniaturized gas-chromatograph," *Sensors Actuators B Chem.*, vol. 141, no. 1, pp. 322–328, 2009, doi: https://doi.org/10.1016/j.snb.2009.06.021.

[28] R. A. Iglesias, F. Tsow, R. Wang, E. S. Forzani, and N. Tao, "Hybrid separation and detection device for analysis of benzene, toluene, ethylbenzene, and xylenes in complex samples," *Anal. Chem.*, vol. 81, no. 21, pp. 8930–8935, Nov. 2009, doi: 10.1021/ac9015769.

[29] I. Lara-lbeas *et al.*, "Sub-ppb level detection of BTEX gaseous mixtures with a compact prototype GC equipped with a preconcentration unit," *Micromachines*, vol. 10, no. 3, p. 187, 2019, [Online]. Available: https://doi.org/10.3390/mi10030187.

SECTION

2. CONCLUSIONS AND RECOMMENDATIONS

2.1. CONCLUSIONS

In this dissertation different polymer-based materials are synthesized and characterized such as optical oxygen sensor, soy polyol-based polyurethane foam, and environmental monitoring of volatile organic compounds using portable gas chromatography during recycling of waste rubber.

Optical oxygen sensors are superior technology for continuous monitoring of oxygen in a growing number of applications. An optical oxygen sensor ink was developed, compatible to print on most of the commonly used polymeric substrate. Immobilization of fluorophore in the polystyrene particles did not alter the optical properties of the fluorophore. These optical sensors showed linear response within 0-21% oxygen concentrations with single quenching constant and very good reproducibility of the signal. Sensor has adequate sensitivity within the required oxygen range, i.e. 0-21% oxygen concentrations and showed good operational stability with very short response time. Low cost fabrication technique suitable to print microparticle-based ink was also developed. Printed sensor patches along with smartphone-based imaging read-out technique made the system suitable for continuous monitoring of oxygen on a two-dimensional surface.

In the second task, soy-polyol based polyurethane (PU) foams were synthesized instead of completely petroleum-based PU foam to mitigate the environmental issue due

to continuous use of petroleum-based products. Rigid PU foams were fabricated for structural and thermal insulation applications. Effect of different additives, such as catalyst, blowing agent, surfactant and polyol functionlaity was investigated by preparing and characterizing different synthetic formulations of PU foams. It was observed that higher catalyst content increased the foam density by increasing the curing rate; whereas higher water content enhanced the blowing rate and produced low density foam with improved thermal resistivity. However, very high amount of water addition produced foams with irregular cell structures and broken cell walls, which might deteriorate the thermal resistivity. Silicone surfactants were used to improve reactant miscibility by aligning along the air-polyol interface and reducing the overall surface tension. Surfactants also helped to generate PU foams of high thermal resistivity by entraping high volume of air bubbles during mechanical mixing and supporting the nucleation and growth of the cell structure without getting coalesced. But, compression force deflection (CFD) values deteriorated for higher surfactant loading due to the plasticizing effect of it. 100% soy polyol-based PU foam has comparable thermal resistivity but poor CFD values with that of the petroleum-based control foam Baydur 683. To improve CFD values comparable with that of the petroleum-based one high functiononlaity polyol (HB 530) was blended with low functionality polyol (HB 230). It was found that mixing of 5g of HB530 with 95g of HB230 along with 0.08g catalyst, 1.50g of water and 5g of surfactant can produce soy-based foam with CFD and R-value similar to that of the control foam (Baydur 683).

Finally, a newly developed transportable gas chromatography with photo ionization detector (GC-PID) was tested for online monitoring of volatile organic

compounds. A high throughput sensitive method was established for instantaneous monitoring of benzene, toluene, ethylbenzene and xylenes (BTEX). Analysis time of the method was extremely short (<2.5 min) with excellent reproducibility. PID is known to be highly sensitive and selective for aromatic volatile compounds with low ionization energy, plus on-line preconcentration capability, resulting this portable GC- PID super sensitive with detection limit for benzene. Longer sampling time, as needed, may further lower detection limit. The method was successfully applied for on-line determination of BTEX emission during hot-mix-asphalt processing containing recycled materials as processing aids.

2.2. RECOMMENDATIONS

Polymer host usually improves stability of the fluorophore in optical sensor. Performance of the prototype patches under different conditions such as variable temperature and moisture can be studied. Future research can focus the further applicability of the sensor patch for different applications such as tissue oxygen monitoring for early detection of pressure ulcer, monitoring of food package conditions, etc.

Soy-based rigid polyurethane foam can be used to fabricate structural insulated panel (SIP) by sandwiching between Oriented Strand Boards structure, which can be tested for overall themal resitivity and compression force deflection test for energy-efficient and modular building construction.

The portable GC-PID along with BTEX method can be used as a teach lab experiment due to its unique advantages, such as extremely short run time, low price, and high

portability. Even this instrument can be employed for different field experiments. It can also be used to monitor several other volatile organic compounds of low ionization energies. Apart from air sample, other matrices can also be analyzed, provided suitable sample preparation method is developed or adopted to extract VOCs from those complex matrices, such as soil, water, etc.

BIBLIOGRAPHY

[1] M. A. Regan, R. W. Teasell, D. L. Wolfe, D. Keast, W. B. Mortenson, and J. A. L. Aubut, "A systematic review of therapeutic interventions for pressure ulcers after cpinal cord injury," *Arch. Phys. Med. Rehabil.*, vol. 90, no. 2, pp. 213–231, 2009, doi: 10.1016/j.apmr.2008.08.212.

[2] S. Schreml *et al.*, "2D luminescence imaging of physiological wound oxygenation," *Exp. Dermatol.*, vol. 20, no. 7, pp. 550–554, Jul. 2011, doi: 10.1111/j.1600-0625.2011.01263.x.

[3] X.-H. Wang *et al.*, "Targetable phosphorescent oxygen nanosensors for the assessment of tumor mitochondrial dysfunction by monitoring the respiratory activity," *Angew. Chemie Int. Ed.*, vol. 53, no. 46, pp. 12471–12475, Nov. 2014, doi: 10.1002/anie.201405048.

[4] M. Fitzgerald *et al.*, "Nondestructive monitoring of oxygen profiles in packaged foods using phase-fluorimetric oxygen sensor," *J. Food Sci.*, vol. 66, no. 1, pp. 105–110, Jan. 2001, doi: 10.1111/j.1365-2621.2001.tb15590.x.

[5] C. McDonagh *et al.*, "Phase fluorometric dissolved oxygen sensor," *Sensors Actuators B Chem.*, vol. 74, no. 1, pp. 124–130, 2001, doi: https://doi.org/10.1016/S0925-4005(00)00721-8.

[6] J. Azimian, N. Dehghan Nayeri, E. Pourkhaleghi, and M. Ansari, "Transdermal wound oxygen therapy on pressure ulcer healing: a single-blind multi-center randomized controlled trial," *Iran. Red Crescent Med. J.*, vol. 17, no. 11, p. e20211, Nov. 2015, doi: 10.5812/ircmj.20211.

[7] S. Schreml, R. M. Szeimies, L. Prantl, S. Karrer, M. Landthaler, and P. Babilas, "Oxygen in acute and chronic wound healing," *Br. J. Dermatol.*, vol. 163, no. 2, pp. 257–268, Aug. 2010, doi: 10.1111/j.1365-2133.2010.09804.x.

[8] C. K. Sen, "Wound healing essentials: let there be oxygen," *Wound Repair Regen.*, vol. 17, no. 1, pp. 1–18, 2009, doi: 10.1111/j.1524-475X.2008.00436.x.

[9] Z. Li *et al.*, "Non-invasive transdermal two-dimensional mapping of cutaneous oxygenation with a rapid-drying liquid bandage," *Biomed. Opt. Express*, vol. 5, no. 11, pp. 3748–3764, Oct. 2014, doi: 10.1364/BOE.5.003748.

[10] S. Cichosz, A. Masek, and M. Zaborski, "Polymer-based sensors: A review," *Polym. Test.*, vol. 67, pp. 342–348, 2018, doi: https://doi.org/10.1016/j.polymertesting.2018.03.024.

[11] B. Adhikari and S. Majumdar, "Polymers in sensor applications," *Prog. Polym. Sci.*, vol. 29, no. 7, pp. 699–766, 2004, doi: https://doi.org/10.1016/j.progpolymsci.2004.03.002.

[12] H. Gábor, "Polymer films in sensor applications: a review of present uses and future possibilities," *Sens. Rev.*, vol. 20, no. 2, pp. 98–105, Jan. 2000, doi: 10.1108/02602280010319169.

[13] M. Quaranta, S. M. Borisov, and I. Klimant, "Indicators for optical oxygen sensors," *Bioanal. Rev.*, vol. 4, no. 2, pp. 115–157, 2012, doi: 10.1007/s12566-012-0032-y.

[14] Y. Amao, "Probes and Polymers for Optical Sensing of Oxygen," *Microchim. Acta*, vol. 143, no. 1, pp. 1–12, 2003, doi: 10.1007/s00604-003-0037-x.

[15] X. Wang and O. S. Wolfbeis, "Optical methods for sensing and imaging oxygen: materials, spectroscopies and applications," *Chem. Soc. Rev.*, vol. 43, no. 10, pp. 3666–3761, 2014, doi: 10.1039/C4CS00039K.

[16] D. B. Papkovsky, G. V Ponomarev, W. Trettnak, and P. O'Leary, "Phosphorescent complexes of porphyrin ketones: optical properties and application to oxygen sensing," *Anal. Chem.*, vol. 67, no. 22, pp. 4112–4117, Nov. 1995, doi: 10.1021/ac00118a013.

[17] S.-K. Lee and I. Okura, "Photostable optical oxygen sensing material: platinum tetrakis(pentafluorophenyl)porphyrin immobilized in polystyrene," *Anal. Commun.*, vol. 34, no. 6, pp. 185–188, 1997, doi: 10.1039/A701130J.

[18] Y. Mao *et al.*, "Highly enhanced sensitivity of optical oxygen sensors using microstructured PtTFPP/PDMS-pillar arrays sensing layer," *Sensors Actuators B Chem.*, vol. 251, pp. 495–502, 2017, doi: https://doi.org/10.1016/j.snb.2017.05.081.

[19] O. Bayer, W. Siefken, H. Rinke, L. Orthner, and H. Schild, "A process for the production of polyurethanes and polyureas," 1937.

[20] S. Tan, T. Abraham, D. Ference, and C. W. Macosko, "Rigid polyurethane foams from a soybean oil-based polyol," *Polymer (Guildf).*, vol. 52, no. 13, pp. 2840–2846, 2011, doi: https://doi.org/10.1016/j.polymer.2011.04.040.

[21] A. A. Abdel Hakim, M. Nassar, A. Emam, and M. Sultan, "Preparation and characterization of rigid polyurethane foam prepared from sugar-cane bagasse polyol," *Mater. Chem. Phys.*, vol. 129, no. 1, pp. 301–307, 2011, doi: https://doi.org/10.1016/j.matchemphys.2011.04.008.

[22] A. Guo, I. Javni, and Z. Petrovic, "Rigid polyurethane foams based on soybean oil," *J. Appl. Polym. Sci.*, vol. 77, no. 2, pp. 467–473, Jul. 2000, doi: 10.1002/(SICI)1097-4628(20000711)77:2<467::AID-APP25>3.0.CO;2-F.

[23] K. S. Chian and L. H. Gan, "Development of a rigid polyurethane foam from palm oil," *J. Appl. Polym. Sci.*, vol. 68, no. 3, pp. 509–515, Apr. 1998, doi: 10.1002/(SICI)1097-4628(19980418)68:3<509::AID-APP17>3.0.CO;2-P.

[24] Y. H. Hu *et al.*, "Rigid polyurethane foam prepared from a rape seed oil based polyol," *J. Appl. Polym. Sci.*, vol. 84, no. 3, pp. 591–597, Apr. 2002, doi: 10.1002/app.10311.

[25] I. Javni, Z. S. Petrović, A. Guo, and R. Fuller, "Thermal stability of polyurethanes based on vegetable oils," *J. Appl. Polym. Sci.*, vol. 77, no. 8, pp. 1723–1734, Aug. 2000, doi: 10.1002/1097-4628(20000822)77:8<1723::AID-APP9>3.0.CO;2-K.

[26] A. Campanella, L. M. Bonnaillie, and R. P. Wool, "Polyurethane foams from soyoil-based polyols," *J. Appl. Polym. Sci.*, vol. 112, no. 4, pp. 2567–2578, May 2009, doi: 10.1002/app.29898.

[27] L.-T. Yang, C.-S. Zhao, C.-L. Dai, L.-Y. Fu, and S.-Q. Lin, "Thermal and mechanical properties of polyurethane rigid foam based on epoxidized soybean oil," *J. Polym. Environ.*, vol. 20, no. 1, pp. 230–236, 2012, doi: 10.1007/s10924-011-0381-6.

[28] D. Ji *et al.*, "Polyurethane rigid foams formed from different soy-based polyols by the ring opening of epoxidised soybean oil with methanol, phenol, and cyclohexanol," *Ind. Crops Prod.*, vol. 74, pp. 76–82, 2015, doi: https://doi.org/10.1016/j.indcrop.2015.04.041.

[29] C. Zhang and M. R. Kessler, "Bio-based polyurethane foam made from compatible blends of vegetable-oil-based polyol and petroleum-based polyol," *ACS Sustain. Chem. Eng.*, vol. 3, no. 4, pp. 743–749, Apr. 2015, doi: 10.1021/acssuschemeng.5b00049.

[30] Y. Li, X. Luo, and S. Hu, "Polyols and Polyurethanes from Vegetable Oils and Their Derivatives," in *Bio-based Polyols and Polyurethanes*, SpringerBriefs in Molecular Science, 2015.

[31] J. John, M. Bhattacharya, and R. B. Turner, "Characterization of polyurethane foams from soybean oil," *J. Appl. Polym. Sci.*, vol. 86, no. 12, pp. 3097–3107, Dec. 2002, doi: 10.1002/app.11322.

[32] A. Guo, Y. Cho, and Z. S. Petrović, "Structure and properties of halogenated and nonhalogenated soy-based polyols," *J. Polym. Sci. Part A Polym. Chem.*, vol. 38, no. 21, pp. 3900–3910, Nov. 2000, doi: 10.1002/1099-0518(20001101)38:21<3900::AID-POLA70>3.0.CO;2-E.

[33] E. F. T. White, "Polyurethane handbook Edited by G. Oertel, Hanser Publishers, Munich, 1985. pp. 629, price E104.70. ISBN 3-446-13671-1," *Br. Polym. J.*, vol. 18, no. 6, pp. 403–404, 1986, doi: 10.1002/pi.4980180626.

[34] M. L. Pinto, "Formulation, Preparation, and Characterization of Polyurethane Foams," *J. Chem. Educ.*, vol. 87, no. 2, pp. 212–215, Jan. 2010, doi: 10.1021/ed8000599.

[35] R. Herrington and K. Hock, *Dow Polyurethanes: Flexible Foams*. Michigan: The Dow Chemical Company, 1997.

[36] K. Aalto-Korte, M. Engfeldt, T. Estlander, and R. Jolanki, "Polyurethane Resins BT - Kanerva's Occupational Dermatology," S. M. John, J. D. Johansen, T. Rustemeyer, P. Elsner, and H. I. Maibach, Eds. Cham: Springer International Publishing, 2018, pp. 1–12.

[37] Y. H. Kim *et al.*, "Properties of rigid polyurethane foams blown by HFC-365 mfc and distilled water," *J. Ind. Eng. Chem.*, vol. 13, pp. 1076–1082, Jan. 2007.

[38] P. Mondal and D. V Khakhar, "Regulation of Cell Structure in Water Blown Rigid Polyurethane Foam," *Macromol. Symp.*, vol. 216, no. 1, pp. 241–254, Sep. 2004, doi: 10.1002/masy.200451223.

[39] M. Szycher, *Szycher's Handbook of Polyurethanes*. Florida: CRC Press, 1999.

[40] D. Perry, "Silicone surface active agents," in *Additives in Water-Borne Coatings*, G. Davison and B. Lane, Eds. Cambridge: The Royal Society of Chemistry, 2003, pp. 77–84.

[41] J. Grimminger and K. Muha, "Silicone surfactants for pentane blown rigid foam," *J. Cell. Plast.*, vol. 31, no. 1, pp. 48–72, Jan. 1995, doi: 10.1177/0021955X9503100104.

[42] X. D. Zhang, C. W. Macosko, H. T. Davis, A. D. Nikolov, and D. T. Wasan, "Role of silicone surfactant in flexible polyurethane foam," *J. Colloid Interface Sci.*, vol. 215, no. 2, pp. 270–279, 1999, doi: https://doi.org/10.1006/jcis.1999.6233.

[43] E. Durmusoglu, F. Taspinar, and A. Karademir, "Health risk assessment of BTEX emissions in the landfill environment," *J. Hazard. Mater.*, vol. 176, no. 1–3, pp. 870–877, 2010, doi: https://doi.org/10.1016/j.jhazmat.2009.11.117.

[44] Y. Ueno, T. Horiuchi, T. Morimoto, and O. Niwa, "Microfluidic device for airborne BTEX detection," *Anal. Chem.*, vol. 73, no. 19, pp. 4688–4693, Oct. 2001, doi: 10.1021/ac010210+.

[45] R. E. Dodson, J. I. Levy, J. D. Spengler, J. P. Shine, and D. H. Bennett, "Influence of basements, garages, and common hallways on indoor residential volatile organic compound concentrations," *Atmos. Environ.*, vol. 42, no. 7, pp. 1569–1581, 2008, doi: https://doi.org/10.1016/j.atmosenv.2007.10.088.

[46] R. Nasreddine, V. Person, C. A. Serra, and S. Le Calvé, "Development of a novel portable miniaturized GC for near real-time low level detection of BTEX," *Sensors Actuators B Chem.*, vol. 224, pp. 159–169, 2016, doi: https://doi.org/10.1016/j.snb.2015.09.077.

[47] F.-H. Chang, T.-C. Lin, C.-I. Huang, H.-R. Chao, T.-Y. Chang, and C.-S. Lu, "Emission characteristics of VOCs from athletic tracks," *J. Hazard. Mater.*, vol. 70, no. 1, pp. 1–20, 1999, doi: https://doi.org/10.1016/S0304-3894(99)00154-5.

[48] F. J. Santos and M. T. Galceran, "The application of gas chromatography to environmental analysis," *TrAC Trends Anal. Chem.*, vol. 21, no. 9, pp. 672–685, 2002, doi: https://doi.org/10.1016/S0165-9936(02)00813-0.

[49] J. Koziel, M. Jia, A. Khaled, J. Noah, and J. Pawliszyn, "Field air analysis with SPME device," *Anal. Chim. Acta*, vol. 400, no. 1, pp. 153–162, 1999, doi: https://doi.org/10.1016/S0003-2670(99)00614-5.

[50] S. Król, B. Zabiegała, and J. Namieśnik, "Monitoring VOCs in atmospheric air I. On-line gas analyzers," *TrAC Trends Anal. Chem.*, vol. 29, no. 9, pp. 1092–1100, 2010, doi: https://doi.org/10.1016/j.trac.2010.05.007.

[51] E. Woolfenden, "Sorbent-based sampling methods for volatile and semi-volatile organic compounds in air: Part 1: Sorbent-based air monitoring options," *J. Chromatogr. A*, vol. 1217, no. 16, pp. 2674–2684, 2010, doi: https://doi.org/10.1016/j.chroma.2009.12.042.

[52] C. Liaud, N. T. Nguyen, R. Nasreddine, and S. Le Calvé, "Experimental performances study of a transportable GC-PID and two thermo-desorption based methods coupled to FID and MS detection to assess BTEX exposure at sub-ppb level in air," *Talanta*, vol. 127, pp. 33–42, 2014, doi: https://doi.org/10.1016/j.talanta.2014.04.001.

[53] J. Ji, C. Deng, W. Shen, and X. Zhang, "Field analysis of benzene, toluene, ethylbenzene and xylene in water by portable gas chromatography–microflame ionization detector combined with headspace solid-phase microextraction," *Talanta*, vol. 69, no. 4, pp. 894–899, 2006, doi: https://doi.org/10.1016/j.talanta.2005.11.032.

[54] T. Horiuchi, Y. Ueno, S. Camou, T. Haga, and A. Tate, "Portable aromatic VOC gas sensor for onsite continuous air monitoring with 10-ppb benzene detection capability," *NTT Tech. Rev.*, vol. 4, no. 1, pp. 30–37, 2006.

[55] A. Allouch, S. Le Calvé, and C. A. Serra, "Portable, miniature, fast and high sensitive real-time analyzers: BTEX detection," *Sensors Actuators B Chem.*, vol. 182, pp. 446–452, 2013, doi: https://doi.org/10.1016/j.snb.2013.03.010.

[56] E. Deef-Allah, M. Abdelrahman, M. Fitch, M. Ragab, M. Bose, and X. He, "Balancing the performance and environmental concerns of used motor oil as rejuvenator in asphalt mixes," *Recycling*, vol. 4, no. 1, p. 11, 2019, [Online]. Available: https://doi.org/10.3390/recycling4010011.

[57] J. Sneddon, S. Masuram, and J. C. Richert, "Gas Chromatography-Mass Spectrometry-Basic Principles, Instrumentation and Selected Applications for Detection of Organic Compounds," *Anal. Lett.*, vol. 40, no. 6, pp. 1003–1012, 2007.

[58] A. Rodríguez-Cuevas, I. Lara-Ibeas, A. Leprince, M. Wolf, and S. Le Calvé, "Easy-to-manufacture micro gas preconcentrator integrated in a portable GC for enhanced trace detection of BTEX," *Sensors Actuators B Chem.*, vol. 324, p. 128690, 2020, doi: https://doi.org/10.1016/j.snb.2020.128690.

[59] J. C. Posner, "Portable Gas Chromatography," in *NIOSH Manual of Analytical Methods*, 1996, p. 74.

[60] S. Ahuja and M. W. Dong, Eds., *Handbook of Pharmaceutical Analysis by HPLC*. Separation Science and Technology, 2005.

[61] J. H. Sun, F. Y. Guan, X. F. Zhu, Z. W. Ning, and T. J. Ma, "The Integrated Mini GC-PID System for Monitoring Air Pollution," InTech, 2015.

[62] A. Garg *et al.*, "Zebra GC: A mini gas chromatography system for trace-level determination of hazardous air pollutants," *Sensors Actuators B Chem.*, vol. 212, pp. 145–154, 2015, doi: https://doi.org/10.1016/j.snb.2014.12.136.

[63] R.-S. Jian, Y.-S. Huang, S.-L. Lai, L.-Y. Sung, and C.-J. Lu, "Compact instrumentation of a μ-GC for real time analysis of sub-ppb VOC mixtures," *Microchem. J.*, vol. 108, pp. 161–167, 2013, doi: https://doi.org/10.1016/j.microc.2012.10.016.

[64] M. Rahman, A. M. A. El-Aty, J.-H. Choi, H.-C. Shin, S. C. Shin, and J.-H. Shim, "Basic Overview on Gas Chromatography," in *Analytical Separation Science*, Wiley-VCH Verlag GmbH & Co. KGaA, 2015, pp. 823–834.

[65] A. Sarafraz-Yazdi, A. H. Amiri, and Z. Es'haghi, "Separation and determination of benzene, toluene, ethylbenzene and o-xylene compounds in water using directly suspended droplet microextraction coupled with gas chromatography-flame ionization detector," *Talanta*, vol. 78, no. 3, pp. 936–941, 2009, doi: https://doi.org/10.1016/j.talanta.2008.12.069.

[66] Q. Li, X. Ma, D. Yuan, and J. Chen, "Evaluation of the solid-phase microextraction fiber coated with single walled carbon nanotubes for the determination of benzene, toluene, ethylbenzene, xylenes in aqueous samples," *J. Chromatogr. A*, vol. 1217, no. 15, pp. 2191–2196, 2010, doi: https://doi.org/10.1016/j.chroma.2010.02.009.

[67] J. A. Dziuban *et al.*, "Portable gas chromatograph with integrated components," *Sensors Actuators A Phys.*, vol. 115, no. 2, pp. 318–330, 2004, doi: https://doi.org/10.1016/j.sna.2004.04.028.

[68] A. F. L. Godoi, E. Y. Sawada, M. R. R. de Marchi, R. Van Grieken, and R. H. M. Godoi, "Determination of BTEX by GC–MS in air of offset printing plants: comparison between conventional and ecological inks," *Water, Air, Soil Pollut. Focus*, vol. 9, no. 3, pp. 163–169, 2009, doi: 10.1007/s11267-009-9219-9.

[69] L. Spinelle, M. Gerboles, G. Kok, S. Persijn, and T. Sauerwald, "Review of Portable and Low-Cost Sensors for the Ambient Air Monitoring of Benzene and Other Volatile Organic Compounds," *Sensors (Basel)*, vol. 17, no. 7, p. 1520, 2017.

[70] F. M. Peng, P. H. Xie, Y. G. Shi, J. D. Wang, W. Q. Liu, and H. Y. Li, "Photoionization Detector for Portable Rapid GC," *Chromatographia*, vol. 65, no. 5, pp. 331–336, 2007, doi: 10.1365/s10337-006-0169-3.

VITA

Mousumi Bose was born in Howrah, West Bengal, India. She received her Bachelor of Science in Chemistry and Bachelor of Technology in Polymer Science and Technology from University of Calcutta, India in July 2008 and August 2011, respectively. In 2011, she started her graduate study and in November 2013 she received her Master of Technology in Polymer Science and Technology from Indian Institute of Technology Delhi, India. After her graduation she worked as an assistant teacher in Chemistry at M.C. Kejriwal Vidyapeeth, Howrah, India. Later she worked as a teaching and research assistant at Indian Institute of Technology Kanpur, India.

In January 2017, Mousumi started her doctoral study at Missouri University of Science and technology, Rolla, USA. She worked in multiple projects under the guidance of Prof. Paul Nam. She presented one of her works at ACS National Meeting, Boston, MA, USA in 2018 and two of her other works at Pittcon Conference and Expo, Chicago, IL, USA in 2020. In May 2021 she received her Doctor of Philosophy in Chemistry from Missouri University of Science and Technology, Rolla, MO, USA. She was a member of American Chemical Society.

Mousumi was one of the inventors of a recently filed U.S. Provisional Patent entitled "Smart wound dressing" (Application Serial No. 63/156,157).